FIELD CALIBRATION METHODOLOGY FOR A MULTIBEAM ECHO SOUNDER USING A SPLIT BEAM SONAR SYSTEM AND A STANDARD TARGET

BY

JOSE CARLOS LANZONI

B.S.E.E., University of New Hampshire, 2002

M.S.E.E., University of New Hampshire, 2007

THESIS

Submitted to the University of New Hampshire

In Partial Fulfillment of

The Requirements for the Degree of

Master of Science

in

Ocean Engineering

December, 2011

UMI Number: 1507825

This thesis has been examined and approved.

Thesis Advisor, Thomas Weber
Research Assistant Professor of Ocean Engineering

Larry Mayer, Professor of Ocean Engineering

Lloyd Huff, Professor of Ocean Engineering

19 Dec 2011
Date

DEDICATION

I would like to dedicate this dissertation to my wife, Neide. Thank you for your continued support to complete this process.

ACKNOWLEDGEMENTS

TABLE OF CONTENTS

LIST OF FIGURES
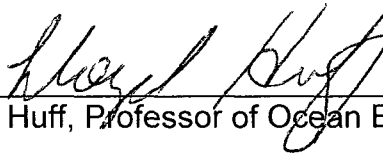
ABSTRACT

FIELD CALIBRATION METHODOLOGY FOR A MULTIBEAM ECHO SOUNDER

USING A SPLIT BEAM SONAR SYSTEM AND A STANDARD TARGET

BY

JOSE CARLOS LANZONI

University of New Hampshire, DECEMBER, 2011

The use of multibeam echo sounders (MBES) has grown more frequent in applications like seafloor imaging, fisheries, and habitat mapping. Calibration of acoustic backscatter – including measurements of beam pattern and fixed calibration offsets – is an important aspect of understanding and validating the performance of MBES. For echo sounders in general, different calibration methodologies have been developed in controlled environments such as a fresh water tank as well as in the field. While calibration in an indoor tank facility can bring excellent results in terms of accuracy, the amount of time required for a complete calibration can be prohibitively large. Field calibration can reveal the beam pattern for ship-mounted sonar systems, accounting for acoustic interferences which may be caused by objects around the installed transducers.

A method to determine the combined transmit/receive beam pattern for a ship-mounted multibeam system was developed and tested at distances of up to 8 m using a RESON 7125 MBES inside the fresh water calibration tank of the University of New Hampshire. The calibration method employed a tungsten

carbide sphere of 38.1 mm diameter as the target and a SIMRAD EK60 split-beam sonar system to provide athwartship and alongship angular information of the target sphere position.

The multibeam sonar system was configured for 256 beams in equi-angle mode with an operating frequency of 200 kHz; the split-beam system was set to work passively at the same frequency. A combined transmit/receive beam pattern was computed for athwartship angular ranges between $-6°$ and $+6°$ and alongship angular ranges between $-1°$ and $+3°$. The target sphere, with target strength of -39 dB at 200 kHz, was suspended in the water column by a monofilament line and manually moved along the range of athwartship and alongship angles. The limited angular range of the measurements is due to the -3 dB beamwidth of $7.0°$ in the alongship and athwartship direction of the split-beam sonar system coupled with the alongship offset of $1.6°$ between the maximum response axes (MRA) of the two systems. Possible acoustic interference caused by the monofilament line was found in the measurements for alongship angles smaller than $-1°$.

Beam pattern measurements for the combined transmit/receive beam pattern at a distance of 8 m show a -3 dB beamwidth of $1.1°$ in the athwartship direction and a -3 dB beamwidth of $2.0°$ in the alongship direction for the most inner beams. The dynamic range for the measurements was approximately -40 dB, limiting the ability to resolve side-lobes.

Tests of the accuracy of the target angle estimates from the split-beam system were also conducted. Errors for athwartship angles were smaller than

0.1° for the most inner angular positions (athwartship and alongship angles closer to the split-beam MRA), increasing to 0.3° for athwartship and alongship angles close to + 4° and –4°. Alongship errors were found to be smaller than 0.1° for the most inner positions increasing to around 0.5° for athwartship angles close to + 4°and –4° and alongship angles close to +4°. Alongship errors for alongship angles less than –1° were much larger (on the order of 5°), which compromised the beam pattern measurements for that angular region. Further tests suggested that interference from the monofilament line used to suspend the sphere may have compromised the angle estimates for alongship angles less than –1°. The acoustic interference from the monofilament line suggested by the tests may be due to the particular configuration of the transducers used here, where the MRAs of both sonar systems were pointed parallel to the water level (horizontally) and approximately perpendicular the monofilament line. Different results may be observed for ship-mounted transducers where the measurement geometry would be different than the one used in the tests described here.

.

CHAPTER 1

FIELD CALIBRATION OF MULTIBEAM ECHO SOUNDERS

1.1 – Introduction

Multibeam echo sounders (MBES) have gained importance in marine research for their high efficiency, using a fan of narrow acoustic beams which allows coverage of large areas. These systems are typically used to make measurements of target range and angle, and to infer target characteristics based on the intensity of the backscattered signals. The interpretation of these signals relies on proper calibration of the multibeam system.

Electro-acoustic transducers can be calibrated for transmit beam pattern for projectors, receive beam pattern for hydrophones, or combined transmit/receive beam pattern for a system using both types of transducers. The transmit radiation beam pattern of an acoustic system can be determined by measuring the magnitude of transmitted signals from the transducer at different angular positions in the along axis and in the axis that is orthogonal to the along axis of the transmit array and ranges using a reference hydrophone. The receive beam pattern can be determined by measuring the magnitude of received signals by the transducer using a reference projector to generate the transmitted signals

at different angular positions and ranges. It is also possible to determine the combined transmit/receive beam pattern using a standard target placed at different positions and measuring the signal return corresponding to that target. Differences in target range, if any, must be compensated for acoustic losses during the computation of the beam pattern. Since sonar systems are often designed to operate installed on vessels, this thesis will designate angles corresponding to the target position as athwartship and alongship angles.

Several methods for calibration have been developed, including calibration in an indoor tank facility using standard hydrophones and the standard-target method [1]. While a calibration in an indoor tank facility can bring excellent results in terms of accuracy, the amount of time required for a complete calibration can be prohibitively large. One example is the RESON 7125 MBES calibration performed in the indoor fresh water tank at Chase Ocean Engineering Laboratory at the University of New Hampshire [2], discussed in Chapter 2. Measurements for transmit and receive beam patterns were performed with resolution on the order of $0.1°$ for athwartship and alongship angles. To achieve the fine resolution of this calibration procedure, it required approximately 120 hours of data acquisition time. Also, this methodology does not account for possible acoustic interference caused by objects close to the transducer arrays when they are mounted on a vessel. Acoustic interference of this type was observed during this calibration procedure which caused small ripples in the transmit beam pattern. This interference may have been due to the presence of the projector not in use in the system (there are two projectors in this system:

one for the operation at a frequency of 200 kHz and another for operation at 400 kHz, mounted side by side in parallel). Field calibrations offer the best chance for accounting for this type of interference.

Many studies have been conducted on beam pattern calibration methodologies using standard spherical targets that can be used to perform calibration of ship-mounted transducers. A target sphere is usually suspended in the water column using monofilament lines chosen to be acoustically transparent at the operating frequency of the sonar under calibration. However, one of the difficulties when using this method for hydrographic MBES is determining the alongship angle of the target relative to the maximum response axis (MRA) of the receive array. Since most hydrographic MBES employ only a single line array, phase difference information from the receive array helps to determine only the athwartship angle of the target. Figure 1.1 below shows an example of a hydrophone array along with the alongship and athwartship angles.
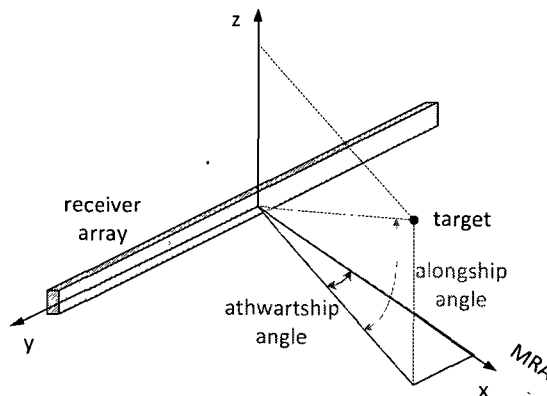
Figure 1.1 – Alongship and athwartship angles

A methodology for field calibration of MBES is proposed here with the use of a standard sphere and a split-beam echo sounder. The split-beam sonar

system is used to provide information about the target sphere location during the MBES calibration procedure. This methodology offers the advantage of significant decrease of the time necessary for the MBES calibration compared to the indoor tank facility procedure, while accounting for acoustic interference caused by objects surrounding the transducers.

1.2 – Target Position Estimation Using a Split-beam Sonar

The working principle of a split beam echo sounder and the feasibility of its use in the field to provide position information of a target sphere during a field calibration are explored here. Sections 1.2.1 and 1.2.2 are derived from Burdic [3] and address the fundamental concepts of a split-array correlator. The angular accuracy of the split-beam system can be investigated by determining the signal-to-noise ratio (SNR) necessary for the split-beam echo sounder to identify the location of a target sphere with a target strength TS.

1.2.1 – Estimation of Angular Position for a Split Array Correlator

Consider a line array of length $L/2$ with a pattern function $G(\psi)$ centered at origin, as shown by figure 1.2.a. Now consider two copies of this array: one is shifted by $+L/4$ and the other is shifted by $-L/4$, as shown by figure 1.2.b. The phase of a signal received by the shifted apertures is changed relative to the signal at the centered aperture by a value proportional to the shifted distance.

(a) line array centered at origin   (b) shifted line arrays
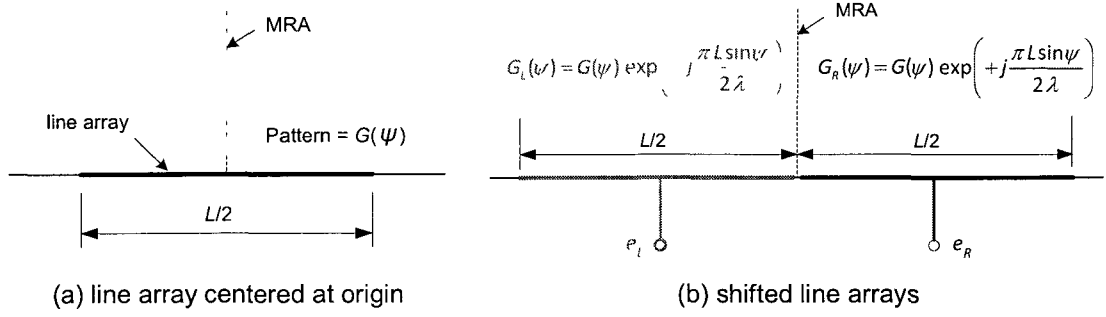
Figure 1.2 – Effect of translation on the pattern function (source: modified from [3])

The pattern functions for the left and right-shifted apertures, G_L and G_R, can be described by

$$G_L = G(\psi)\, exp\left(-j\,\frac{\pi L\, sin\psi}{2\,\lambda}\right)$$

(1.2.1)

and

$$G_R = G(\psi)\, exp\left(+j\,\frac{\pi L\, sin\psi}{2\,\lambda}\right),$$

(1.2.2)

where ψ is the spatial angle between the MRA and the target and λ is the signal wavelength.

The output signals for the right and left arrays, e_R and e_L, for a plane wave signal with single frequency f and amplitude a can be expressed by

$$e_L(t,\psi) = a\, G(\psi)\, exp\left(\omega t - j\,\frac{\pi L\, sin\psi}{2\,\lambda}\right)$$

(1.2.3)

and

$$e_R(t,\psi) = a\, G(\psi)\, exp\left(\omega t + j\,\frac{\pi L\, sin\psi}{2\,\lambda}\right),$$

(1.2.4)

where ω is the angular frequency and t is time ($\omega = f / t$).

These two signals are identical except for an electrical phase difference ϕ due to the half-array separation and the spatial angle ψ. The electrical phase difference is given by

$$\phi = \frac{\pi L}{\lambda} \sin\psi .$$

(1.2.5)

For small ψ, the expression for ϕ becomes

$$\phi \cong \frac{\pi L}{\lambda} \psi .$$

(1.2.6)

This electrical phase difference can be used to measure the target direction relative to the MRA.

1.2.2 – Estimation of Target Bearing Using Split-beam Sonar

Consider the diagram depicted by figure 1.3.a below. This figure shows a split-beam mounted on a vessel used to identify the location of a target sphere. This configuration is represented in figure 1.3.b for the one-dimensional problem of finding the target bearing angle θ, which will be analyzed.

(a) system with target sphere on the vessel   (b) one-dimensional target bearing problem
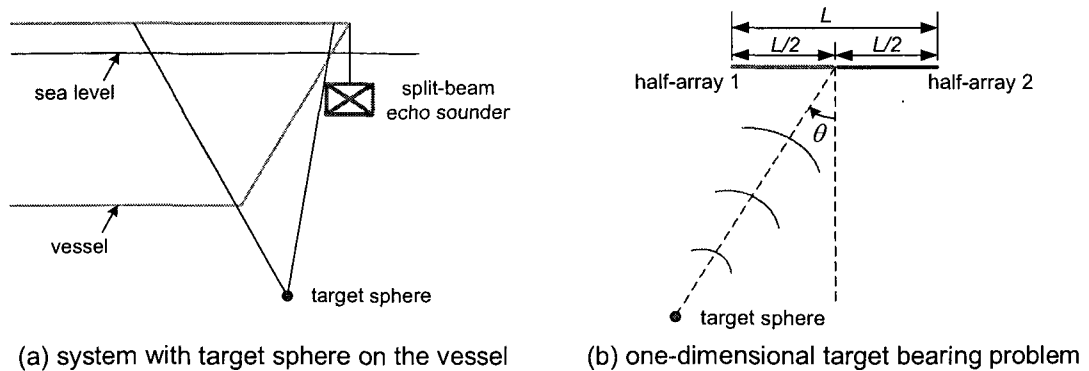
Figure 1.3 – Split-beam echo sounder using standard target sphere setup

According to [3], the variance of the estimated angular position θ, σ_θ^2, for a split-aperture correlator is given by

$$\sigma_\theta^2 = \frac{N_o}{2E} \frac{2\lambda^3}{\pi^2 L^3} ,$$ (1.2.7)

where

λ: wavelength of the signal,

E: energy in the real signal waveform, and

$N_o/2$:   spectral density amplitude of real noise.

Using the following relationship of signal-to-noise ratio SNR_o for a line array (from [3]),

$$SNR_o = \frac{2E}{N_o} \frac{2L}{\lambda} ,$$ (1.2.8)

in 1.2.7, the expression for the variance σ_θ^2 becomes

$$\sigma_o^2 = \left(\frac{N_o}{2E}\right)\left(\frac{\lambda}{2L}\right)(2)\frac{2\lambda^2}{\pi^2 L^2} = \frac{4\lambda^2}{SNR_o \, \pi^2 L^2} .$$ (1.2.9)

The signal-to-noise ratio required to meet a specific value of angular position variance, σ_θ^2, can be determined using (1.2.9) for a given signal wavelength λ and aperture length L. Table 1.1 shows values for $L = \lambda/2$, $L = 2\lambda$, and $L = 10\lambda$ for an angular standard deviation (σ_θ) of 0.1°.

Table 1.1 – Signal-to-noise ratio for some values of wavelength and aperture length

	$L = \lambda/2$	$L = 2\lambda$	$L = 10\lambda$
SNR_o (dB)	57	45	31

Table 1.1 shows that it is to have necessary a signal-to-noise ratio of 57 dB using an aperture length of $\lambda/2$ to achieve a standard deviation of $0.1°$.

1.2.3 – SNR Estimation at the Split-beam Transducers Using a MBES as Transmitter and a Target Sphere

Now consider that a multibeam echo sounder (MBES) is mounted close to a split-beam echo sounder (SBES) and a target sphere is at a distance *r* from both sonar systems, as depicted by figure 1.4. With this setup, the MBES transmits a signal; the transmitted signal is reflected by the target sphere and reaches the SBES.
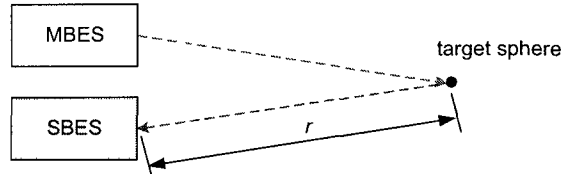
Figure 1.4 – Split-beam using standard target sphere setup

The echo level EL at the split-beam transducers, in decibel (dB), is given by (not accounting for the directivity of the transducers)

$$EL = SL - 2TL + SL,\qquad(1.2.10)$$

where

SL: source level in dB,

TL: one-way transmission loss in dB, and

TS: target strength in dB.

The transmission loss TL is given by

$$TL = 20\log_{10}(r) + \alpha r, \qquad \cdot \qquad (1.2.11)$$

where α is the absorption coefficient in dB/m. For a distance between the transducers and the target sphere of 10 m (r = 10) used during the calibration measurements, the absorption loss term (αr) becomes very small compared with the spreading loss term (20 $\log_{10}(r)$). Therefore, the two-way transmission loss for this range is approximately 40 dB.

For a source level of 220 dB (provided by the MBES) and using a sphere with a target strength value of –45 dB, the echo level at the SBES transducers will be of 135 dB.

Assuming that the conditions are ambient noise limited, rather than self-noise limited, the noise level (NL) is given by

$$NL = ambient\ noise + 10\log_{10}(bw), \qquad (1.2.12)$$

where bw is the bandwidth of the system. With the frequency of operation of 200 kHz, the value of the ambient noise may be considered around 40 dB (from Wenz curves). When using a bandwidth bw of 10 kHz, the total noise level NL will be of 80 dB.

The signal-to-noise ratio SNR is given by

$$SNR = EL - NL. \qquad (1.2.13)$$

Considering the echo level of 135 dB and a noise level of 80 dB, the signal-to-noise ratio (SNR) will be 55 dB. This SNR value would be sufficient to achieve a standard deviation of 0.13° for an aperture length L of $\lambda/2$ using the split-array correlator. If a sphere with target strength of –30 dB is used, then the

SNR value can be raised to 70 dB, which would be sufficient to determine the target sphere position using the split-beam system for an aperture length L of $\lambda/2$ achieving a standard deviation σ_θ of $0.02°$. Table 1.2 shows standard deviation values for different values of aperture length and signal-to-noise ratio.

Table 1.2 – Standard deviation of angular position (σ_θ) for different values of aperture length L and SNR

	$L = \lambda/2$	$L = \lambda$	$L = 2\lambda$	$L = 3\lambda$	$L = 9\lambda$	$L = 13\lambda$	$L = 27\lambda$
SNR = 35 dB	1.30°	0.65°	0.32°	0.22°	0.07°	0.05°	0.024°
SNR = 55 dB	0.13°	0.06°	0.03°	0.02°	0.01°	0.005°	0.002°
SNR = 70 dB	0.02°	0.01°	0.006°	0.004°	0.001°	< 0.001°	< 0.001°

An acceptable for the standard deviation of the estimated angular position (σ_θ) can be achieved by using the split-beam system SIMRAD EK60 operating at a frequency of 200 kHz and with an aperture value close to 9 λ for SNR values of 35 dB and above.

1.3 – Proposed Methodology for Field Calibration of MBES

A field calibration methodology for MBES was developed employing a SIMRAD EK60 split-beam echo sounder with a 200 kHz split-beam transducer ES200-7CD and a target sphere. This methodology was tested on a RESON Seabat 7125 MBES, with operational frequency of 200 kHz for both systems, in

the acoustic tank of the University of New Hampshire. The tank has dimensions of 18 m long, 12 m wide, and 6 m deep. The transducers of both systems were installed in the same mounting, with enough separation between them to minimize and/or avoid acoustic interference from one another.

To perform the calibration, the MBES operates actively, transmitting 200 kHz signals and receiving echoed returns from the target sphere. The target sphere is manually moved at an approximately constant range from the transducers, sweeping an area defined by the athwartship and alongship angular range of interest for the beam pattern of the MBES. The split-beam system operates passively, listening to the echo return signals from the target sphere. The task of the split-beam system is to determine the target sphere position during the calibration procedure using the split-phase difference data. The two systems are synchronized in time, employing an NTP (Network Time Protocol) time server protocol, so that their data sets can be cross-referenced.

As indicated in Section 1.2, better target angle estimation is found by working with higher SNR values. Therefore, a target with large target strength should be chosen for the methodology. The target chosen for the tests described herein was a tungsten carbide sphere of 38.1 mm diameter (WC38.1), that has average target strength of −39 dB at a frequency of 200 kHz. The target sphere is suspended in the water column by a monofilament fishing line. This monofilament line is considered to have very small acoustic target strength.

In the interest of working with high SNR values, the operator may choose to set maximum values for the MBES transmitted power. However, it is desirable

to avoid/minimize the nonlinearities that have been identified with the electric circuitry of the system. The proposed methodology employs measurements to determine proper settings for transmitted power and receive gain of the MBES under test to be operated in a linear range, as discussed by Greenaway and Weber [4].

Tests to determine angular accuracy of the target sphere position provided by the split-beam were conducted using the same configuration employed in the field MBES calibration tests described in Chapter 4. The position information corresponding to the target sphere, provided by the split-beam echo sounder, is given in values relative to the split-beam system coordinates. This information needs to be converted into values relative to the MBES coordinates, requiring the development of a coordinate transformation method. Although the tests to validate the proposed methodology were performed with the target sphere in the near field of the MBES, it nonetheless provides a proof-of-concept and brings some level of confidence that this methodology can be applied to ship-mounted MBES in the operating field.

1.4 – Thesis Organization

This thesis presents a methodology to perform a field calibration of a multibeam echo sounder, discussing both theoretical and practical aspects of the methodology. Chapter 2 discusses the indoor calibration procedure of a RESON 7125 MBES conducted in the acoustic tank of the University of New Hampshire

[2]. This procedure generates three-dimensional transmit and receive beam patterns with high resolution and high accuracy, albeit at the expense of a large amount of time employed in the measurements. The results of this procedure also demonstrate the importance of calibrating ship-mounted systems in the field, showing acoustic interference which is believed to be related to the mount of the transducers.

The estimation of the angular accuracy of the split-beam system is explored and presented in Chapter 3. This chapter discusses the setup in the acoustic tank, where an angular grid of known positions was designed to accurately and precisely place the target sphere. It provides details on the coordinate conversion for this particular configuration and the pulse length tests employed to determine an optimal pulse length value for the calibration measurements. The influence of the monofilament line used to suspend the target sphere on the measurements was also investigated in this chapter.

Chapter 4 presents the proposed methodology for field calibration of MBES, with details on the setup in the acoustic tank, the mount of the transducers, the analysis of multipath acoustic interference in the tank, the coordinate system transformation, and the time synchronization procedure used to match the records from both sonar systems. This chapter also describes the data processing steps used to compute the beam pattern of the MBES, as well as the results of the proposed field calibration methodology. Problems encountered during the procedure are also analyzed and alternatives to minimize

them are discussed. Chapter 5 discusses the results of the presented methodology, its accuracy, limitations, benefits, and future research.

Appendix A describes the procedure used to determine optimal operational settings for transmitted power and gain of the MBES, allowing the MBES to operate with high power values, helping to increase the signal-to-noise ratio (SNR) of the return signals from the target sphere. Appendix B contains the MATLAB code used in the computation of the beam pattern using the recorded data from both sonar systems during the calibration measurements and the MATLAB code employed in the angular accuracy tests discussed in Chapter 3.

CHAPTER 2

CONVENTIONAL RELATIVE CALIBRATION OF A MULTIBEAM ECHO SOUNDER IN AN ACOUSTIC TANK

2.1 – Introduction

Acoustic radiation beam pattern calibration in a controlled environment can provide excellent results in terms of accuracy and resolution and is essential to achieving improved performance of multibeam echo sounders (MBES) [5]. A high-resolution calibration procedure to determine the three dimensional transmit and receive beam patterns of a RESON SeaBat 7125 MBES was developed using the acoustic tank of Chase Ocean Engineering Laboratory at the University of New Hampshire and documented by Lanzoni & Weber [2]. A similar procedure is described here to illustrate the importance of this type of calibration, along with its limitations, leading to the motivation for developing a calibration procedure which could be applied in ship-mounted systems.

2.2 – The Acoustic Tank

The dimensions of the acoustic tank at the University of New Hampshire Ocean Engineering Laboratory used to perform the measurements are 18 m long, 12 m wide and 6 m deep. The tank has a main bridge (powered) and a secondary bridge (non-powered) on a rail system with variable positioning along the 18 m length of the tank. On the top of the main bridge there is a cart (also powered) which can move along the 12 m width of the tank. A Yuasa rotator (with a programmable controller) is installed on the main bridge cart and can control the angular position of a carbon fiber pole attached to it. Designed to hold mounted transducers, this pole can slide into the rotator chucks and allows variable vertical positioning of transducers inside the tank. The secondary bridge is used for mounting reference transducers. Figure 2.1 depicts the acoustic tank used in the calibration procedure.
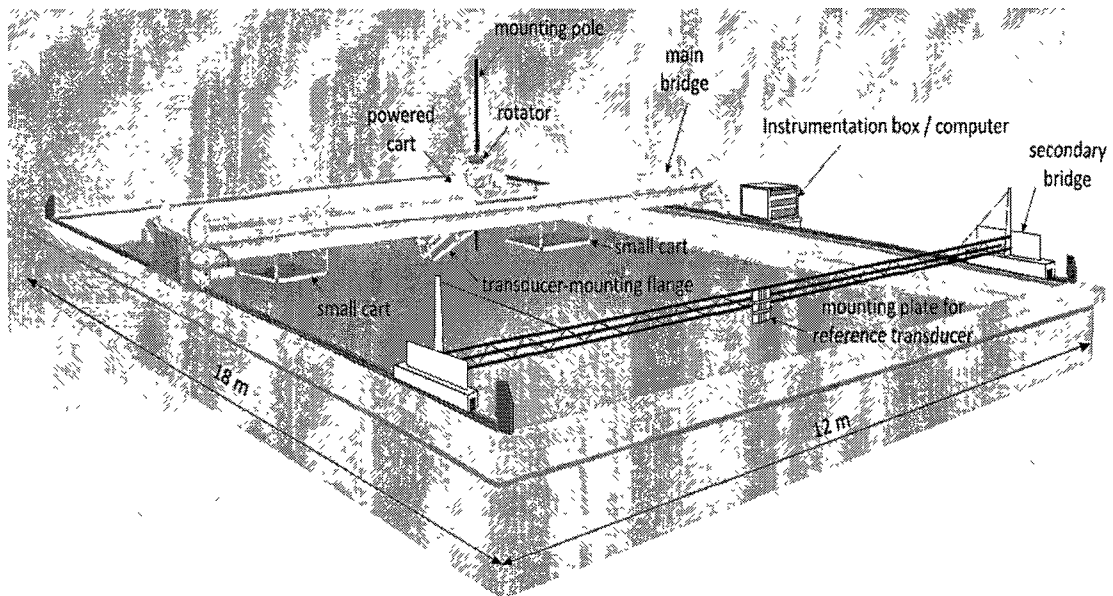
Figure 2.1 – Acoustic tank at Chase Ocean Engineering Laboratory

2.3 – Beam Pattern Measurement Setup in the Acoustic Tank

A SeaBat 7125 mounting bracket supplied by RESON was used to mount the transducers to be calibrated and then fixed to a mounting support. This support was attached to the rotating pole, as illustrated by Figure 2.2. As seen from this figure, the MBES has two projector arrays and one hydrophone array. One projector array is designed to operate at the frequency of 400 kHz, while the other is designed to operate at the frequency of 200 kHz. The center of gravity of the submerged mounted MBES transducers was determined and was aligned with the rotating pole center. This alignment procedure was performed to avoid bending the pole with the weight of the mounting, minimizing errors on the angular position during the measurements.
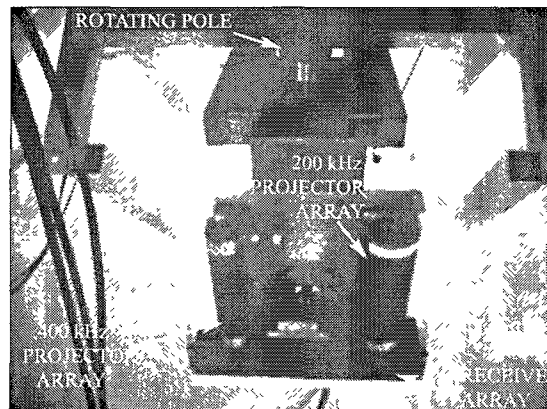
Figure 2.2 – Mounting bracket with the 7125 transducers attached to the rotating pole

The multibeam sonar system was configured for 256 beams operating in equi-angle mode and at a frequency of 396 kHz. An omni-directional RESON TC4034 hydrophone/projector was used as a reference transducer in the

measurements. The setup in the acoustic tank is depicted by Figure 2.3. As defined in this figure, the athwartship direction of the MBES is on the y-axis, while its alongship direction is on the z-axis. The athwartship angular position is determined by the Yuasa rotator, while the alongship angular position is determined by the depth of the TC4034 transducer. The 7125 transducers and the TC4034 hydrophone/projector were positioned inside the tank in such a way to avoid multi-path signals in the measurements from the tank walls, as well as from the tank bottom and the water surface.

The distance between the 7125 projector and the reference transducer was fixed at 13 meters. The TC4034 transducer was positioned at a distance of 3 meters from the tank wall behind it, while the 7125 transducers were at a distance of 2 meters from the wall behind them. Using this configuration, the first reflected signals to arrive at the reference transducer are from the bottom of the tank and from the water surface. They arrive approximately 880 μs after the direct path signal arrival at the reference transducer, providing the sufficient time separation in order to uniquely identify the direct path arrival.

secondary bridge

main bridge

tank walls

6 m

3 m

13 m

2 m

rotation

hydrophone
TC4034

7125
projector/hydrophone
arrays

6 m

x — z

y

tank walls

(a) – top view

tank wall

height adjustable pole

water level

rotating pole

tank wall

3 m

13 m

2 m

z

3 m

z = 0

hydrophone
TC4034

3 m

7125
projector/hydrophone
arrays

z

x — y
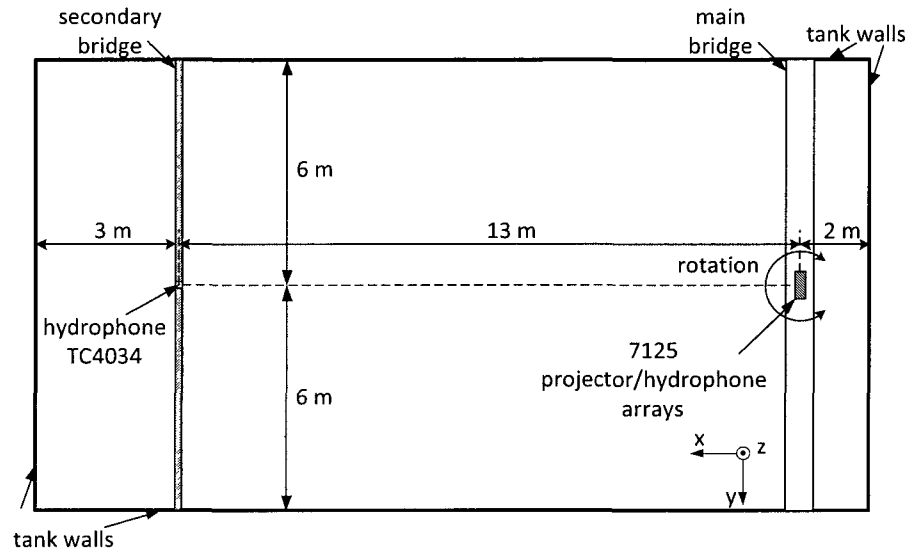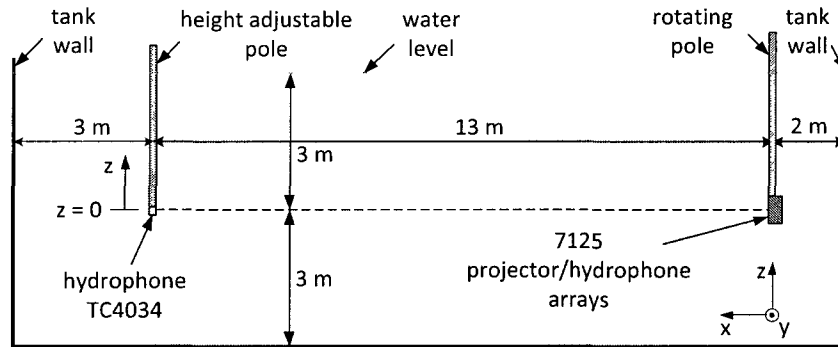
(b) – side view

Figure 2.3 – Beam pattern measurements setup

2.4 – Transmit Beam Pattern Measurements

The transmit beam pattern measurement procedure was performed using

a program code written in LabVIEW running on a personal computer with an NI

PCI-6110 data acquisition board. This code was used for acquiring the received

signal from the TC4034 transducer while automatically changing the athwartship

angular position of the 7125 transducers after the desired number of pings for each position. The current date and time from a GPS device were acquired for each athwartship angular position during the signal acquisition by the LabVIEW code, along with the raw waveforms and processed rms values of the received signal. Recording time data from the GPS device allowed synchronization between data recorded by the MBES computer and by the LabVIEW code. Figure 2.4 shows the block diagram for the transmit beam pattern measurements.

A function generator, triggered by the MBES trigger signal, was used to generate a copy of the signal transmitted by the 7125 projector. This copy of the signal was used by the LabVIEW code to trigger the data acquisition process and to calculate the rms values of the acquired waveforms. A pre- amplifier was used to filter and amplify the signal from the TC4034 transducer to a reasonable level.
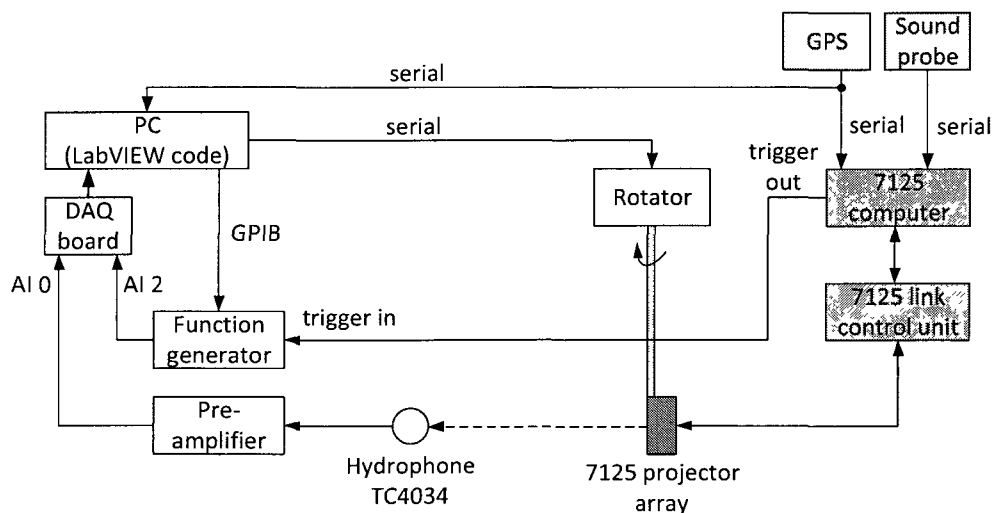
Figure 2.4 – Transmit beam pattern set up: block diagram

After positioning the transducers in the tank, it was necessary to perform

athwartship and alongship alignments to find the maximum response axis (MRA)

of the 7125 transducers. The athwartship alignment was performed by setting

the MBES to transmit and observing the pressure amplitude on the MBES screen

for the two most inner beams (beams 128 and 129). The LabVIEW code was

used to rotate the 7125 transducers while observing the pressure amplitude of

beams 128 and 129 corresponding to the position of the TC4034 transducer.

The MBES was rotated until the pressure amplitudes for beans 128 and 129

(corresponding to the position of the TC4034) reached the same values (on the

screen of the MBES display). At this point, the athwartship angular position was

set to zero degrees by resetting the rotator controller. Figure 2.5 illustrates this

setup.
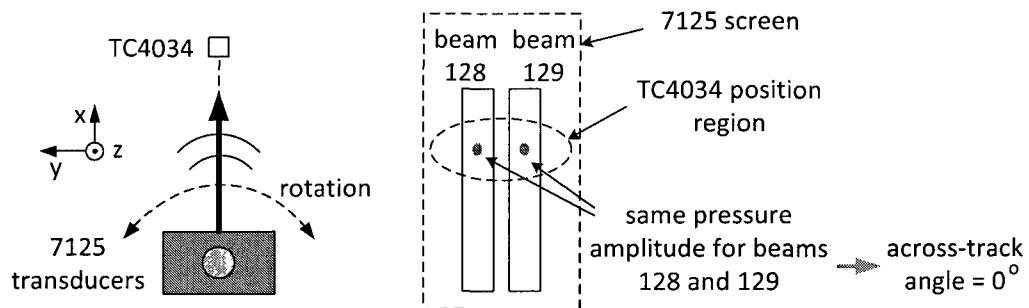
Figure 2.5 – Athwartship alignment

The alongship alignment was done by setting the MBES to transmit and

observing the amplitude value of the received signal from the TC4034 transducer

with an oscilloscope as the pole height (where the TC4034 transducer is

attached to) varied. When the signal amplitude was at a maximum level, the

position was set at zero meters on the z-axis, corresponding to the alongship

.

angle of zero degree (central acoustic axis). After the athwartship alignment procedure, the alongship alignment was performed again to verify the position of maximum response after changing the athwartship angular position of the 7125 transducers. Fig. 2.6 depicts the alongship alignment procedure. According to the geometry from Fig. 2.7, the alongship angles were calculated using the vertical displacement of the TC4034 transducer (Δz) and the horizontal distance between the 7125 transducers and the TC4034 (13 m). The values for the alongship angles are given by

$$alongship\ angle = tan^{-1}\left(\frac{\Delta z\ (in\ meters)}{13\ meters} \right).$$
(2.4.1)
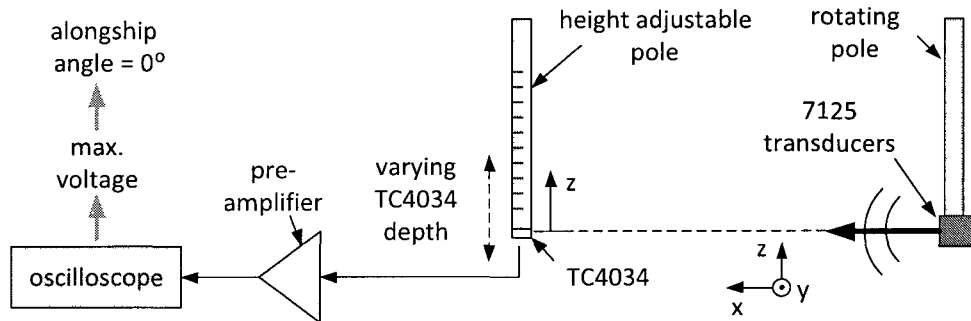
Figure 2.6 – Alongship alignment
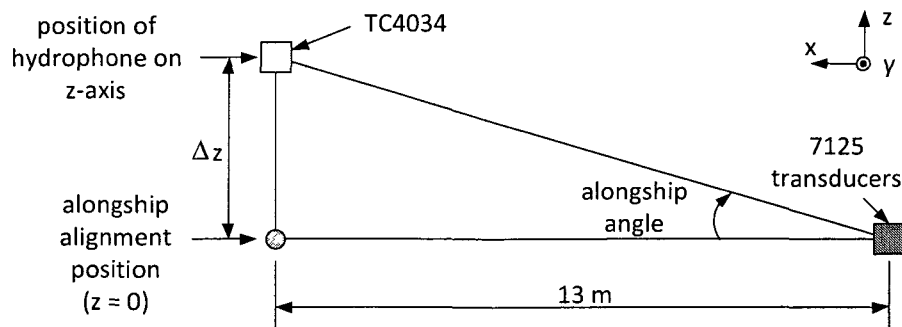
Figure 2.7 – Alongship angle calculation

Transmit beam pattern measurements were taken for reference

transducer positions (Δz) between +/–0.58 meters in 0.02 meters increments,

corresponding to alongship angles ranging between +/–2.55° in 0.09° increments

in a total of 59 measurements. Each of these measurements was taken for

athwartship angles ranging between +/–90° in 0.1° increments, with 20 pings per

athwartship angular position at a rate of 4 pings per second, using a 396 kHz

transmitted signal with a pulse length of 300 µs. The time spent for each

complete beam pattern measurement was about 50 minutes. With these

measurements, it was possible to obtain a three-dimensional plot of the transmit

beam pattern for those angular ranges. Table 2.1 shows the sonar settings used

for the measurements.

Table 2.1 – 7125 settings for transmit beam pattern measurements

Power (dB)	Pulse Length (µs)	Rate (pings/s)	Gain (dB)	Range (m)
200	300	4	20	30

2.5 – Receive Beam Pattern Measurements

The receive beam pattern measurements were performed using a similar

LabVIEW program code as the one used in the transmit beam pattern

measurements. This code was used for controlling the generation of the

transmitted signal sent to the TC4034 transducer while changing automatically

the athwartship angular position of the 7125 transducers after the desired

number of pings per angle. The current date and time was also recorded from the GPS device. Since the athwartship angular position was only recorded in the computer running the LabVIEW code, the time data were used to reference the recorded data from the MBES to the athwartship angle data recorded by the LabVIEW code. Figure 2.8 shows the block diagram for the receive beam pattern measurements.
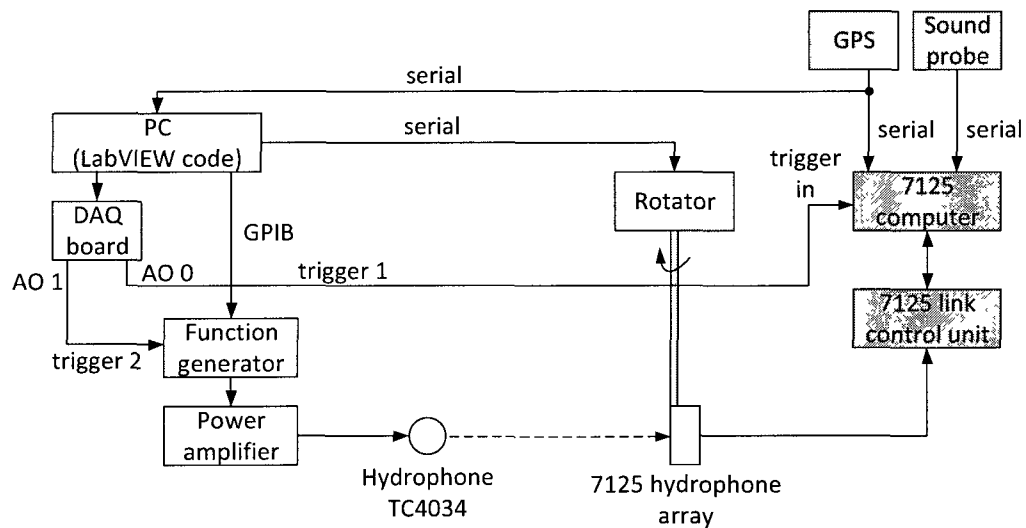
Figure 2.8 – Receive beam pattern set up: block diagram

The function generator was used to produce the 396 kHz sinusoidal pulses. This signal was applied to a power amplifier and sent to the TC4034 transducer, which worked as a projector to send the signal to the 7125 receive array. In preliminary tests, one trigger signal generated by the LabVIEW code (using a data acquisition board analog output channel) was used to trigger the function generator and the MBES computer at the same time. It was observed that the MBES was triggering with a delay of approximately 3 ms after the function generator was triggered. Therefore, it was necessary to generate two

separated trigger signals: one to trigger the MBES computer, and another one to trigger the function generator after that delay. The generation of these trigger signals was implemented in the LabVIEW code using two analog outputs from the data acquisition board. The code allowed adjustment for the values of ping rate, number of pings per athwartship angular position, time delay between the two trigger signals, and time between changes in athwartship angular positions.

Receive beam pattern measurements were first performed for athwartship angles between +/−120° in 0.1° increments for the alongship angle of 0°. The pulse length of the transmitted signal was set to 300 μs at a rate of 4 pings per second. These settings allowed one set of beam pattern measurements per alongship angular position for the specified athwartship angular range in 4.5 hours. Table 2.2 shows the sonar settings used for these measurements. The alongship and athwartship alignments for these measurements were performed using the same methodology described in the transmit beam pattern measurement procedure.

Table 2.2 – 7125 settings for receive beam pattern measurements

Power (dB)	Pulse Length (μs)	Rate (pings/s)	Gain (dB)	Range (m)
0	300	4	20	25

Measurements for the athwartship angular range between +/−90° in 0.1° increments and alongship angular positions in the range of +/−1.23° in 0.18° increments were also performed, generating a three dimensional receive beam pattern for each of the 256 beams. The beam patterns were measured using the

same settings for the signal transmitted to TC4034 transducer as used in the previously described measurements, providing the same sound pressure level of 154 dB at the 7125 hydrophone array. However, the MBES gain setting was adjusted to 50 dB (instead of the value of 20 dB used in the first receive beam pattern measurement), in an effort to increase the dynamic range. The amplitude of the receive beam pattern for the alongship angle of 0° was then amplified to align its main lobe amplitude with the main lobe amplitudes of the beam patterns for the adjacent alongship angles (+0.18° and −0.18°).

2.6 – Results

2.6.1 – Transmit Beam Pattern Results

Figure 2.9 shows the three dimensional transmit beam pattern plot from the measurements performed for the 400 kHz projector array of the Reson 7125 MBES. The top view of the three dimensional plot is depicted by Figure 2.10. It can be observed from Figure 2.10 that the 7125 transmit beam pattern looks curved. Ripples in the beam pattern can also be seen in an athwartship angular region between +30° and +75°. The two dimensional plot of the transmit beam pattern for the 0° alongship angle and athwartship angular range between +/–90° is shown in more detail in Figure 2.11.

The two dimensional plot of Figure 2.11 shows that the beam pattern amplitude is above the −3 dB line for athwartship angles between approximately +/–75°. Ripples can be observed in the beam pattern for the athwartship angular

region between +30° and +75°, where the amplitude gradually decreases. This leads to the hypothesis that the 200 kHz projector installed parallel to the side of the 400 kHz projector could be interfering with the transmitted signal. To investigate this phenomenon, the transmit beam pattern for the 200 kHz projector was measured for a 0° alongship angle using the same setup for the 400 kHz projector. Figure 2.12 shows the results for the 200 kHz transducer transmit beam pattern.
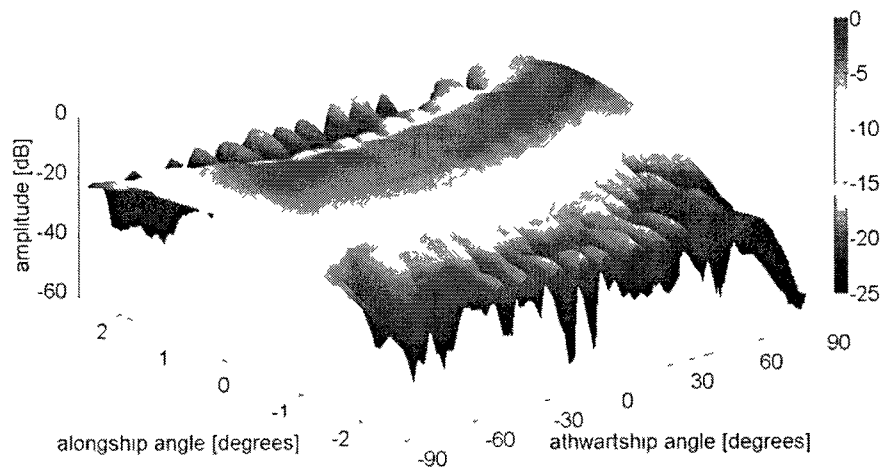
Figure 2.9 – 3-D plot of RESON 7125 transmit beam pattern
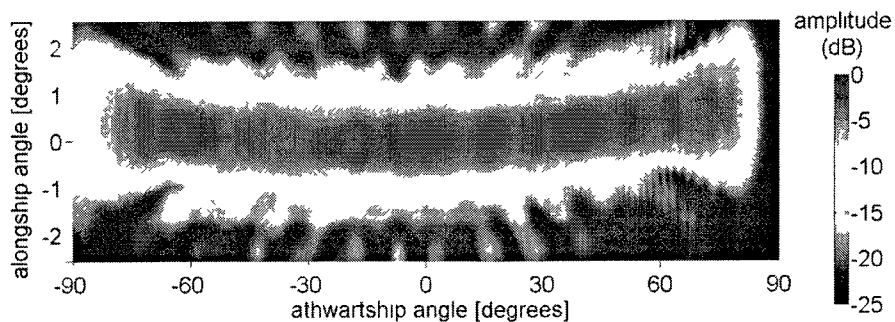
Figure 2.10 – Top view of 3-D plot of RESON 7125 transmit beam pattern
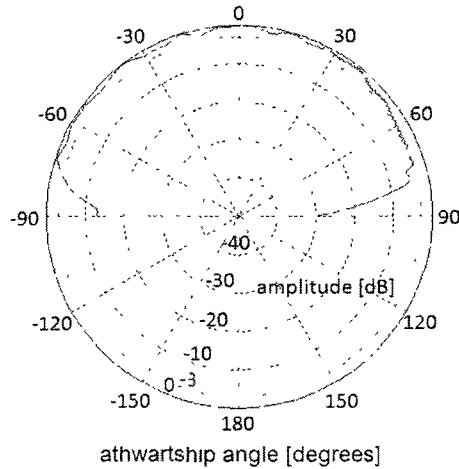
Figure 2.11 – 2-D plot of RESON 7125 transmit beam pattern (400 kHz projector) – alongship angle: 0°

The plot of figure 2.12 shows that the transmit beam pattern for the 200 kHz is very similar to the beam pattern obtained for the 400 kHz, except that the ripples appear in the region between –30° and –75°, approximately. This result supports the hypothesis that the unused projector interferes with the transmit beam pattern of the one in use.

Figure 2.13 depicts the plots of the along-track transmit beam pattern for across-track angular positions of –60°, 0°, and +60°.
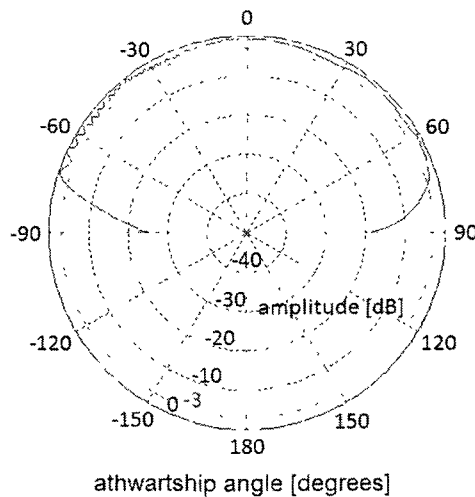
Figure 2.12 – 2-D plot of RESON 7125 transmit beam pattern (200 kHz projector) – alongship angle: 0°
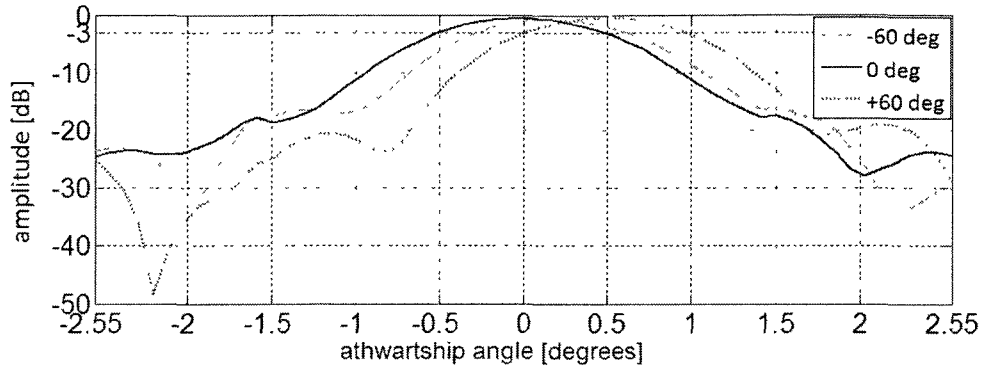
Figure 2.13 – 7125 alongship transmit beam pattern – athwartship angles: 60°, 0°, and –60°

According to figure 2.13, the transmit beam pattern for the range of 13 m and athwartship angle of 0° has a –3 dB beamwidth of 0.99° and side lobes below –17 dB. The main lobe of the transmit beam pattern for the athwartship angle of +60° is centered at approximately 0.5°, while for the –60° athwartship angle it is centered at approximately 0.1°. The –3 dB beamwidth is 0.89° for the athwartship angle of –60°, while for the +60° athwartship angle it is 0.98°, approximately. The manufacturer specification datasheet reports a value of 1° for the –3dB beamwidth in the alongship direction.

2.6.2 – Receive Beam Pattern Results

The three dimensional receive beam pattern was computed using all the measurements for the athwartship angular range between ±90° and alongship angular range between +/–2.55°. Figure 2.14 shows the receive beam pattern for beam 128. The plot of this figure was obtained by aligning the main lobe of the beam pattern for the alongship angular position of 0° with the adjacent beam pattern main lobes, since it was used a lower gain setting for the first set of measurements.
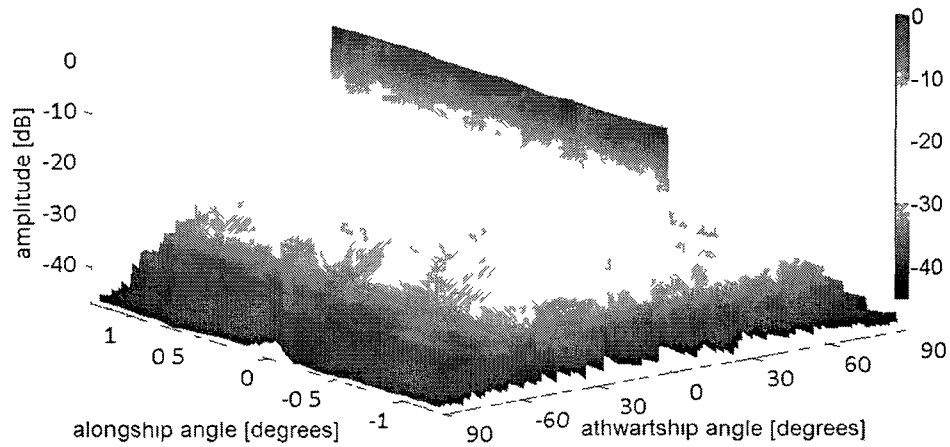
Figure 2 14 – 3-D plot of 7125 receive beam pattern for beam 128

After aligning the main lobe maximum levels, as shown by the 3-D plot of

the receive beam pattern from figure 2.14, it is possible to see the potential

saturation effects (low side lobe amplitudes at alongship angle of 0°).

The athwartship receive beam pattern for the alongship angular position of

0° for beam numbers 128, 129, 1, and 256 (the two most inner and the two most

outer beams) are depicted by figures 2.15, 2.16, 2 17, and 2.18.
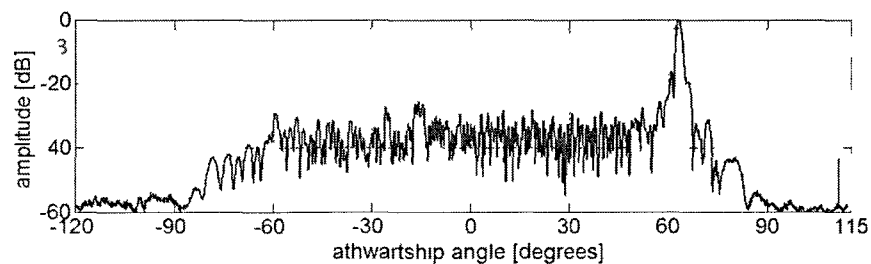
Figure 2 15 – Receive beam pattern for alongship angle of 0° for beam 1
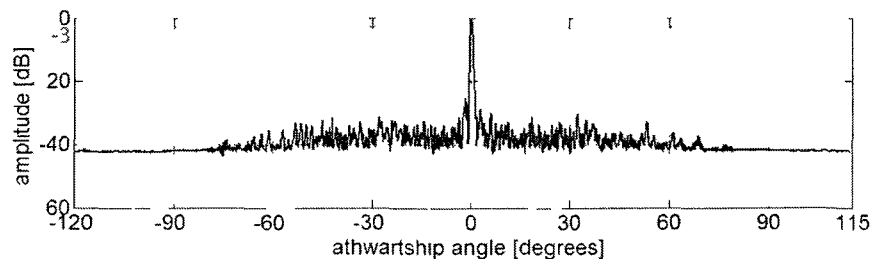
Figure 2 16 – Receive beam pattern for alongship angle of 0° for beam 128
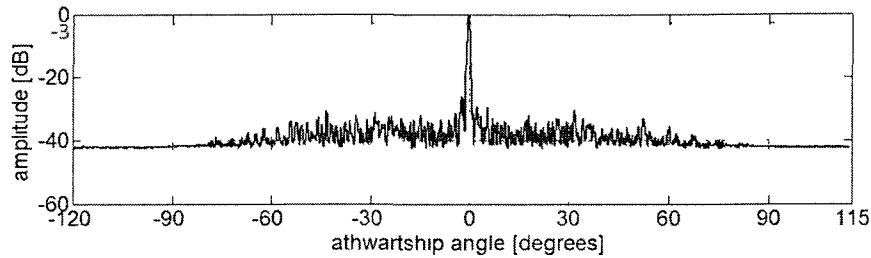
Figure 2.17 – Receive beam pattern for alongship angle of 0° for beam 129
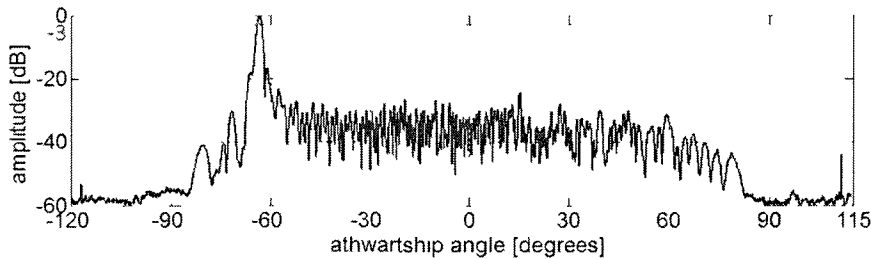
Figure 2.18 – Receive beam pattern for alongship angle of 0° for beam 256

Table 2.3 shows the beamwidth for beams 128, 129, 1, and 256, determined from the plots of figures 2.15 to 2.18. The manufacturer specification datasheet reports a value of 0.5° for the –3dB beamwidth in the athwartship direction.

Table 2.3 – Reson 7125 Receive Beam Pattern: –3 dB Beamwidth

	Beam 128	Beam 129	Beam 1	Beam 256
Beamwidth	0.614°	0.617°	1.395°	1.392°

2.7 – Conclusion

A calibration procedure for the Reson 7125 MBES was performed for the operating frequency of 396 kHz and 256 beams/equi-angle mode at an acoustic

distance of 13 m using the fresh water acoustic tank at the University of New Hampshire. These measurements allowed the computation of a three dimensional plot of the transmit beam pattern for athwartship angular range between +/-90° in 0.1° increments and alongship angular range between +/-2.55° in 0.09° increments. The -3 dB beamwidth of the transmit beam pattern for athwartship angle of 0° was observed to be approximately 0.99°, with side lobes below -17 dB (the manufacturer specification value for this -3 dB beamwidth is 1°). The transmit beam pattern plot appears to be curved. This curvature in the beam pattern would have gone un-noticed during a two dimensional beam pattern measurement.

Interferences from the transducer not in use (200 kHz projector) were observed in the transmit beam pattern of the 400 kHz projector array. Ripples and attenuation were observed in the transmit beam pattern measurements at the athwartship angular region between +30° and +75° with gradual decrease in amplitude of about 3 dB. This suggests that the two projectors should be mounted farther apart to avoid undesirable interferences.

The receive beam pattern was measured for athwartship angular range between +/-120° in 0.1° increments and alongship angular position of 0°. From these measurements, the beam pattern revealed that the -3 dB beamwidth for the most inner beams (beams 128 and 129) was approximately 0.62°, with side-lobes below -26 dB. For the most outer beams (beams 0 and 256), the beamwidth was approximately 1.40°, with side-lobes below -17 dB. The manufacturer specification value for the -3 dB beamwidth in the athwartship

direction is 0.5°. The near-field/far-field transition region of the tested multibeam system is in the range of 10 m. Performed at a range of 13 m, the beam pattern measurements are not quite in the far-field but the results meet the expectations for the beamwidths in the far-field to a good degree.

Measurements to compute a three dimensional plot of the 7125 receive beam pattern were also performed. While measurements for alongship angle of 0° were taken using a sonar gain setting of 20 dB, measurements for the alongship ranges from −1.23° to −0.18° and from +0.18° to +1.23° in 0.18° increments were performed with a sonar gain setting of 50 dB in an attempt to increase the dynamic range. However, after aligning the main lobe maximum levels for all the measurements, the three dimensional receive beam pattern shows lower side lobe amplitudes at alongship angle of 0° compared to other alongship angular values. This is an evidence of possible saturation effects, which limited the receive beam pattern main lobe amplitude for the measurements taken with higher sonar gain setting. This effect, which would not have been observed without the three-dimensional measurements, would have caused large artifacts in the beam pattern measurements.

A single transmit beam pattern measurement set (one set for each alongship angular position) required an acquisition time of 50 minutes. Fifty nine sets of measurements were performed to compute the three dimensional plot of the transmit beam pattern for the described angular ranges, which is the equivalent of 50 hours of data acquisition time. For the receive beam pattern measurements, a single set of measurements required approximately 4.5 hours.

Fifteen sets of measurements were taken to compute a three dimensional plot of the receive beam pattern for the described angular ranges, corresponding to approximately 68 hours of data acquisition time. Considering the set up time, the total time spent to perform the all the measurements for transmit and receive beam patterns for the described angular ranges required three weeks.

CHAPTER 3

SPLIT-BEAM ECHO SOUNDER ACCURACY

3.1 – Introduction

Given that 3 weeks is often not allowable to calibrate a MBES, here an approach is proposed for calibration in the field using a split-beam echo sounder. The role of the split-beam system in this methodology is to provide the position of the target necessary to compute the beam pattern of the MBES. Consequently, the accuracy of this methodology strongly depends on the performance of this auxiliary sonar system in providing accurate values for the measured angles corresponding to the target position. Tests to evaluate the performance of the SIMRAD EK60 split-beam sonar system used in the proposed calibration methodology were conducted in the acoustic tank of the University of New Hampshire. The transducers of both systems (RESON Seabat 7125 and SIMRAD EK60 ES200-7CD) were employed with the same configuration as described in Chapter 4, while the target sphere was placed on a grid of pre-defined angular positions. These tests were performed employing an operating frequency of 200 kHz for two cases: i) using the MBES active and split-beam system passive and ii) using the split-beam system active and the MBES sections.

3.2 – Split-beam Accuracy Measurements Setup/Procedure

An angular grid with values from –6° to +6° in 0.5° increments for alongship and athwartship angles was established to position the target sphere in the acoustic tank at a distance of approximately 8 m from the transducers. Figure 3.1 shows the angular grid and the –3 dB beamwidth of the split-beam sonar system.

The vertical position of the target sphere determined the alongship angle, while its horizontal position determined the athwartship angle. The sphere was held by a monofilament line attached to a sliding pole, as shown by Figure 3.2. The sliding pole was held by a small cart fixed on the main bridge of the tank, being able to slide horizontally to bring the target sphere to appropriate athwartship angular positions by using marked positions on the pole. Marked positions on the monofilament were also used to position the target sphere in the vertical direction at appropriate alongship angular values. Angular errors are expected to be smaller than 0.02° using this positioning mechanism, considering a maximum error of 0.5 cm when aligning the marks on the pole with the reference mark on the cart and the knots on the line with the pole reference mark.

The MBES was configured for 256 beam equi-angle mode at an operating frequency of 200 kHz. Its power and gain setting was adjusted to 220 dB and 40 dB, respectively. The configuration used for both sonar systems are the same as the one used in the tests to evaluate the field calibration methodology, described

in Chapter 4. During the first set of tests to evaluate the performance of the split-beam system, it was set to work passively and the MBES was set to work actively. The second set of tests used the opposite configuration (MBES passive/split-beam system active). Tests of pulse length were first conducted to evaluate the performance of the split-beam system as this parameter was varied for the two cases. After determining a proper pulse length set for the field calibration procedure based on smaller angular error and smaller angular standard deviation, accuracy tests were conducted by placing the target sphere at different positions in the described angular grid.
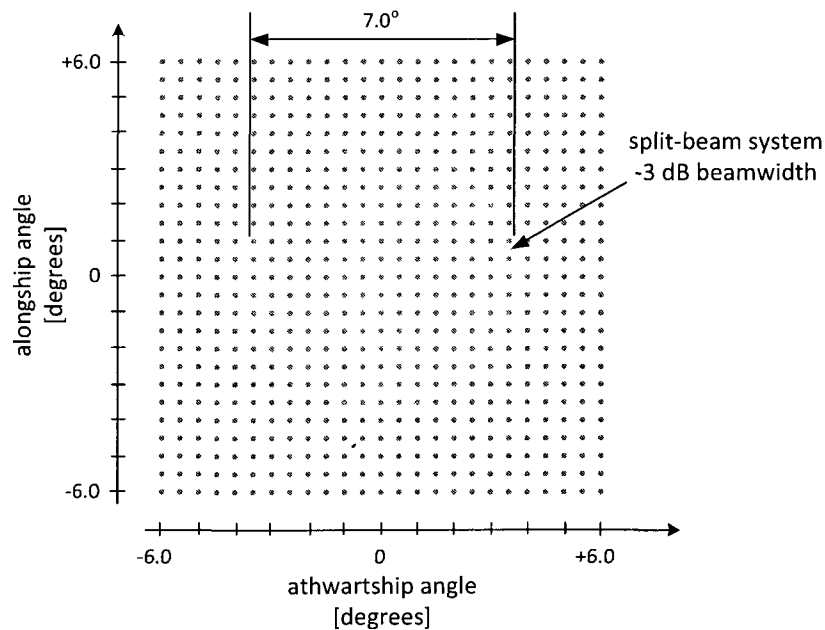
Figure 3.1 – Grid for angular accuracy tests
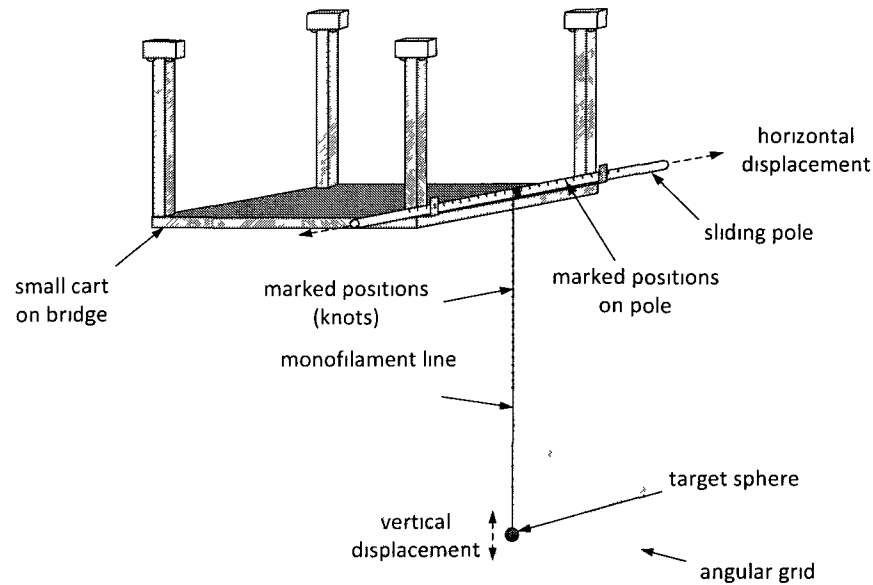
Figure 3 2 – Angular grid implementation

3.3 – Conversion of Angles from the Designed Angular Grid to the Split-beam Coordinates

The performance of the split-beam system was investigated by comparing its measured angular values to angular values from the angular grid corresponding to the target sphere position. The angular grid was designed to be parallel to the yz-plane of the MBES coordinate system and centered at the origin of the y-axis and z-axis of the MBES coordinate system. The horizontal and vertical values from the marked positions on the monofilament line and on the sliding pole corresponding to the position of the target sphere on the grid need to be converted into athwartship and alongship angles in the split-beam coordinate system. In another way: given the position (y,z) of the target sphere on the

angular grid, find the actual angles (alongship and athwartship angles) in the split-beam coordinates corresponding to this position.

3.3.1 – Athwartship Angular Conversion

Consider the target sphere positioned at the MRA of the MBES as depicted by Figure 3.3. The definitions of angles and distances according to this figure are:

r: distance between the MBES transducers and the target sphere,

y_T: distance between the MBES transducers and the split-beam transducer,

y_{7125}:   y-axis of MBES coordinate system,

y^*_{EK60}:   modified y-axis from split-beam coordinate system,

y_o: distance between the origins of y^*_{EK60} and y_{7125} axes,

d_{xyo}:   distance from the split-beam transducer to the intersection of the MRA of split-beam system projected on xy-plane and y_{7125} axis,

y_a: distance between the origin of y^*_{EK60} axis and the position of the split-beam transducer projected on the y^*_{EK60} axis,

α_{EK60o}:   measured athwartship angle from split-beam system corresponding to the target sphere position at the MRA of MBES (athwartship angular offset),

a: angle from the MRA of split-beam system to the perpendicular line passing through the position of the split-beam transducer, and

b: angle from the line connecting the position of the split-beam

transducer and the sphere positioned at the MRA of the MBES.
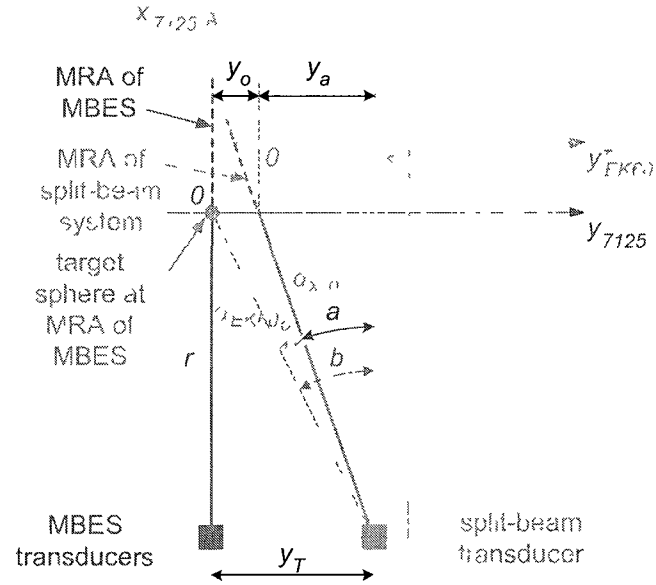
Figure 3.3 – Athwartship angular conversion: target sphere at the MRA of MBES

According to the geometry of figure 3.3, the angle b is given by

$$b = tan^{-1}\left(\frac{y_T}{r}\right)$$

(3.3.1)

and the angle a is given by

$$a = b + \alpha_{EK60o} ,$$

(3.3.2)

since the measured angles by the split-beam system (α_{EK60}) have negative

values for the target at the left side of the MRA of the split-beam system and

positive values for the target at the right side of it.

The distances y_a, y_o and d_{xyo} are calculated using

$$y_a = r\,tan(a) ,$$

(3.3.3)

$$y_o = y_T - y_a,\qquad (3.3.4)$$

and

$$d_{xyo} = \sqrt{r^2 + y_a{}^2}.\qquad (3.3.5)$$

The position of the target sphere on the y^*_{EK60} axis given its position on the

y_{7125} axis is given by

$$y^*_{EK60\_sph} = y_{7125\_sph} - y_o.\qquad (3.3.6)$$

Now consider the target sphere positioned at a general position on the

defined angular grid, as depicted by Figure 3.4. The definition of angles and

distance according to this figure are:

y_{7125_sph}:   position of the target sphere at y_{7125} axis,

$y^*_{EK60\_sph}$:   position of the target sphere at y^*_{EK60} axis,

α_{7125_sph}:   athwartship angle corresponding to the target sphere in the MBES

coordinates,

α_{EK60_sph}:   athwartship angle corresponding to the target sphere in the split-

beam system coordinates,

d_{xy_sph}:   distance between the split-beam transducer and the target sphere,

and

c: angle from the line connecting the split-beam transducer and the

sphere to the y_{7125} axis.

All other angles and distances shown by Figure 3.4 follow the same definitions as

for Figure 3.3.
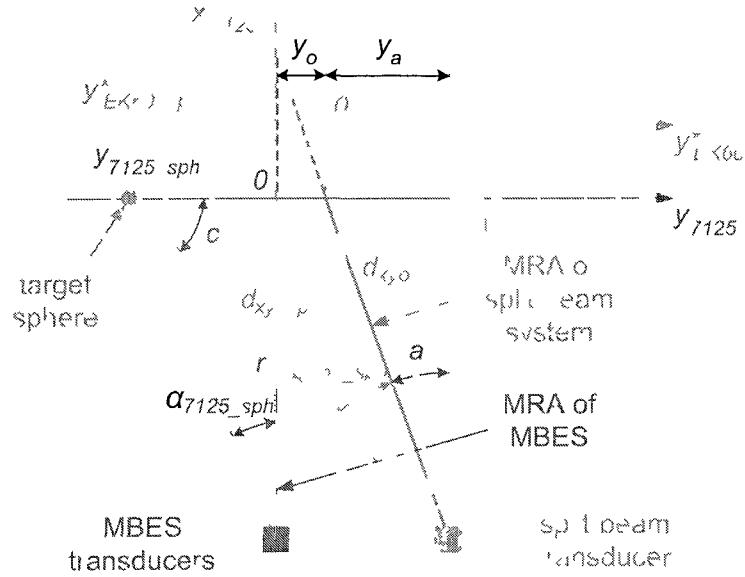
Figure 3 4 – Athwartship angular conversion target sphere at a general position on the angular grid, xy-plane

According to the geometry of Figure 3.4, the distance d_{xy_sph} is given by

$$d_{xy\_sph} = \sqrt{r^2 + \left(y_a - y_{EK60\_sph}^*\right)^2} .$$

(3.3.7)

The angle c is given by

$$c = \sin^{-1}\left(\frac{r}{d_{xy\_sph}}\right) ,$$

(3.3 8)

and applying the trigonometric law of sines, it gives

$$\frac{d_{xyo}}{\sin c} = \frac{y_{EK60\_sph}^*}{\sin \alpha_{EK60\_sph}}$$

(3.3 9)

Applying (3.3.8) in (3.3.9), the athwartship angle corresponding to the position of the target sphere on the defined angular grid in the split-beam coordinate system is given by

$$\alpha_{EK60\_sph} = sin^{-1}\left(\frac{y^*_{EK60\_sph} \left(\frac{r}{d_{xy\_sph}}\right)}{d_{xyo}}\right). \qquad (3.3.10)$$

3.3.2 – Alongship Angular Conversion

Consider the target sphere positioned at the MRA of the MBES, as shown by Figure 3.5. As observed from this figure, the transducers from both systems have the same coordinates in the xz-plane, but their MRAs may have an alongship angular offset. The definitions of distances and angles according to Figure 3.5 are:

z_{7125}:   z-axis of MBES coordinate system,

z^*_{EK60}:   modified z-axis from split-beam coordinate system,

z_o: coordinate in z^*_{EK60} axis corresponding to the offset between the

origins of z_{7125} and z^*_{EK60} axes,

d_{xzo}:   distance from the split-beam transducer to the intersection of the

MRA of split-beam system projected on xz-plane and z_{7125} axis,

x_{7125}:   x-axis of MBES coordinate system, and

β_{EK60o}:   measured alongship angle from split-beam system corresponding

to the target sphere position at the MRA of MBES (alongship

angular offset).

All other angles and distances shown by Figure 3.5 follow the same definitions as for Figure 3.3.
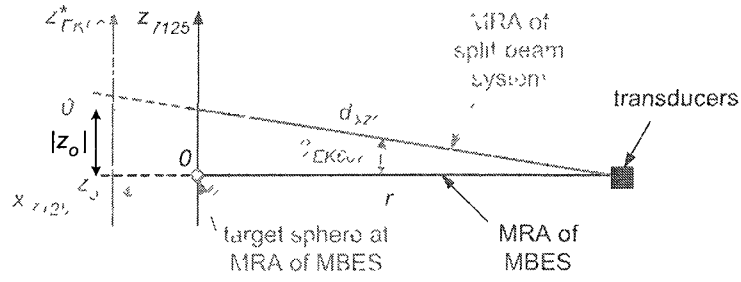
Figure 3.5 – Alongship angular conversion: target sphere at the MRA of MBES, xz-plane

The angular offset β_{EK60o} is given by the measured alongship angle from the split-beam system. From the geometry of Figure 3.5, the value of z_o is given by

$$z_o = r \ tan\left(\beta_{EK60o}\right)$$ (3.3.11)

and the coordinate of the target sphere in the $z^*{}_{EK60}$ axis given its coordinate in the z_{7125} axis is given by

$$z^*_{EK60} = z_{7125} + z_o \ ,$$ (3.3.12)

while the distance d_{xzo} is calculated using

$$d_{xzo} = \sqrt{r^2 + z_o{}^2} \ .$$ (3.3.13)

Now consider the target sphere placed at a general position on the defined angular grid as shown by Figure 3.6. The definitions of distances and angles according to this figure are:

z_{7125_sph}:   position of the target sphere at z_{7125} axis,

$z^*_{EK60\_sph}$:   position of the target sphere at z^*_{EK60} axis,

β_{7125_sph}:   alongship angle corresponding to the target sphere in the MBES coordinates,

β_{EK60_sph}:   alongship angle corresponding to the target sphere in the split-beam system coordinates,

d_{xz_sph}:   distance between the split-beam transducer and the target sphere projected on the xz-plane, and

e: angle from the line connecting the split-beam transducer and the sphere to the z_{7125} axis.

All other angles and distances shown by Figure 3.6 follow the same definitions as for Figures 3.3 and 3.5.
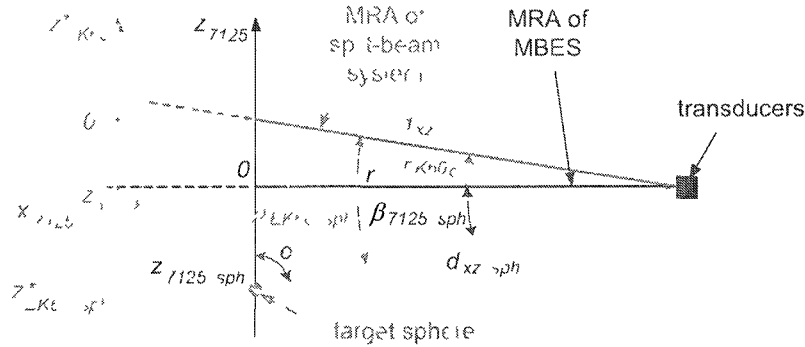
Figure 3.6 – Alongship angular conversion: target sphere at a general position on the angular grid

From the geometry of Figure 3.6, the distance d_{xz_sph} is given by

$$d_{xz\_sph} = \sqrt{r^2 + \left(z_1 - z_o\right)^2} \qquad (3.3.14)$$

and the angle e is calculated from

$$e = sin^{-1}\left(\frac{r}{d_{xz\_sph}}\right) . \qquad (3.3.15)$$

Using the trigonometric law of sines, it can be written

$$\frac{d_{xz\_sph}}{sin(e)} = \frac{z_{EK60\_sph}^*}{sin\left(\beta_{EK60\_sph}\right)} . \qquad (3.3.16)$$

Applying (3.3.15) in (3.3.16), the value of the alongship angle corresponding to the target sphere position in the defined angular grid is finally calculated by using

$$\beta_{EK60\_sph} = sin^{-1}\left(\frac{z^*_{EK60\_sph}\left(\dfrac{r}{d_{xz\_sph}}\right)}{d_{xzo}}\right).$$

(3.3.17)

3.4 – Pulse Length Tests

Pulse length tests were performed to investigate the performance of the split-beam system as this parameter was varied. Pulse lengths values of 64 μs, 130 μs, and 260 μs were used for two configurations: 1) MBES passive and split-beam system active and 2) MBES active and split-beam system passive. These tests were conducted using the same configuration as described in Chapter 4, with the target sphere placed at a distance of approximately 8 m from the transducers. The alongship angle corresponding to the target sphere location was kept at a constant value of 0° in the MBES coordinates, while the athwartship angle was set to –7.10°, –3.10°, 0.00°, 3.60°, and 6.40° in the MBES coordinates. The target sphere was placed in the first of these angular positions and measurements were conducted using the three pulse length values. This procedure was repeated for each of the described angular positions. Two hundred pings for each of the angular positions were recorded during the

measurements, and the measured values of the angles were averaged before computing the angular errors.

A displacement of 0.005 m on the target sphere position using the sliding pole corresponds to an angular change of 0.04° when the distance from the target to the transducers was 8 m. Therefore, the estimated error for the actual angular position of the target sphere is in the order of 0.02°. The calculated error from measured angles were calculated using

$$angle\ error = measured\ angle\ -\ actual\ angle.$$ (3.4.1)

Table 3.1 shows the athwartship angular measurement results from the split-beam system in its coordinate system for pulse lengths of 64 μs, 130 μs, and 260 μs.

Table 3.1 – Athwartship angular error and standard deviation from pulse length tests

Actual Athwartship Angle [degrees]	MBES coordinates	-7.10	-3.10	0.00	3.60	6.40
	Split-beam coordinates	-7.76	-3.71	-0.67	2.81	5.47
Pulse Length 64 μs	Athwartship Angular Error [degrees]	Split-beam active	0.67	0.15	0.00	0.06	0.03
		MBES active	0.70	0.17	0.00	0.01	0.02
	Athwartship Standard Deviation [degrees]	Split-beam active	0.07	0.01	0.03	0.01	0.02
		MBES active	0.25	0.01	0.01	0.01	0.01
Pulse Length 130 μs	Athwartship Angular Error [degrees]	Split-beam active	0.70	0.10	0.00	0.07	0.09
		MBES active	0.60	0.12	0.00	0.06	0.00
	Athwartship Standard Deviation [degrees]	Split-beam active	0.03	0.01	0.00	0.00	0.01
		MBES active	0.03	0.03	0.02	0.02	0.03
Pulse Length 260 μs	Athwartship Angular Error [degrees]	Split-beam active	0.60	0.10	0.00	0.07	-0.01
		MBES active	0.70	0.10	0.00	0.06	0.04
	Athwartship Standard Deviation [degrees]	Split-beam active	0.02	0.02	0.02	0.02	0.02
		MBES active	0.03	0.00	0.00	0.00	0.00

Figures 3.7, 3.8, and 3.9 show plots of these results as well as the results for the alongship angles. The actual angles shown on these figures were converted to the split-beam coordinate system using the procedure described in Section 3.3.

The results from the three pulse length tests show that the split-beam system performed well in providing athwartship angles corresponding to the target sphere position, except for the athwartship angular position of $-7.76°$, which is much larger than the -3 dB beamwidth of the sonar system (see Figure 3.1).

(a) – Athwartship angles: split-beam active

(b) – Athwartship angles: MBES active

(c) – Alongship angles: split-beam active

(d) – Alongship angles: MBES active
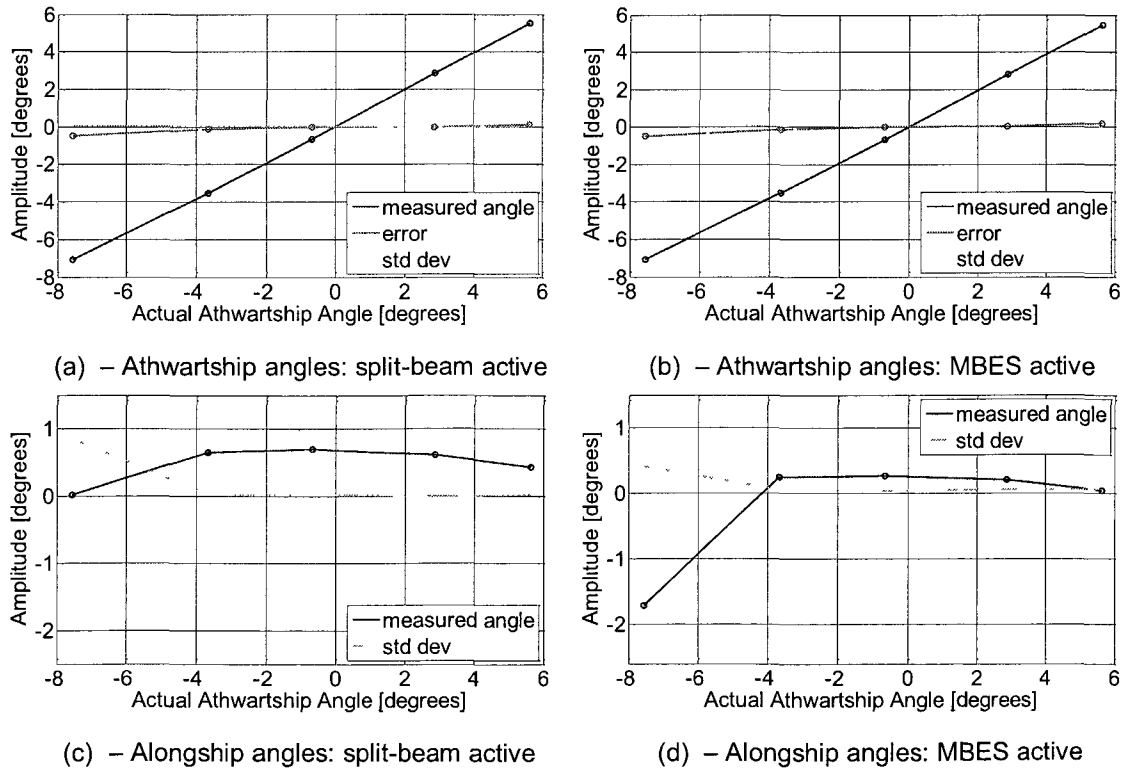
Figure 3.7 – Pulse length: 64 μs, angles in split-beam coordinate system
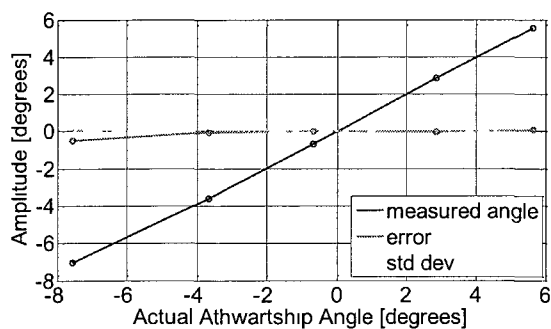
(a) – Athwartship angles: split-beam active   (b) – Athwartship angles: MBES active
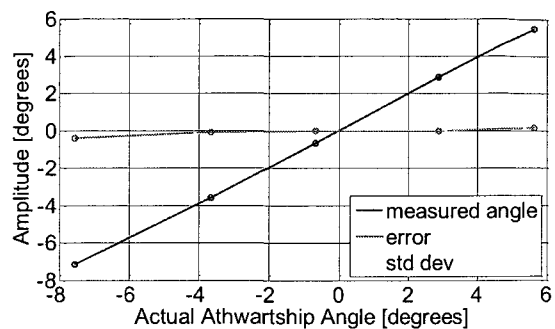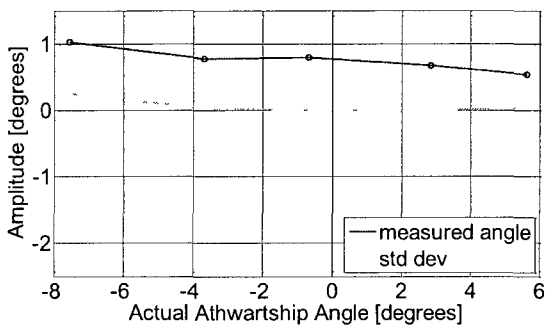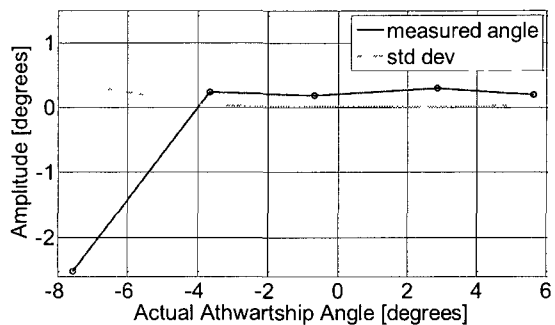
(c) – Alongship angles: split-beam active   (d) – Alongship angles: MBES active

Figure 3.8 – Pulse length: 130 µs, angles in split-beam coordinate system
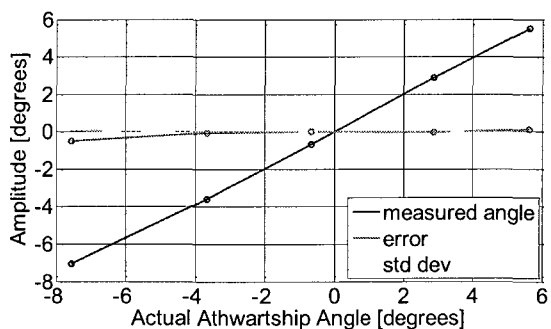
(a) – Athwartship angles: split-beam active   (b) – Athwartship angles: MBES active
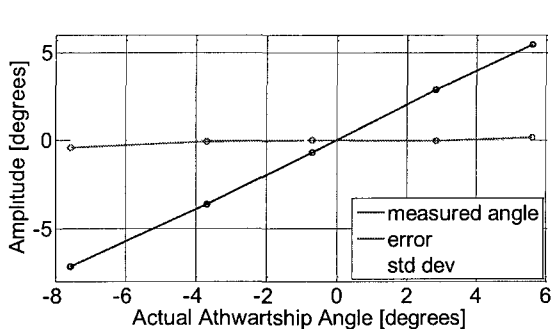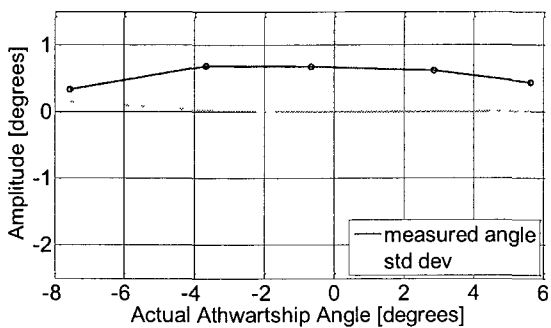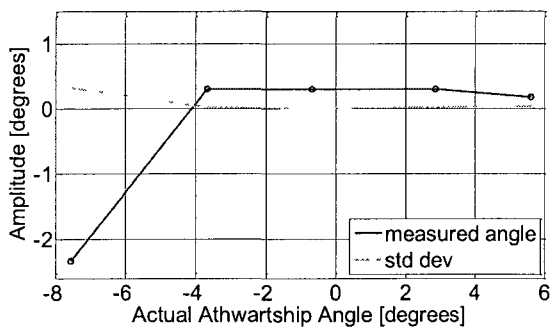
(c) – Alongship angles: split-beam active   (d) – Alongship angles: MBES active

Figure 3.9 – Pulse length: 260 µs, angles in split-beam coordinate system

For the three pulse length tests, athwartship angular errors ranged from 0.00° to 0.17° for the last four angular positions, with corresponding standard deviation values ranging from 0.00° to 0.03°. Athwartship angular error results for the three sets of pulse length measurements are very similar, while the standard deviation for pulse length of 260 µs is the smallest one.

The results for the alongship angles from these tests, as observed from Figures 3.7, 3.8, and 3.9, show consistent low standard deviation values ranging from 0.00° to 0.06° for the last four angular measurements. As observed for the athwartship angle measurements, the standard deviation values of the alongship angle corresponding to the athwartship angular position of −7.76° are much larger than the ones corresponding to the other athwartship angular positions, ranging from 0.25° to 0.41°. Values for measured alongship angles are more consistent for the first four athwartship positions when using pulse length of 260 µs with the MBES active. These results from athwartship and alongship angular measurements indicate that the pulse length value of 260 µs is an acceptable choice to be employed in the proposed calibration procedure. Transmitted signals with longer pulse length cause longer returned echoes from the target, increasing the ability of the sonar system of detecting the target more accurately.

3.5 – Split-beam Sonar System Accuracy Measurements

Tests to evaluate the accuracy of the SIMRAD EK60 split-beam echo sounder for athwartship and alongship ranges from −6° to +6° in 0.5° increments

(in the MBES coordinate system) were also conducted using the configuration previously described in Section 3.4. These tests employed transmitted signals with pulse length of 260 μs and 50 pings per angular position. These measurements were also averaged for each of the positions before computing the angular error. As in Section 3.4, the actual angular positions were converted from the MBES coordinate system to the split-beam coordinate system using the procedure described in Section 3.3.

These tests employed a 30 lb. test monofilament fishing line (0.3 mm diameter) to suspend the target sphere in the water column. As in Section 3.4, these tests were performed for two cases: i) split-beam sonar system active and MBES passive and ii) split-beam system passive and MBES active. Figure 3.10 presents the results from these tests, showing regions for angular errors in the range of +/−1.0°.

The results shown in Figure 3.10 indicate that angular errors increase as the target sphere is positioned farther from the MRA of the split-beam system, as expected. Athwartship angle errors are smaller when the MBES is active than when the split-beam is active. This is due to the higher transmitted power provided by the MBES, with larger covered range in the athwartship direction than when the split-beam system is active. Alongship angle errors are a little higher than the athwartship angle errors. These angle errors become larger than 1° for alongship values lower than −0.3° when the MBES is active; which are higher than the corresponding alongship angle errors for the case when the split-beam system is active. This may be an indication of acoustic interference caused

by reflections coming from the monofilament line, which is used to suspend the target sphere in the water column, a phenomena that is discussed in the following section of this chapter.

(a) – Athwartship angle error: split-beam active

(b) – Athwartship angle error: MBES active

(c) – Alongship angle error: split-beam active

(d) – Alongship angle error: MBES active
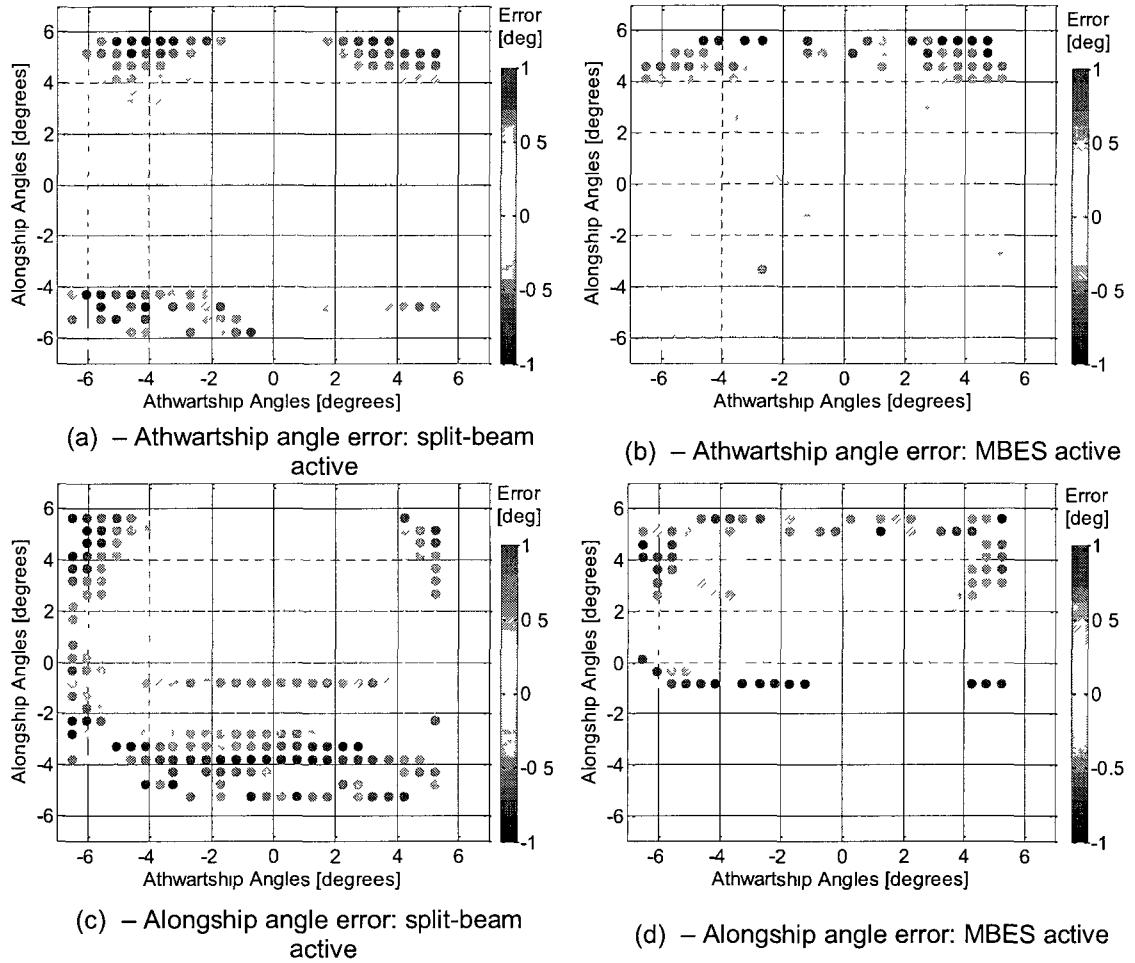
Figure 3.10 – Split-beam accuracy test: error magnitude smaller than 1°

Figure 3.11 presents more detailed plots of the angular errors, showing regions of angular errors values within the range of +/–0.5°. From the plots of this figure, it is possible to verify that for angular values inside the –3 dB beamwidth range of the split-beam system (+/–3.55° in both alongship and athwartship directions), the athwartship angle error values for both cases (split-beam active and MBES active) vary from +/–0.2°, with smaller angle errors for angular

positions closer to the MRA of the split-beam system. Inside this −3 dB

beamwidth range, alongship angle errors when the split-beam is active, vary from

0° to 0.2° for alongship angles from −0.3° to +3.5° and from 0° to 0.6° for

alongship angles from −0.3° to −3.5°. For the case when the MBES is active, the

alongship angle errors vary from 0° to 0.3° for alongship angles from −0.3° to

+3.5° and from 0° to more than 1° for alongship angles from −0.3° to −3.5°.

(a) − Athwartship angle error: split-beam active

(b) − Athwartship angle error: MBES active

(c) − Alongship angle error: split-beam active

(d) − Alongship angle error: MBES active

Figure 3.11 − Split-beam accuracy test: error magnitude smaller than 0.5°

Figure 3.12 shows the plots of standard deviation values corresponding to

the described accuracy test measurements. It can be observed from the plots in

this figure that for athwartship angles, in both cases (split-beam system active

and MBES active), the standard deviations are less than 0.1° for most of the covered angular range. The standard deviations for alongship angles are lower than 0.1° for the range of alongship angles higher than −1°, when the split-beam is the active system. When the MBES is the active system, the standard deviations are smaller than 0.2° for alongship angles higher than −1°. The increased standard deviations for the region of alongship angle values smaller than −1° may be also an indication of acoustic interference of the monofilament line used to suspend the target sphere in the water column.

(a) − Athwartship angle standard deviation:
split-beam active

(b) − Athwartship angle standard deviation:
MBES active

(c) − Alongship angle standard deviation:
split-beam active

(d) − Alongship angle standard deviation:
MBES active
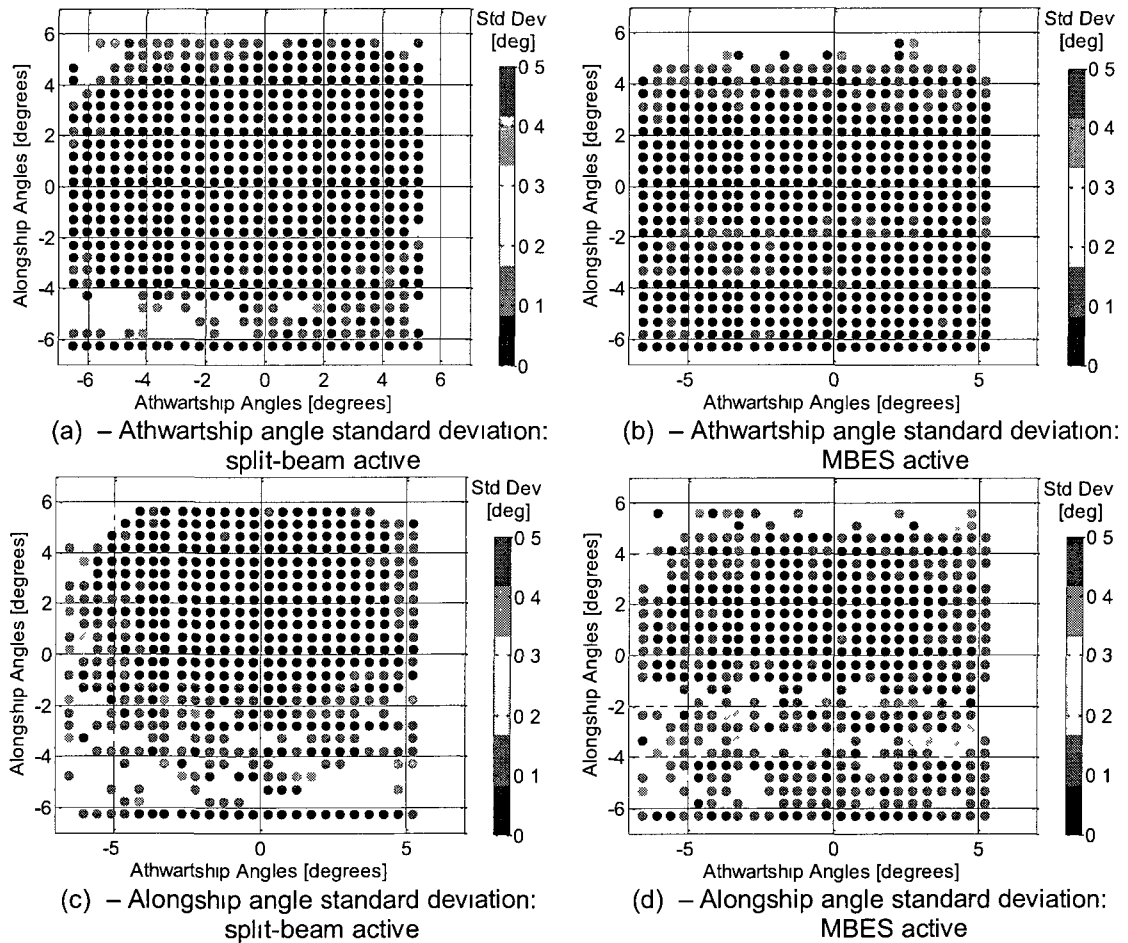
Figure 3.12 − Split-beam accuracy test: standard deviation

3.6 – Investigation of Acoustic Interference from Monofilament Line on the

Measurements

Tests were conducted to check the influence of the monofilament line (used to suspend the target sphere in the water column) on the angular measurements made by the split-beam system using the configuration described in Chapter 4. These tests employed two different monofilament lines types (30 and 6 lb. test) with two different configurations for the split-beam transducer: i) transducer mounted in its original position and ii) transducer mounted with a rotation of 180° (upside down when compared to its original position).

The angular grid used to place the target sphere was defined for athwartship and alongship angle values from +/–6° in 2° increments. Only the SIMRAD EK60 split-beam system was utilized in these tests, which employed 50 pings for each angular position of the target sphere.

The split-beam transducer was fixed with a rotation of 180° in its mount relative to its original position and the target sphere was held inside the tank by a 30 lbs. test monofilament line. With this configuration, measured angle values from the split beam system are negative in comparison with angle values from the previous accuracy tests.

Figure 3.13 shows the plots of angle error and standard deviation values for measured athwartship and alongship angles. The values for athwartship angle error and standard deviation remain approximately the same as for the previous accuracy tests, with small values for the region within the –3 dB

beamwidth of the split-beam system (errors within the range of 0° and 0.2° and standard deviations lower than 0.1°). The values for alongship angle error and standard deviation, however, are reversed from the corresponding results from the previous tests when the transducer was mounted in its original position. The magnitude of the alongship angle error starts becoming higher than 0.5° for increasing alongship angles higher than 2°, while standard deviations start becoming higher than 0.5° in the same angular region. These results suggest that the monofilament line may be interfering in the angular measurements from the split-beam system, since the transducer was mounted upside down relative to its original position and larger errors and standard deviation values appear now on the positive side of alongship angle values.

The possible acoustic interference from the monofilament line used to hold the target sphere inside the tank was further investigated by replacing the 30 lb. test monofilament line by a thinner one. A 6 lb. test monofilament line was employed to verify the accuracy of the angular measurements from the split-beam system for the two cases: i) transducer mounted in its original position and ii) transducer mounted with a rotation of 180° relative to its original position (mounted upside down). The test was to observe if the characteristics of the monofilament line would cause different values for the errors in the angular measurements by comparing the measurement results when using two different types of monofilament line to hold the target sphere in the tank.

(a) – Athwartship angle error   (b) – Athwartship angle standard deviation

(c) – Alongship angle error   (d) – Alongship angle standard deviation
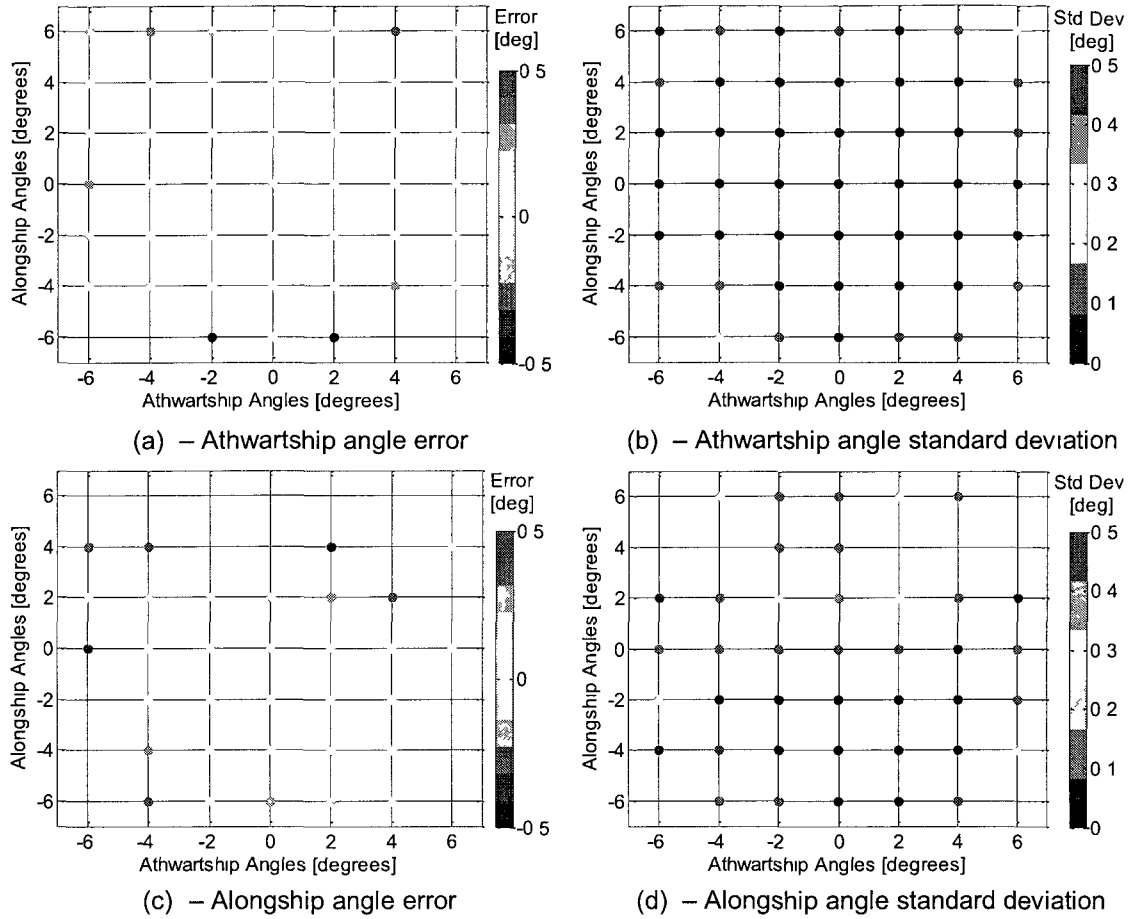
Figure 3.13 – Split-beam accuracy test: angular error and standard deviation - transducer mounted upside down

Figure 3.14 presents the athwartship and alongship angle errors and standard deviations for measured athwartship and alongship angles for the case when the split-beam transducer was mounted in its original position. As expected, values for athwartship angle error and standard deviation are smaller inside the region defined by the –3 dB beamwidth of the split-beam system, increasing as the angular range gets larger than that region. Athwartship angle errors are between $0°$ and $0.1°$ inside this –3 dB beamwidth region, while the corresponding standard deviations are smaller than $0.1°$. Values for alongship angle error using the thinner monofilament line are between $+/–0.1°$ inside the –3

dB beamwidth region, and less or equal than +/–0.4° inside the alongship angle

region of +/–4.0°. The standard deviations are smaller than 0.2° for the region

inside the –3 dB beamwidth of the split-beam system.

The use of the thinner monofilament line to suspend the target sphere in

the water column resulted in smaller angular error values from the

measurements of the split-beam system when compared to the use of the thicker

monofilament line when the transducer is mounted in its original position.

(a) – Athwartship angle error

(b) – Athwartship angle standard deviation

(c) – Alongship angle error: split-beam active

(d) – Alongship angle standard deviation: split-beam active
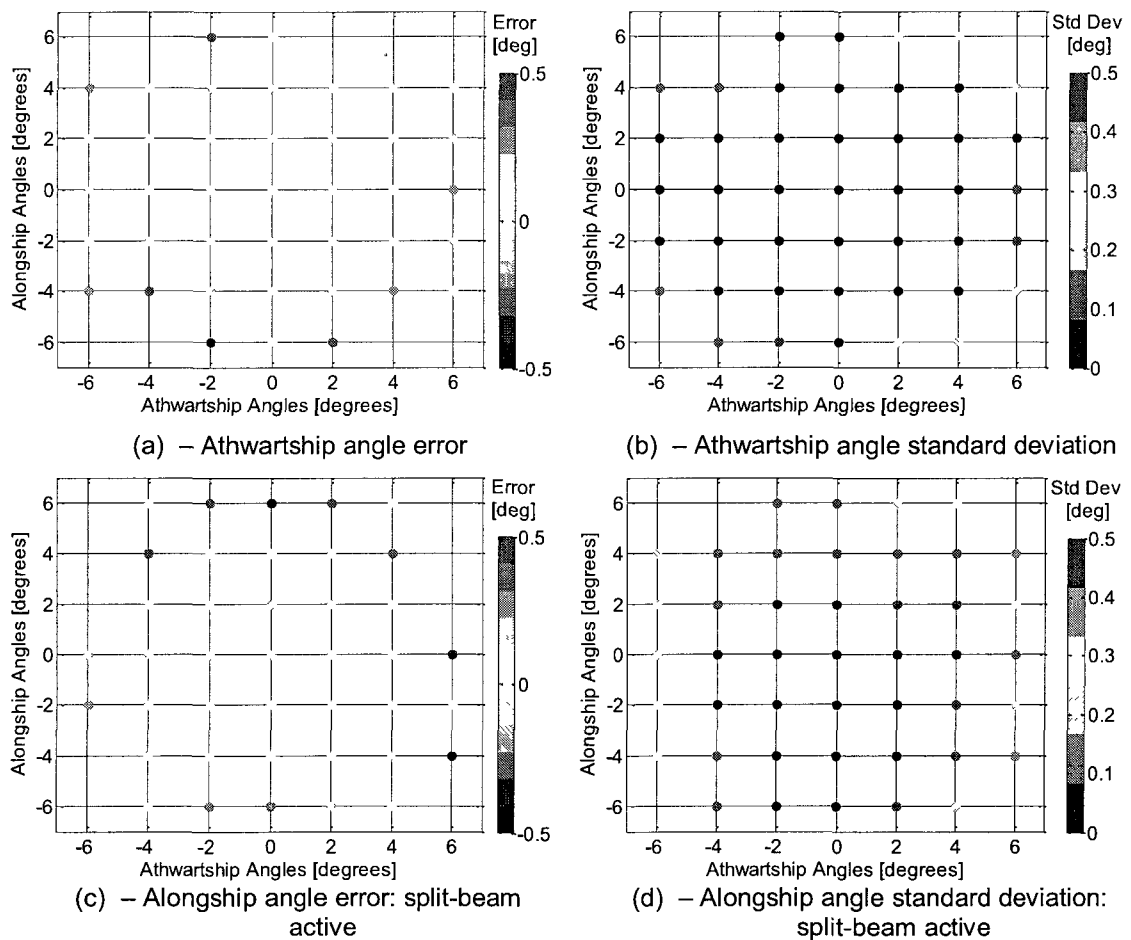
Figure 3.14 – Split-beam accuracy test: angular error and standard deviation - transducer in original position, 6 lbs. test monofilament line

The next set of the split-beam accuracy measurements was performed

employing the 6 lb. test monofilament line to hold the target sphere inside the

tank and the transducer fixed with a rotation of 180° from its original position.

Figure 3.15 presents the athwartship and alongship angle errors and standard

deviations resulting from these measurements.

Athwartship angle errors inside the −3 dB beamwidth region of the split-

beam system are between 0.0° and 0.1°, while the corresponding standard

deviations are smaller than 0.1°. Alongship angle errors are between −0.3° and

0.0° inside the alongship angle region of +/−4.0°. The corresponding standard

deviations for this angular region are smaller than 0.2°.

(a) − Athwartship angle error

(b) − Athwartship angle standard deviation

(c) − Alongship angle error

(d) − Alongship angle standard deviation
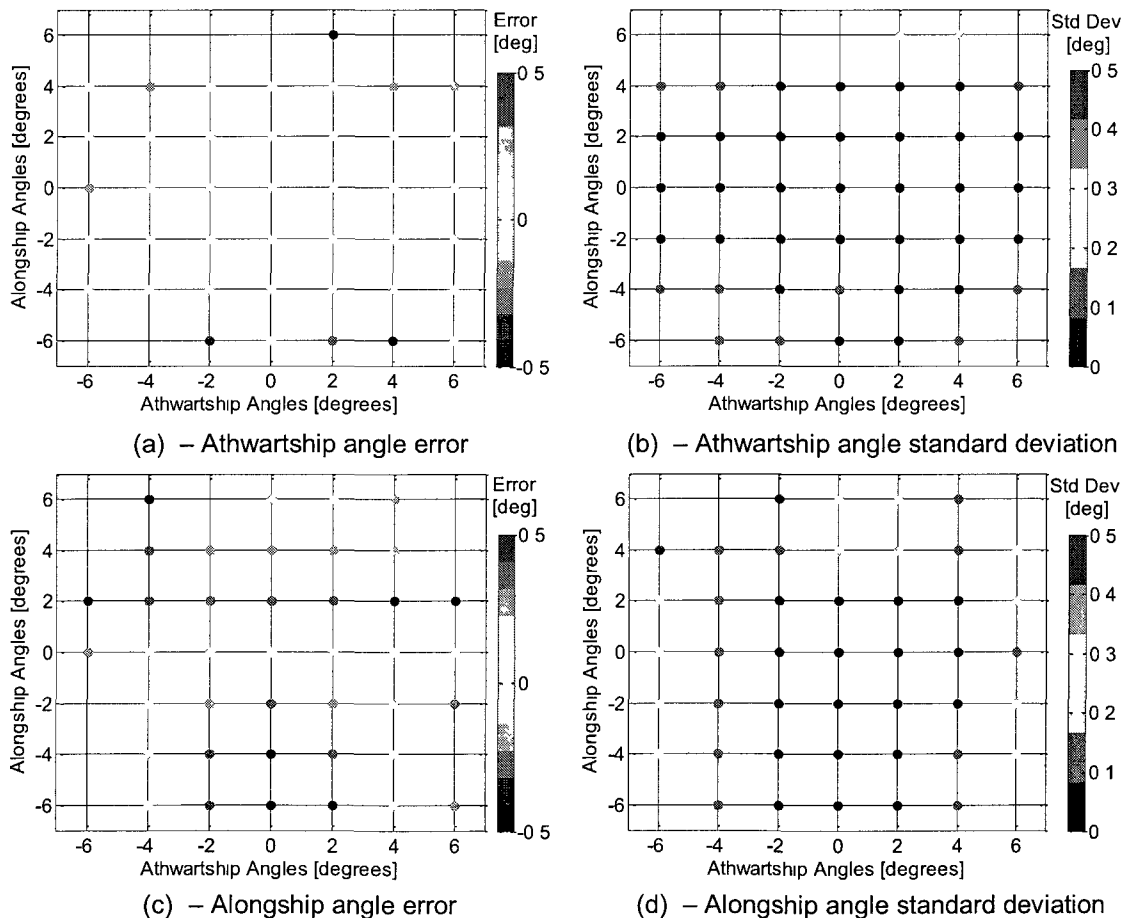
Figure 3.15 − Split-beam accuracy test: angular error and standard deviation - transducer
mounted upside down, 6 lbs. test monofilament line

The results from these tests show smaller angular errors when employing the thinner monofilament line to hold the target sphere in the water column when comparing to the use of the thicker monofilament line. Also, the results from the cases when the transducer was installed with a rotation of 180° from its original position and for when it was installed in its original position show evidence of acoustic interference in the angle measurements from the split-beam system. It was verified that there are large alongship angle error values for negative alongship angle values when the transducer was mounted in its original position, and large alongship angle error values for positive alongship angle values when the transducer was mounted with an 180° rotation from its original position. Further tests necessary to identify the cause of this type of interference were left for future research.

3.7 – Remarks

The accuracy tests of the SIMRAD EK60 split-beam system indicate that it is important to have the MRA of both sonar systems well aligned to minimize error in the angle measurements from the split-beam system. If the MRA of the split-beam has a large alongship angular offset, then, depending on the offset being positive or negative, the area insonified by the MBES would be centered above or below the MRA of the split-beam system. This may cause the upper or lower portion of the beam pattern of the split-beam system to receive very low signal returns from the target, causing larger error in the angular measurements.

The tests described in this chapter were also helpful for assessing the possibility of acoustic interference from the monofilament line in the angular measurements from the split-beam system. The tests suggest that a thin monofilament line should be employed to suspend the target sphere in the water column to minimize errors in the angular measurements. However, one concern about using thin monofilament lines during a field calibration procedure is to lose the target sphere if the line breaks. Therefore, the choice of the monofilament line needs to be considered carefully.

CHAPTER 4

AIDED FIELD CALIBRATION METHODOLOGY FOR A MULTIBEAM ECHO SOUNDER

4.1 – Introduction

The conventional tank calibration procedure discussed in Chapter 2 illustrates the importance of calibrating a MBES, as it provides valuable results in terms of accuracy and high resolution. However, it also illustrates the need for a calibration procedure for ship-mounted sonar systems, which would account for mount-related acoustic interferences and possibly be performed consuming less amount of time.

A methodology developed to calibrate a MBES in the field, providing the combined transmit/receive beam pattern and calibration offset factor for each beam, is described in this chapter. It employs a tungsten carbide sphere of 38.1 mm of diameter (WC38.1) as the standard target and a SIMRAD EK60 split beam echo sounder with a 200 kHz transducer ES200-7CD. The split-beam system is used to provide information about the position of the target necessary to compute the beam pattern of the MBES. A 200 kHz RESON Seabat 7125 MBES, widely used by NOAA (National Oceanic and Atmospheric

Administration) vessels for hydrographic purposes, was used to test the procedure.

The tests to validate this methodology were conducted in the acoustic tank at the University of New Hampshire, which has dimensions of 18 m long, 12 m wide, and 6 m deep, as described in Chapter 2. The procedure may be extended for use in the field for ship-mounted systems, addressing transducer mount-related acoustic interferences and minimizing the time necessary to calibrate the MBES.

In the proposed calibration procedure, the transducers of both sonar systems are mounted side by side, with a separation distance between them set to minimize and/or avoid acoustic interference from one another. The split-beam transducer is adjusted to have its MRA intercepting the MRA of the MBES transducers at the target range, as depicted by Figure 4.1. According to the manufacturer specifications, the −3 dB beamwidth for the RESON 7125 MBES is 1° in the athwartship direction and 2° in the alongship direction while for the SIMRAD EK60 split-beam echo sounder the −3 dB beamwidth is 7.0° in the athwartship and alongship directions. Figure 4.2 shows the superposition of the − 3 dB beamwidth of both systems when their MRAs are aligned.

The MBES is set to work actively (transmitting and receiving acoustic signals) and used to trigger the split-beam system, which is set to work passively (only receiving acoustic signals). Beamformed data is recorded by the MBES, which is used to compute the target range from the MBES and the amplitude of the returns corresponding to the target position. Data recorded by the split-beam

is used to compute the corresponding athwartship and alongship angular coordinates of the target sphere, as well as its range from the travel of the acoustic signal from the MBES to target sphere and to the split-beam system.
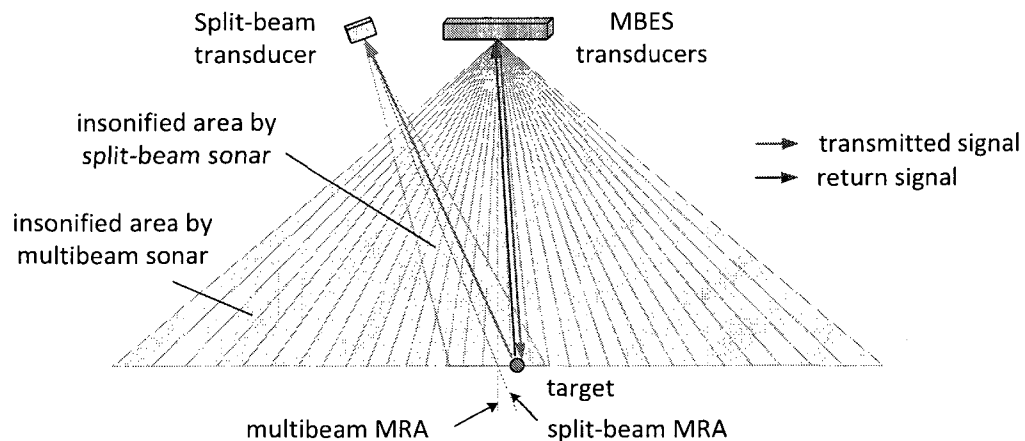
Figure 4.1 – Field calibration methodology overview
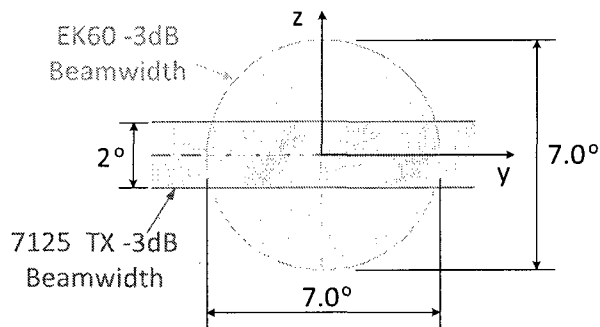
Figure 4.2 – Alignment of MRAs, showing the RESON 7125 alongship -3 dB beamwidth and the SIMRAD EK60 -3 dB beamwidth on the yz-plane

A computational algorithm written in MATLAB was developed to convert the angular coordinates of the target from the split-beam system coordinates to the MBES coordinates and process the amplitude values of the return signals to the MBES, producing a plot of the combined transmit/receive radiation beam pattern. The *readEKRaw EK/ES60 ME/MS70* MATLAB toolkit written by Rick

Towler (NOAA Alaska Fisheries Science Center) was used to extract the data

from the raw files recorded by the split-beam system. This MATLAB toolkit can

be found at http://www.hydroacoustics.net/viewtopic.php?f=36&t=131&start=0.

Although the split-beam is triggered by the MBES, there is a small time

delay between the start of acquisition time of each system. To minimize this

delay and account for missing pings, the recorded data from both sonar systems

were synchronized using the Network Time Protocol (NTP). Figure 3.3 shows the

simplified block diagram for the field calibration methodology. A Garmin GPS

device (GPS 18x LVC) was also used to provide a PPS (pulse per second) signal

and GGA sentences to both system in order to provide synchronization.
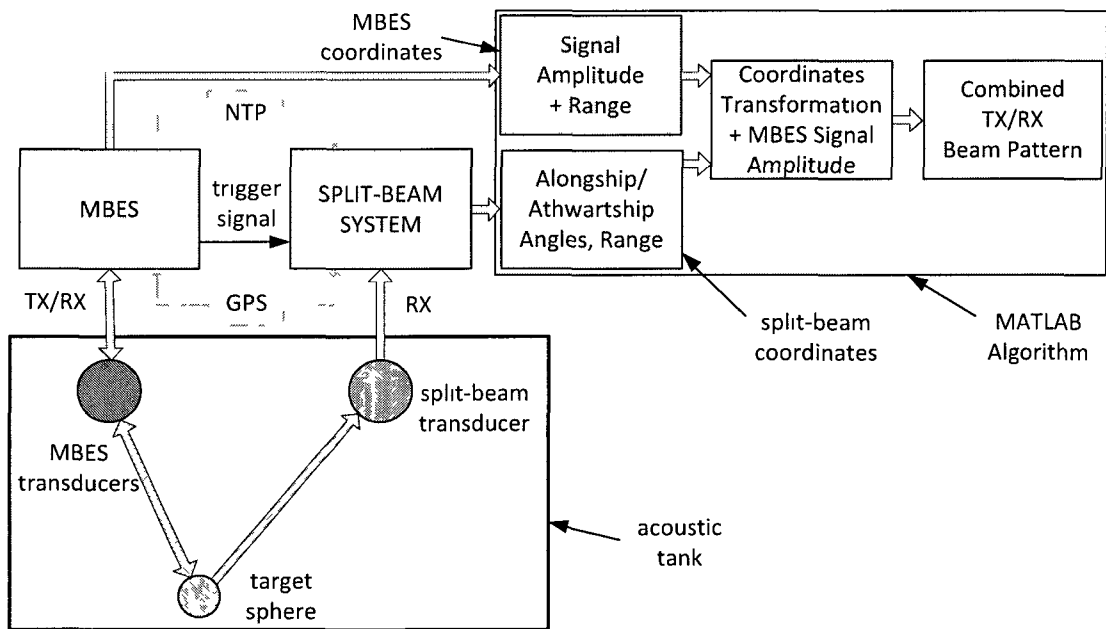
Figure 4.3 – Field calibration methodology: simplified block diagram

The following sections describe details of the field calibration methodology

including the setup in the acoustic tank, analysis of multipath acoustic

interference in the tank, the transformation of coordinates necessary to convert measured angles corresponding to the target by the split-beam system from its coordinate system to the multibeam coordinate system, and the time synchronization mechanism employed to exclude invalid data. The procedure for the combined transmit/receive beam pattern measurements, the data processing stage, and the results are also presented later in this chapter.

4.2 – Setup in the Acoustic Tank

The SIMRAD EK60 split-beam transducer and the RESON 7125 projector and hydrophone arrays were mounted to a rigid metallic structure as depicted in Figure 4.4. As seen from this figure, the transducers of both systems are placed side-by-side in parallel, with a separation distance of 0.955 m between their geometric centers. This distance was chosen to be short enough to keep the mounting structure rigid and, therefore, minimizing possible mechanical vibrations while minimizing acoustic interferences between the two systems. The rigid metallic structure (with the transducers of the two sonar systems) was held by a carbon fiber pole, fixed at the center of gravity of the transducers mount and attached to the main bridge of the tank. The EK60 transducer was tilted to adjust its MRA to intercept the multibeam MRA at a distance of 8 m (this can be done in the field by placing the EK60 transducer on a mount that can rotate using a motor and a controller). This angular offset was calculated using the geometry depicted by Figure 4.5.

(a) – front view

(b) – top view
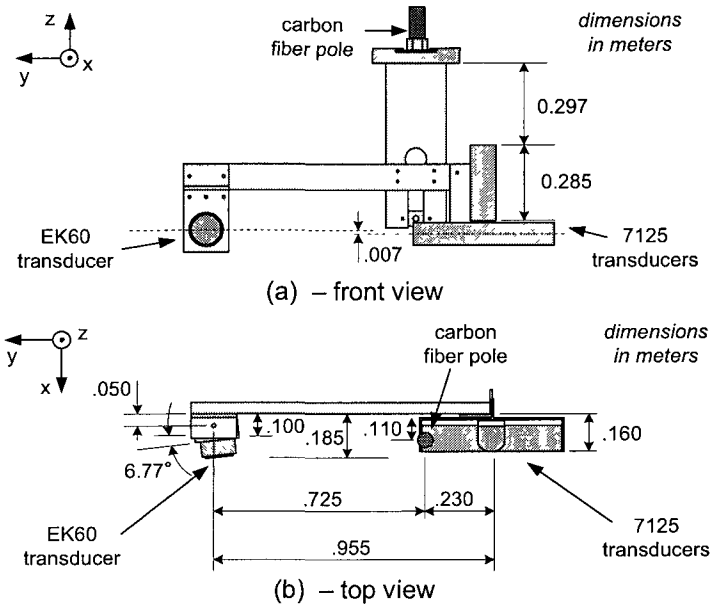
Figure 4.4 – Transducers mounting
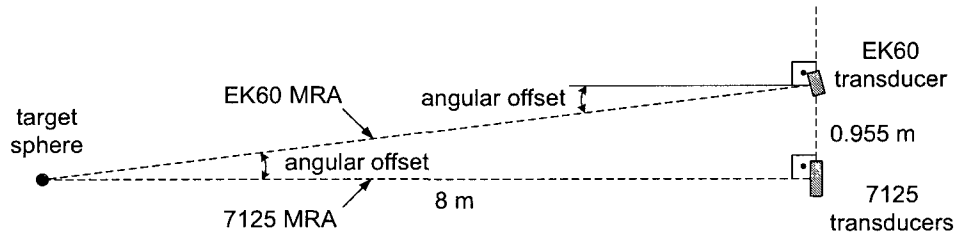
Figure 4.5 – EK60 angular offset calculation

According to the above geometry, the EK60 angular offset is given by

$$angular\ offset = tan^{-1}\left(\frac{0.955\ m}{8\ m}\right) \cong 6.81^{\circ}\ . \tag{4.1.1}$$

The position and direction of the mounted transducers and the target sphere in the tank were chosen to minimize the effects of acoustic signals reflected from the water surface, the bottom, and the walls of the tank during the tests. To avoid the interference in the range of the target sphere position, the

orientation of the transducers of both sonar systems in the acoustic tank had to be modified from the orientation of the transducers used during the calibration procedure described in Chapter 2. This change of the orientation of the transducers was necessary due to the nature of the calibration methodology presented here, where a combined transmit/receive beam pattern is produced using a standard target sphere. With this change in the orientation of the transducers, however, the range of the target was reduced from the one used in the procedure described in Chapter 2. The transducers were placed in the tank at 2 m from the back wall, at 9 m from each of the sidewalls, and at the mid-depth of the tank (3 m). Ideally, the range of the target sphere should be large enough to achieve measurements in the far-field of the transducers. However, having the tank side walls at 9 m of range and working with transmitted signals with pulse lengths of 300 μs (0.45 m of length in water) would allow the target sphere to be at a maximum safe range of 8 m.

The target sphere was manually swept through the region of interest by a person holding a 30 lb. test monofilament fishing line (0.3 mm diameter) on the small cart over the bridge during the beam pattern measurements. Figure 4.6 shows the described setup in the acoustic tank.
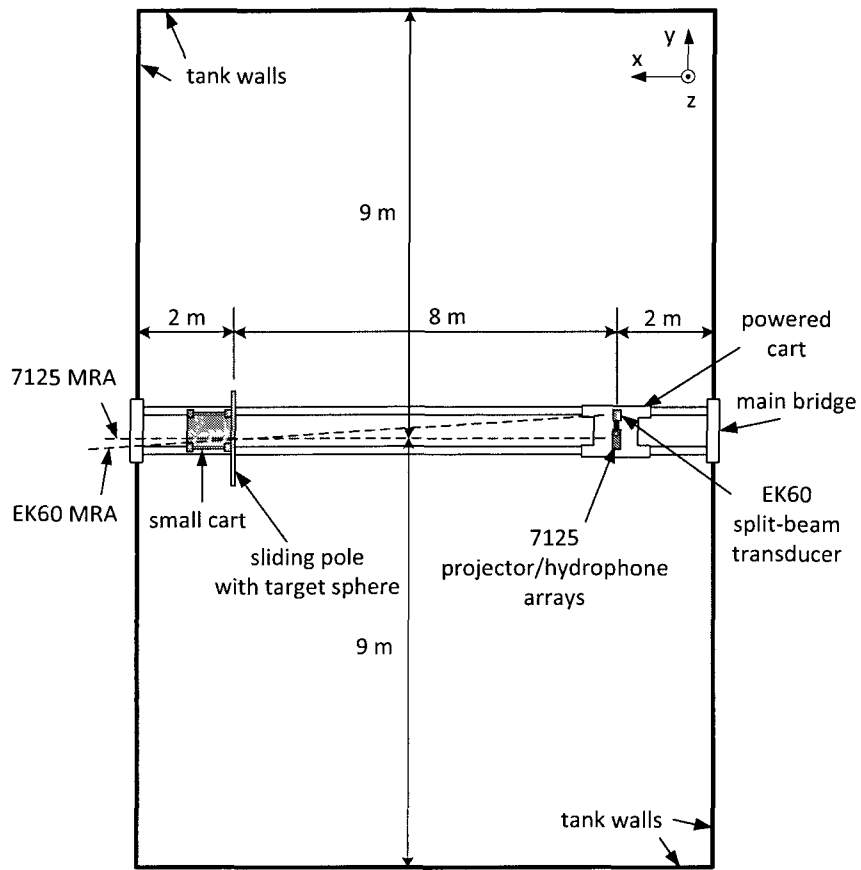
(a) – top view
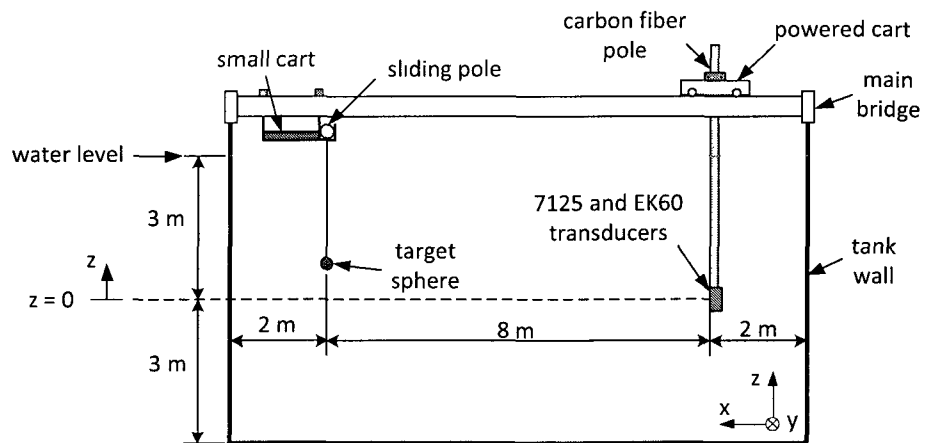
(b) – side view

Figure 4.6 – Acoustic tank setup

4.3 – Analysis of Acoustic Multipath Interferences

Figure 4.7 illustrates the main acoustic paths involved in the calibration procedure performed in the acoustic tank. Since the athwartship coverage of the RESON 7125 MBES is wide, scattered signals from the side walls start to show in the measurements at the range of 9 m. For this reason, the target sphere was placed at a range of 8 m from the transducers. This distance summed with the pulse length of the transmitted signal of 0.45 m is equal to 8.45 m, which gives 0.55 m of extra space for the returned signal from the target to arrive at the transducers without interference from the side walls. Reflections from the surface and the bottom reach the target sphere at a distance of 10 m, arriving at the transducers at a much later time.

Other types of acoustic multipath interference were caused by sidelobes of the MBES and split-beam transducers. First consider the case where the signal transmitted by the MBES is scattered by the split-beam transducer (due to sidelobes from the MBES projector) and it reaches the target later on. Since the split-beam transducer is at a distance of 0.955 m from the multibeam projector, the echo returned from the target sphere corresponding to the transmitted signal scattered by the split-beam transducer does not interfere with the echo returned from the direct path. Now consider echoes returned from the target sphere and scattered either by the MBES transducers or by the split-beam transducer. In either of these cases, the separation distance from the transducers of both systems makes these multipath returned signals arrive at the corresponding

receive transducer after the echo returned from the direct path, causing no acoustic interference either in the split-beam (phase-difference) or in the beam pattern measurements.

(a) – Side view

(b) – Top view
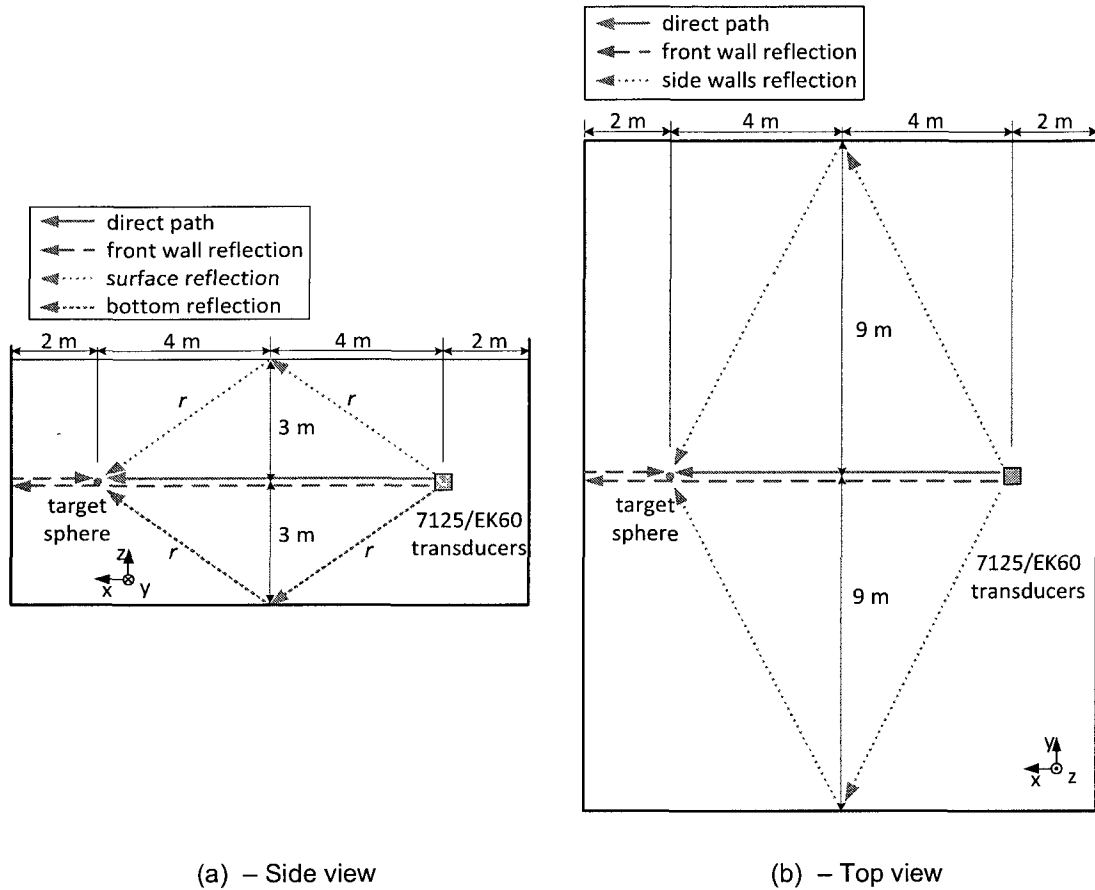
Figure 4.7 – Main acoustic paths for field calibration setup in the acoustic tank

4.4 – Coordinate System Transformation

The position of the target sphere is provided by the split-beam system as athwartship angle (β_{EK60}), alongship angle (α_{EK60}), and range (d_{EK60}). These values, which are given in the split-beam system coordinates, need to be converted to the MBES coordinate system. The split-beam transducer was

placed on the y-axis of the MBES transducers at a distance y_T of 0.955 m. Figure 4.8 depicts the configuration of the mounted transducers using the MBES coordinate system along with the definitions of the angles and distances used to compute the transformation of coordinates. In this figure, the angles and distances are:

d_{7125}:   distance between the target sphere and the multibeam transducers,

d_{7125xy}:   distance d_{7125} projected on the xy-plane,

d_{EK60}:   distance between the target sphere and the split-beam transducer,

d_{EK60xy}:   distance d_{EK60} projected on the xy-plane,

α_o: split-beam system athwartship angle offset (angle between the multibeam system MRA and the projection of the split-beam system MRA on the xy-plane),

β_o: split-beam system alongship angle offset (angle between the multibeam system MRA and the projection of the split-beam system MRA on the xz-plane),

α_{EK60}:   split-beam system athwartship angle,

β_{EK60}:   alongship angle of target in split-beam system coordinates,

α_{7125}:   athwartship angle of target in multibeam system coordinates,

β_{7125}:   alongship angle of target in multibeam system coordinates,

y_T: coordinate of split-beam transducer on y-axis,

y_{sph}:   coordinate of target sphere on y-axis, and

z_{sph}:   coordinate of target sphere on z-axis.
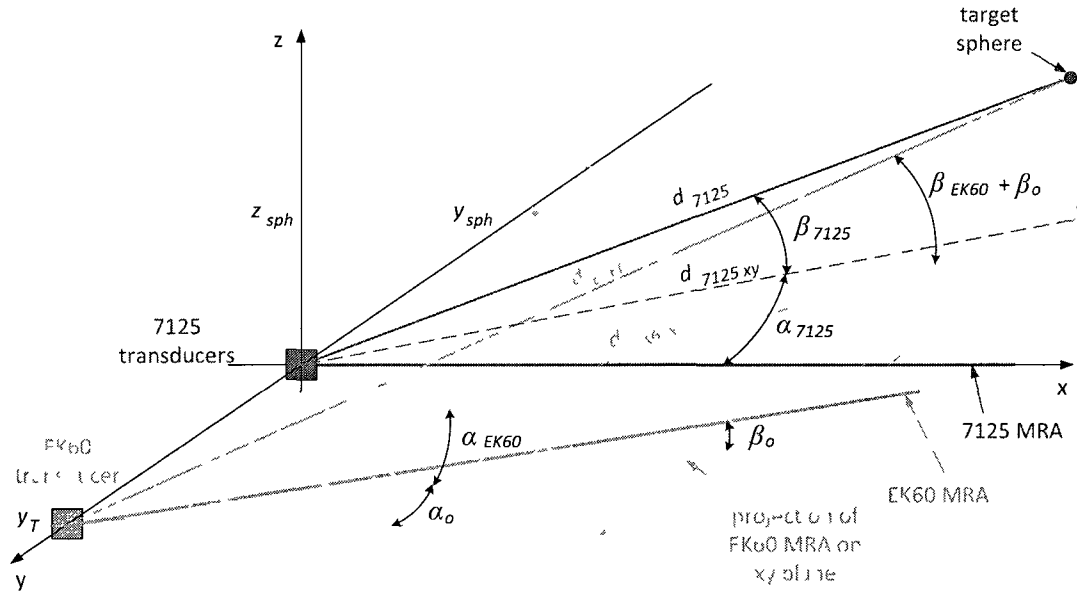
Figure 4 8 – 7125/EK60 coordinate system definition of angles and distances

4.4.1 – Alongship and Athwartship Angles Conversion

The alongship angle corresponding to the target position in the MBES

coordinates is calculated using the geometry shown by Figure 4.9 below. The

split-beam system alongship angle offset β_o has negative value for the shown

configuration, while the split-beam system alongship angle of the target β_{EK60} has

positive value. Therefore, the value of the alongship angle of the target in the

MBES coordinates, β_{7125}, is given by

$$\beta_{7125} = \beta_{EK60} - \beta_o \qquad (4.4.1)$$
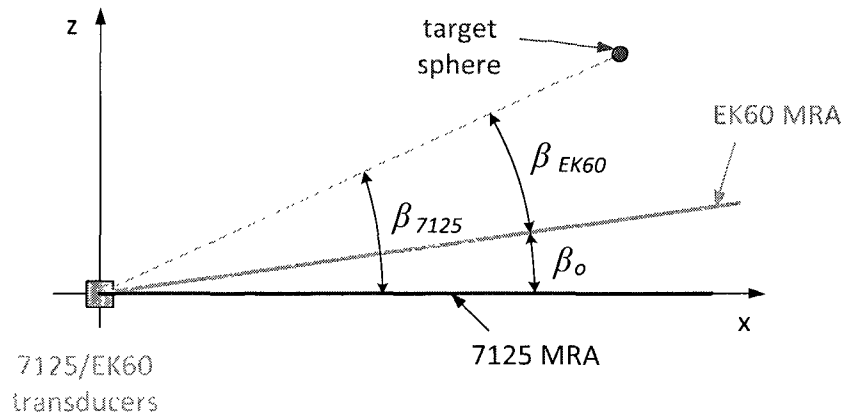
Figure 4.9 – Alongship angles calculation

The distances d_{7125} and d_{EK60} projected on the xy-plane are calculated using the geometry depicted by Figures 4.10 and 4.11 respectively. These distances are used to compute the athwartship angular position of the target in the MBES coordinates. They are given by

$$d_{7125xy} = d_{7125} \cos\left(\beta_{7125}\right) \qquad\qquad (4.4.2)$$

and

$$d_{EK60xy} = d_{EK60} \cos\left(\beta_{EK60} - \beta_o\right). \qquad\qquad (4.4.3)$$

Substituting (4.4.1) into (4.4.3) gives

$$d_{EK60xy} = d_{EK60} \cos\left(\beta_{7125}\right). \qquad\qquad (4.4.4)$$
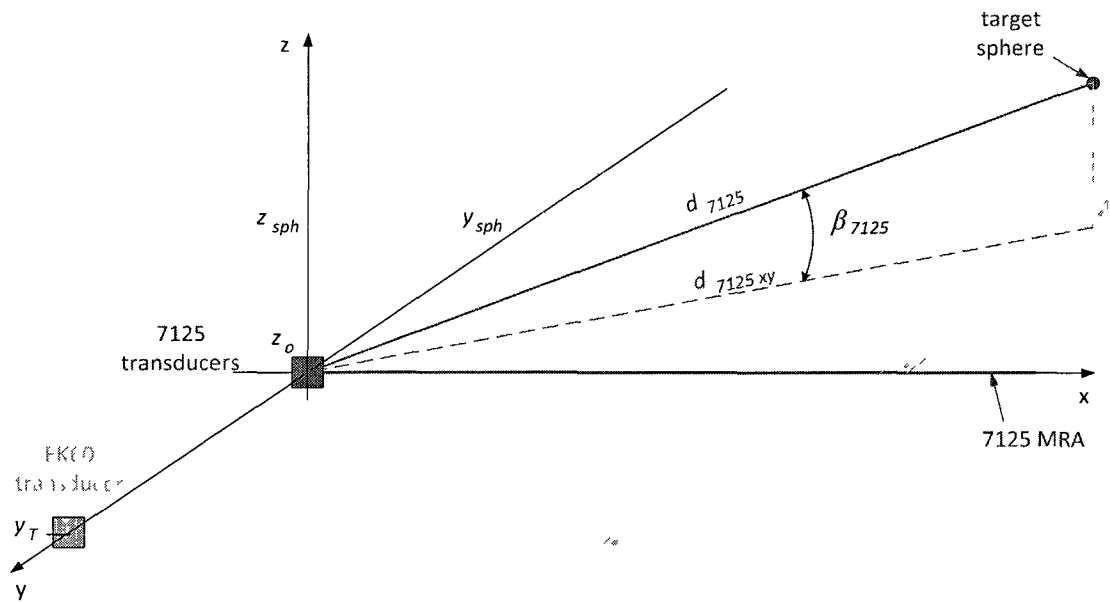
Figure 4 10 – d_{7125xy} calculation
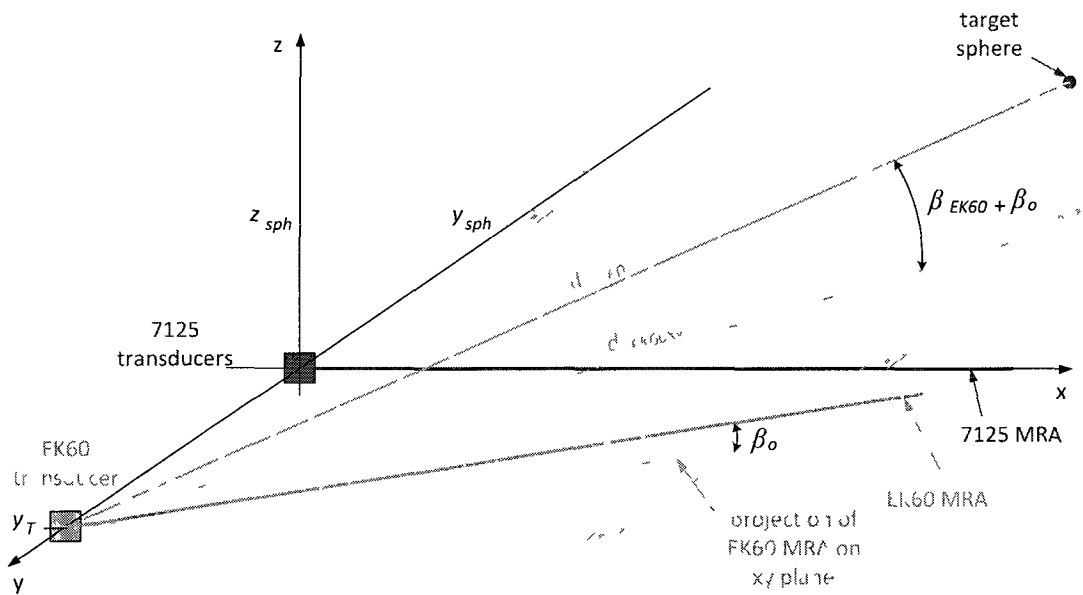
Figure 4.11 – d_{EK60xy} calculation

The angle offset α_o is calculated by positioning the target sphere at the

MRA of the MBES and using the geometry depicted by Figure 4.12.
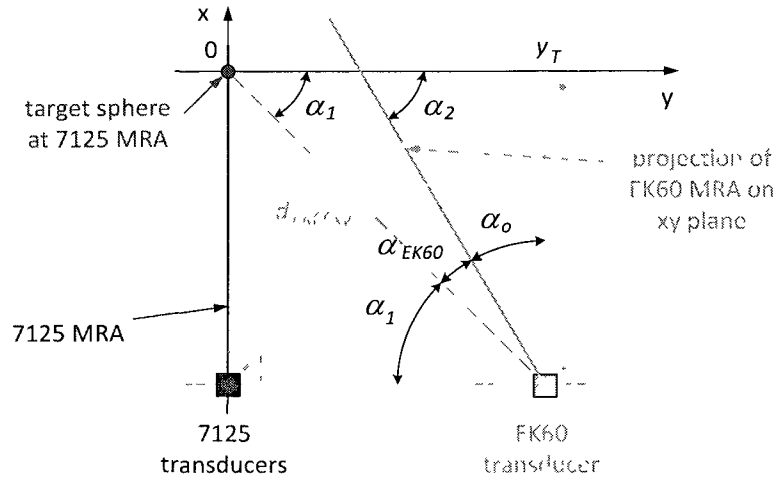
Figure 4.12 – Angle offset α_o calculation

From this figure, the angles α_1, α_2, and α_o are given by

$$\alpha_1 = cos\left(\frac{y_t}{d_{EK60xy}}\right),$$

(4.4.5)

$$\alpha_2 = \alpha_1 - \alpha_{EK60},$$

(4.4.6)

and

$$\alpha_0 = 90^o - \alpha_2.$$

(4.4.7)

Applying (4.4.5) and (4.4.6) into (4.4.7), the angle offset α_o is calculated from

$$\alpha_0 = 90^o - cos^{-1}\left(\frac{y_t}{d_{EK60xy}}\right) + \alpha_{EK60}.$$

(4.4.8)

Figure 4.13 shows the geometry used to compute the athwartship angular position of the target sphere in the MBES coordinates. In this figure, Δy_{sph} is the distance between the target sphere and the split-beam transducer position on the y-axis:

$$\Delta y_{sph} = y_T - y_{sph}.$$

(4.4.9)
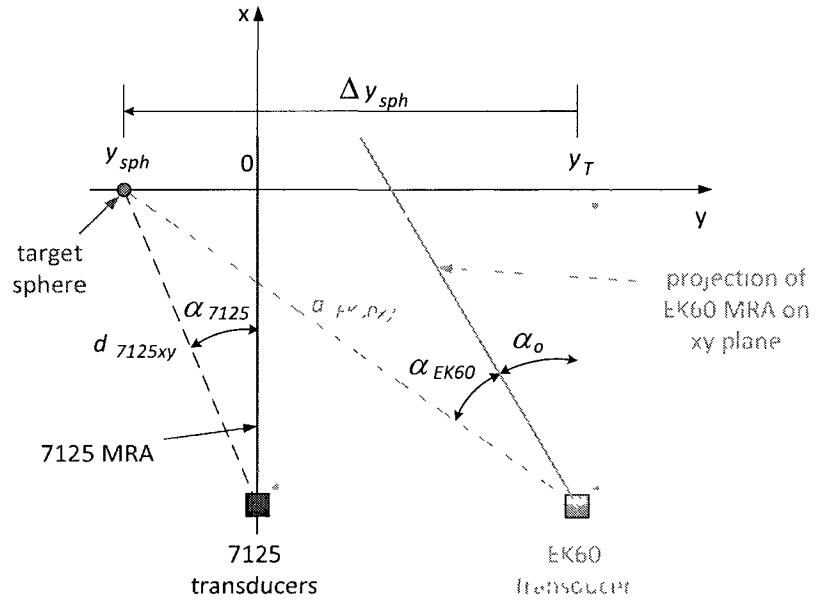
Figure 4.13 – Athwartship angles calculation

The value of Δy_{sph} can be obtained from the geometry of Figure 4.13:

$$\Delta y_{sph} = d_{EK60}\, sin\left(\alpha_o - \alpha_{EK60}\right).$$ (4.4.10)

Applying (4.4.10) into (4.4.9) gives

$$y_{sph} = y_T - d_{EK60}\, sin\left(\alpha_o - \alpha_{EK60}\right).$$ (4.4.11)

Also, the athwartship angular position of the sphere in the MBES coordinates is given by

$$\alpha_{7125} = sin^{-1}\left(\frac{y_{sph}}{d_{7125xy}}\right).$$ (4.4.12)

Applying (4.4.2) and (4.4.11) into (4.4.12), the value of the athwartship angular position of the target in the MBES coordinates becomes

$$\alpha_{7125} = sin^{-1}\left(\frac{y_T - d_{EK60}\, sin\left(\alpha_o - \alpha_{EK60}\right)}{d_{7125}\, cos\left(\beta_{7125}\right)}\right).$$ (4.4.13)

4.4.2 – Coordinate System Conversion Using MBES and Split-beam System Data Sets

The distances between the target and the MBES transducers and between the target and the split-beam transducer, d_{7125} and d_{EK60} respectively, must be obtained from the echo from the target sphere at the MBES and at the split-beam system. Ideally, the two systems should be triggered at the same time and these distances would be computed from the travel time of the transmitted signal to each one of the sonar systems. However, there is a trigger delay between the MBES (the master) and the split-beam system (the slave). It is necessary to account for this delay when computing the true travel time of the signal on both systems to obtain the distances d_{7125} and d_{EK60}.

This time delay can be determined by positioning the target sphere at the multibeam MRA and obtaining the time interval taken by the transmitted signal to reach the target and to return to the MBES receiver array, t_1, and also the time interval taken by the transmitted signal to reach the target sphere and then the split-beam transducer, t_2. Figure 4.14 depicts this setup. The time interval t_1 is obtained from the MBES data set, while the time interval t_2 is obtained from the split-beam system data set.
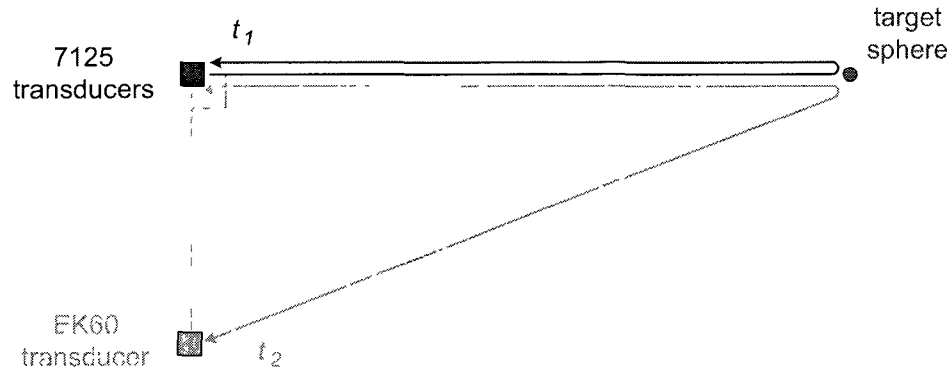
Figure 4.14 – Time delay calculation

The time for the transmitted signal to travel from the MBES projector array to the target is given by

$$t_{7125} = \frac{t_1}{2}.$$

(4.4.14)

The distances d_{7125} and d_{EK60} are calculated from the geometry of Figure 4.15 by

$$d_{7125} = c \ t_{7125}$$

(4.4.15)

and

$$d_{EK60} = \sqrt{d_{7125}^2 + y_T^2},$$

(4.4.16)

where c is the sound speed in the water. This information can be used to compute the expected time interval for the transmitted signal to travel from the MBES projector array, reach the target, and then reach the split-beam transducer. This time interval, $t_{7125\text{-}target\text{-}EK60\_EXPECTED}$, is given by

$$t_{7125\text{-}TARGET\text{-}EK60\_EXPECTED} = \frac{d_{7125} + d_{EK60}}{c}.$$

(4.4.17)
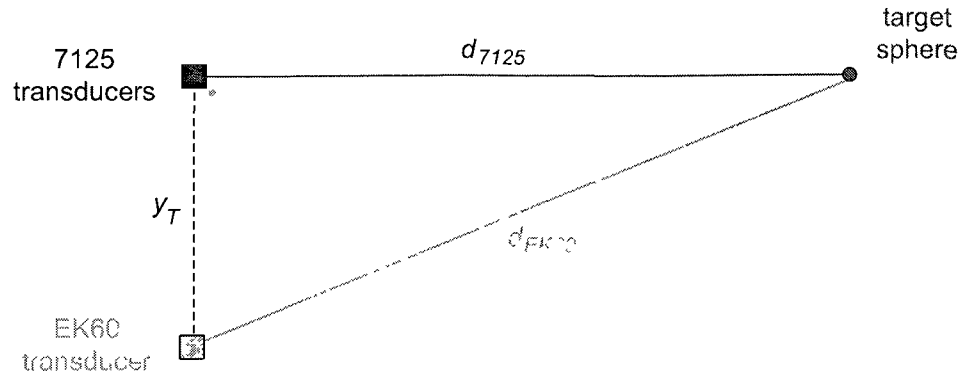
Figure 4.15 – d_{7125} and d_{EK60} calculation for target at MRA

The time delay between the two sonar systems, $t_{system\,delay}$, is finally

calculated using

$$t_{system\,delay} = t_2 - t_{7125-TARGET-EK60\_EXPECTED}.$$ (4.4.18)

Once the time delay between the two sonar systems is found, a correction

is applied to the split-beam system data to account for this delay and obtain the

correct value of the distance between the target and the split-beam transducer

when the target sphere is at an arbitrary position. The distance d_{7125} is calculated

as described for the target sphere at the MBES MRA. The distance d_{EK60} is

calculated by first applying the calculated time delay to the value of t_2:

$$t_{2\_CORRECTED} = t_2 - t_{system\,delay}.$$ (4.4.19)

The time interval corresponding to the travel of the signal from the target

sphere to the split-beam transducer, t_{EK60}, is given by

$$t_{EK60} = t_{2\_CORRECTED} - \frac{t_1}{2}.$$ (4.4.20)

Finally, the distance between the target sphere and the split-beam transducer is obtained from

$$d_{EK60} = c \ t_{EK60}.$$

(4.4.21)

The conversion of the target sphere angular position from the split-beam coordinate system to the MBES coordinate system is then achieved using the procedure described in Section 4.4.1.

4.5 – Time Synchronization

The time information recorded for each ping on each of the systems during the beam pattern calibration procedure is used to verify the existence of missing pings in their records and determine the correct ping pairs. For this reason, the recorded data sets from the two sonar systems need to have the same time reference. The proposed field calibration procedure employs the Network Time Protocol (NTP) to synchronize both sonar systems.

4.5.1 – The Network Time Protocol (NTP)

NTP is a public domain software package which is an implementation of the TCP/IP network protocol. It adjusts the time in the system computer according to a particular configuration. Each NTP daemon (service program running in the background of the computer) can work as client, server, or peer for other NTP daemon. As client, it adjusts its time by checking a reference time from one or more servers. As server, it makes its time available for other clients.

As a peer, the computer checks other peers and they agree about a time for synchronization. A hierarchical time synchronization structure can be built using these features, where each level on this hierarchy is called a stratum. Higher hierarchy levels in such a structure have lower stratum numbers, with more accurate time. The stratum level of a NTP daemon is always one level below the one of its time reference (Meinberg [6]).

The NTP package used for the beam pattern calibration procedure was downloaded from the Meinberg website (www.meinberg.de) and installed on both sonar system computers. The split-beam system computer was set as server to provide the synchronization time for the MBES computer working as client. Figure 4.16 shows the NTP Status tab on the NTP Time Server Monitor window on each system. As shown by this figure, the split-beam computer is a stratum 2, while the MBES computer is a stratum 3 with a synchronization offset of approximately 4 msec. The operational ping rate is much lower than the value of this time offset, allowing pairing the recorded pings of both sonar systems in a proper manner to be used in the beam pattern computations. The time server used by the NTP server daemon installed at the split-beam system is not of importance here, since the only interest is to keep the MBES synchronized in time with the split-beam sonar system.
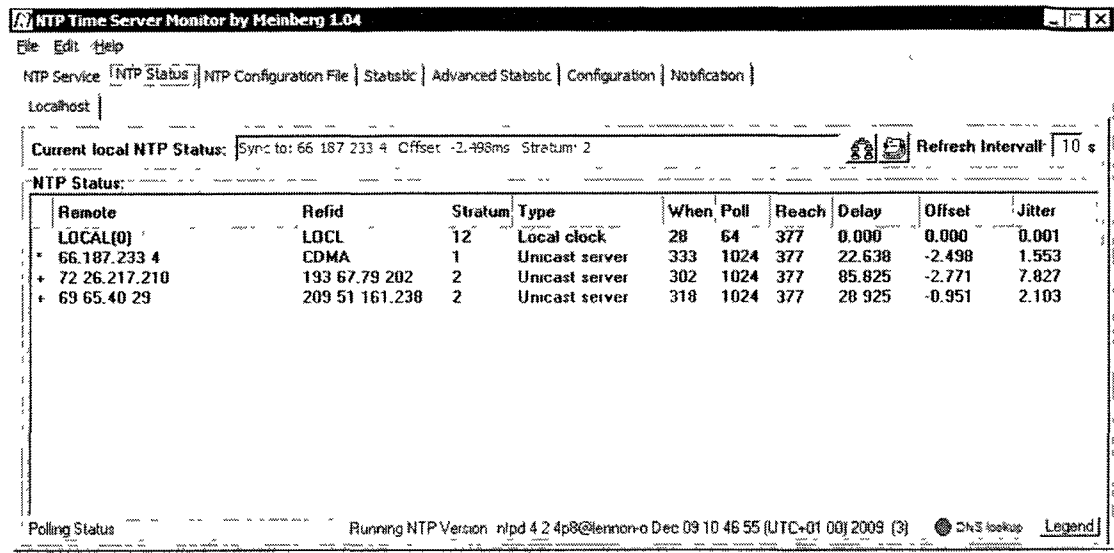
(a) – Split-beam computer
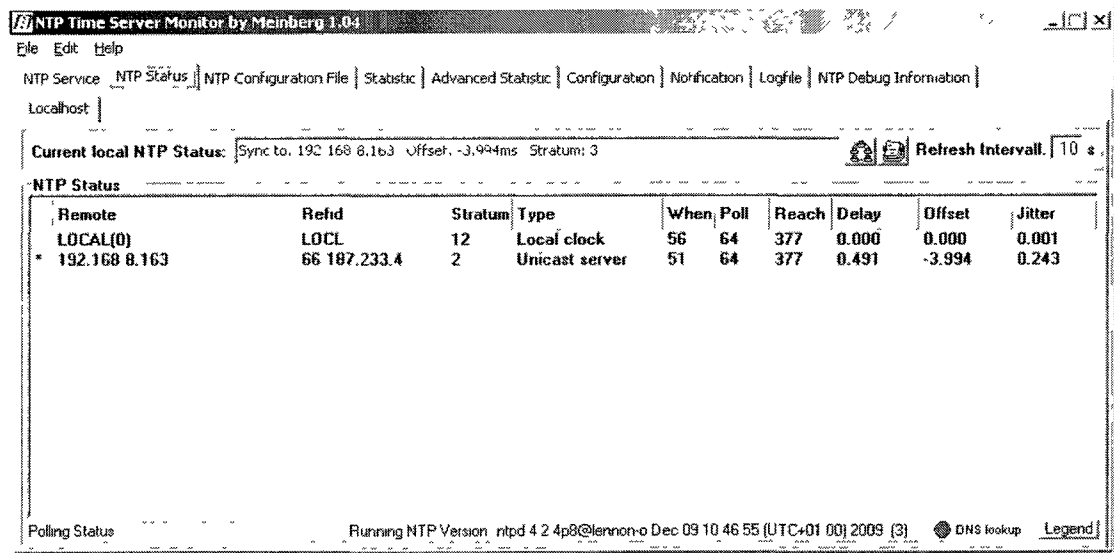
(b) – MBES computer

Figure 4.16 – NTP Time Server Monitor by Meinberg: NTP Status tab

4.5.2 – Check of Missing Pings on Recorded Data from Both Sonar Systems

Even after having both sonar systems synchronized in time, the existence

of missing pings on either of the systems or both systems must be checked

before pairing pings for the beam pattern computation. This is performed by

checking the time stamp for each ping of each system. If a ping is missing in one sonar system, the corresponding ping in the other system needs to be discarded. Figure 4.17 illustrates the missing ping problem.
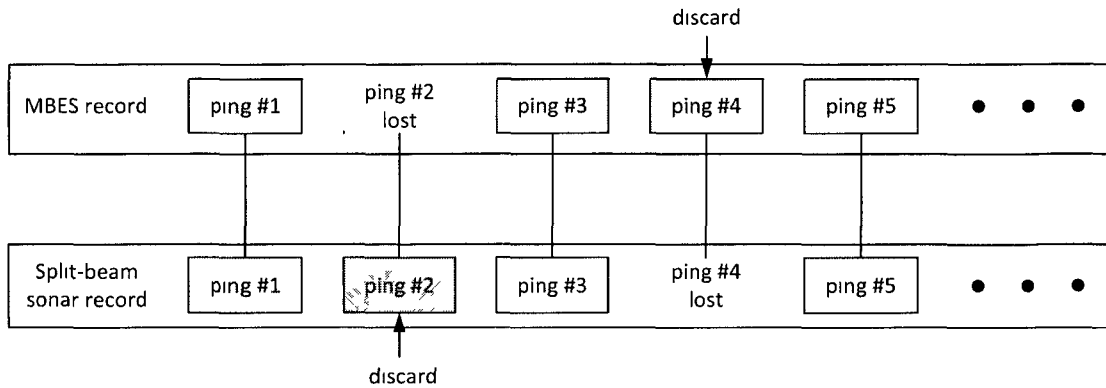
Figure 4.17 – The missing ping problem

A MATLAB program called *missPingsIDX.m* was designed to check for missing pings in both sonar system records and to discard the corresponding ping in the other system record. The time records of both systems were first transformed into the same format and used to identify pings with time stamps of the same value. If a ping in one system record does not have a corresponding ping in the other system record, then that ping is discarded. The algorithm returns two vectors indicating the indices of the recorded pings to be discarded on each of the systems, along with the valid number of pings and an error flag. The code takes into consideration the time delay between the two systems explained in Section 4.4.2 and the time synchronization offset. Figure 4.18 shows the block diagram of the *missPingsIDX.m* code.
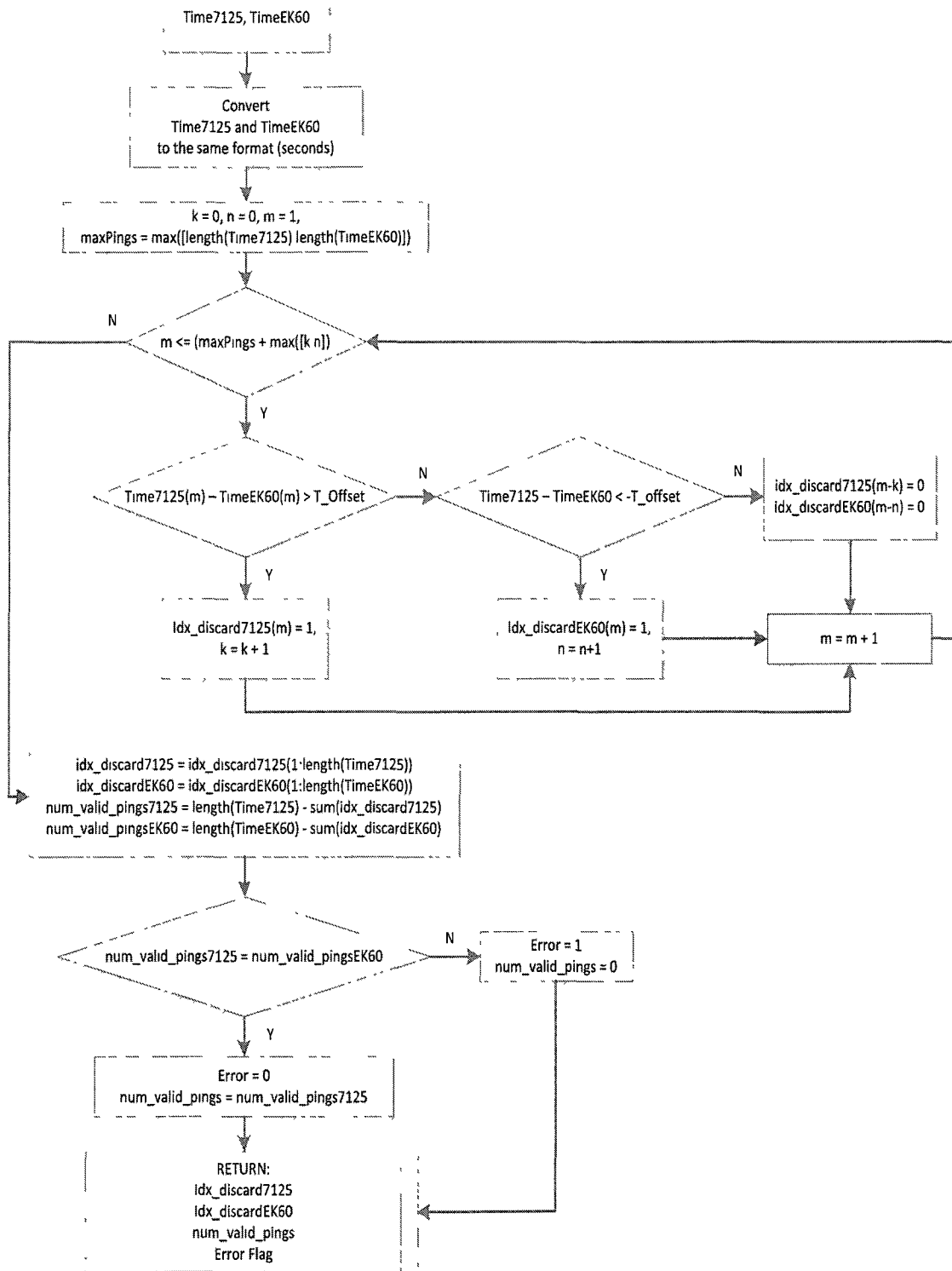
Figure 4.18 – Block diagram of code used to identify missing pings

The difference between the time stamp of a ping from one sonar system and the time stamp of a ping from the other sonar system is compared to a time offset T_{offset} given by

$$T_{offset} = t_{system\ delay} + time\ synchronization\ offset.\tag{4.5.1}$$

If the difference between the time stamps is greater than the absolute value of T_{offset}, then the two pings are not paired.

4.6 – Beam Pattern Measurements Procedure

The proposed calibration methodology is applied in two parts: i) collection of measurements with the target sphere at the MBES MRA and ii) collection of measurements with the target sphere sweeping an area containing the angular limits of interest, but at approximately constant distance from the transducers. The first part is necessary to determine the angle offset in the athwartship direction between the MRAs of the two sonar systems (α_o) and the time delay between their triggers ($t_{system\ delay}$). Since the beam pattern is a relative measurement, the determination of the angle offset in the alongship direction between the MRAs of the two systems is not required for the described configuration. The alongship angle offset in the resulting beam pattern of the MBES is subtracted at a final stage of the data processing.

Figure 4.19 depicts the main window of the software which controls the MBES (7k Control Center), showing the target sphere between beams 128 and

129 (the MRA of the MBES) at the range of 8 m. Figure 4.20 shows the main window of the software which controls the split-beam system (SIMRAD ER60).
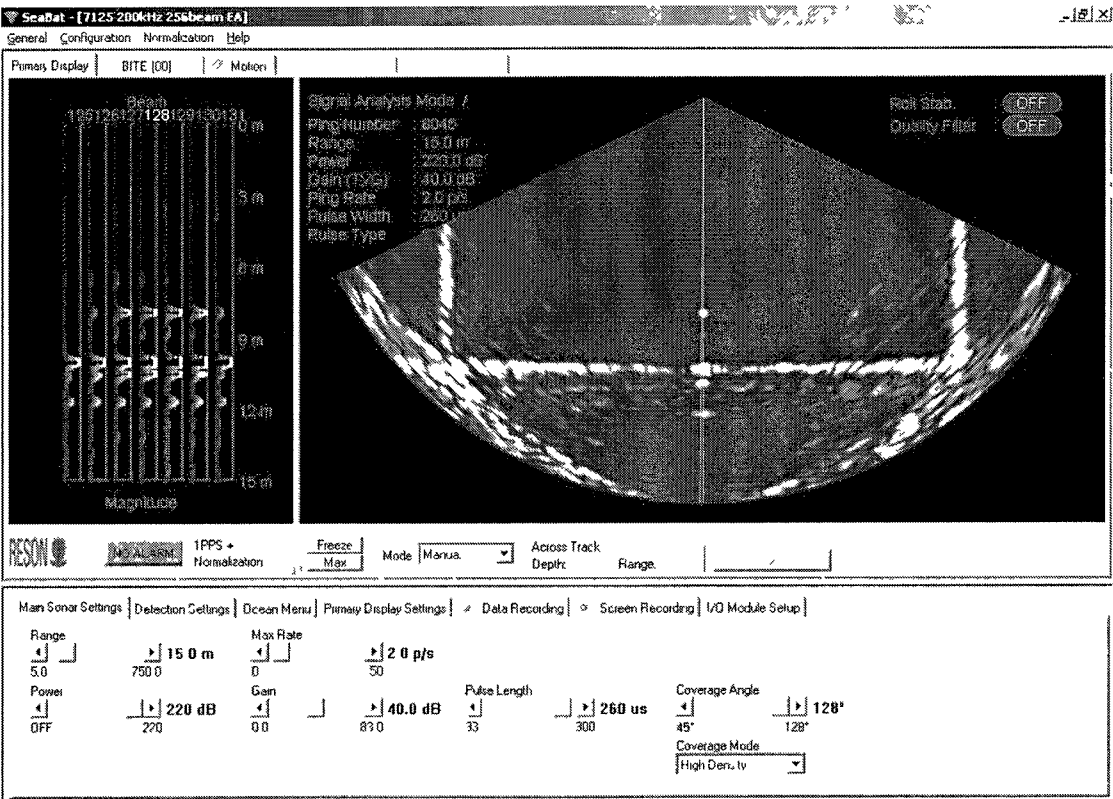
Figure 4.19 – Main window of 7k Control Center, target sphere at MBES MRA
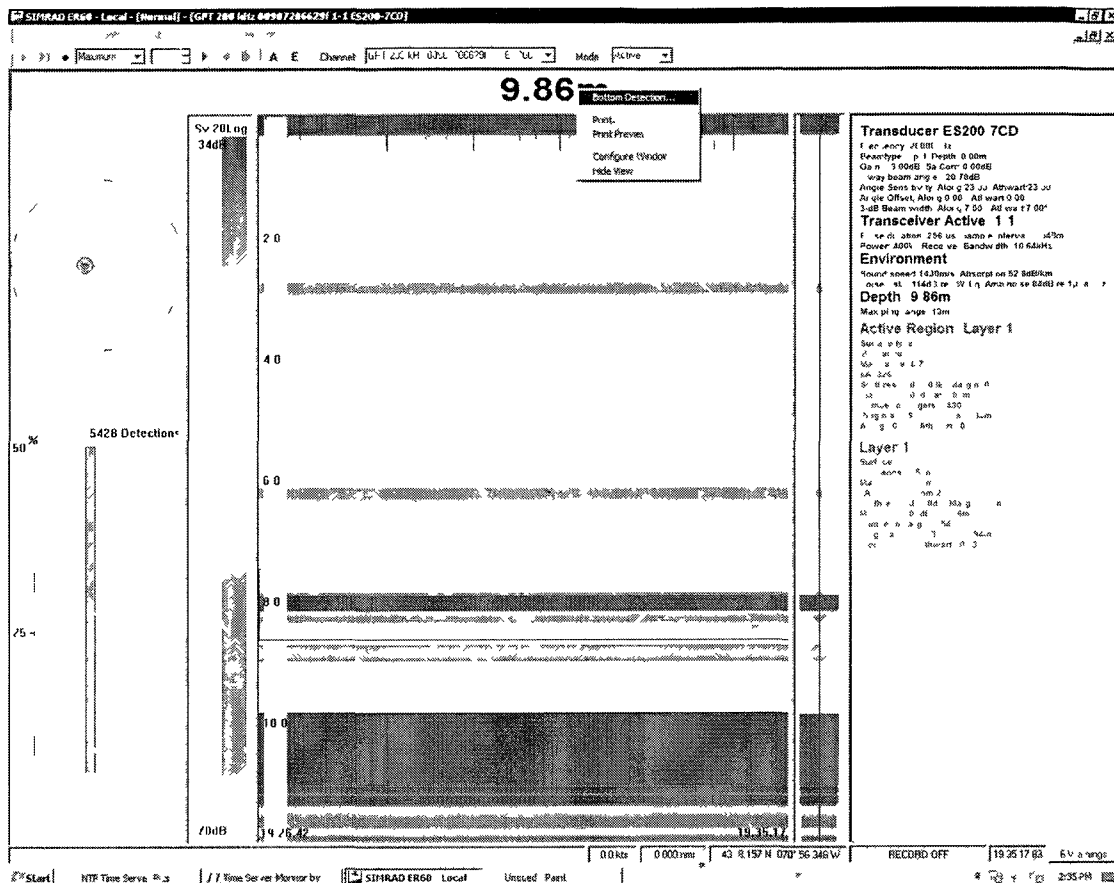
Figure 4 20 – Main window of SIMRAD ER60, target sphere at MBES MRA

The second part of the calibration procedure uses the resulting data from the first part to provide the amplitude of the returned signals from the target sphere along with its corresponding position information, for computing the combined transmit/receive radiation beam pattern of the MBES.

Settings for both sonar systems were kept the same during measurements of parts 1 and 2. Tables 4.1 and 4.2 present the main settings for the RESON 7125 MBES and for the SIMRAD EK60 split-beam echo sounder, respectively. The MBES was configured for 256 beams equi-angle mode at an operating frequency of 200 kHz. It was set to operate at a power setting of 220 dB and a

gain setting of 40 dB. Those power and gain settings were chosen to optimize the transmitted power and the linear range usage of the MBES. The importance of working in the linear range was discussed in the results from the procedure described in Chapter 2 and presented in more detail by Greenaway & Weber [4]. Appendix A presents the methodology used to determine the optimal power and gain settings of the MBES for use in the field calibration procedure. The split-beam system was set to work passively at the same frequency of the MBES. The same sound speed of 1490 m/s was set to both sonar systems, which are used later on the data processing stages (the sound speed in the tank was measured with a digi-bar).

Table 4.1 – RESON 7125 MBES main settings

Power Mode	Power (dB)	Gain (dB)	Pulse Length (µs)	Range (m)	Sound Velocity (m/s)
Active	220	40	260	15	1490

Table 4.2 – SIMRAD EK60 split-beam echo sounder main settings

Power Mode	Pulse Length (µs)	Surface Range (m)	Sound Velocity (m/s)
Passive	256	Start: 0 Range:12	1490

Three complete sets of measurements were performed to compute the beam pattern of the RESON 7125 MBES with ping rates of 2 pings/sec, 3 pings/sec, and 4 pings/sec. Data sets with higher ping rates were expected, however, the bottom detection range setting at the split-beam system was set too

high and many missed pings occurred during the higher ping rate measurements. As a result, the three data sets ended up with approximately the same number of valid pings during the data processing stage. The transducers of both systems and the target sphere were soaped with detergent before the measurements to reduce possible formation of air bubbles on their surfaces and therefore minimize acoustic interference.

It was observed during preliminary tests that the first few pings recorded by the EK60 split-beam sonar system corresponded to pings received from its last operation. For this reason, the first 4 pings from both systems were discarded for the measurements during the data processing stages.

An algorithm written in MATLAB called *fcbp_7125_EK60.m* was designed to read and process the raw files from both sonar system recorded in parts 1 and 2 and to produce a plot of the beam pattern of the MBES. The tasks executed by this algorithm are explained in the following sections.

4.7 – Beam Pattern Measurements Data Processing

4.7.1 – Part 1: Target Sphere at MBES MRA

Data was recorded from both sonar systems for 50 pings transmitted by the MBES with the target sphere placed at its MRA. This data was then processed to provide the angular offset between the MRA of the two systems (α_o) and the time delay between their triggers ($t_{system\,delay}$). The tasks performed by the MATLAB algorithm in part 1 are presented next.

In this code, the user inputs the minimum and maximum range (in meters) for which the sphere is expected to be from the transducers (*maxRange* and *minRange*, respectively). The EK60 raw file is read, providing for each ping the alongship and athwartship angles for the whole range of the record (*AlongAngEK60_o* and *AthwartAngEK60_o*, respectively), the sound velocity (*SoundVelEK60*), the point backscattering strength (*Sp*) values for the whole range of the record (*SpEK60_o*), the time stamp (*TimeEK60*), the sample interval (*SampleIntervalEK60*), and the number of pings (*numPingsEK60*). The maximum and minimum range values corresponding to the range which the target is expected to be are used to compute the corresponding maximum and minimum time indexes (*ibrEK60* and *isrEK60*, respectively). These indices define the target region and are given by

$$ibrEK60 = (minRange * 2)/(SampleIntervalEK60 * SoundVelEK60) \qquad (4.7.1)$$

and

$$isrEK60 = (maxRange * 2)/(SampleIntervalEK60 * SoundVelEK60). \qquad (4.7.2)$$

The location of the target sphere in the records is determined by finding the maximum *Sp* value within the target region. Figure 4.21 shows the *Sp* values for one ping record of the SIMRAD EK60, highlighting the data at the target region in red. The time index of maximum *Sp* value for each ping (*indMaxSpEK60*) is used to extract the alongship and athwartship angles corresponding to the target sphere position. Figure 4.21 shows the records of these angles for one ping, highlighting the data at the target region in red.

The time interval taken from the transmitted signal to reach the target

sphere and then the EK60 transducer (t_2) is given by

$$t_2 = SampleIntervalEK60 * indMaxSpEK60 . \qquad (4.7.3)$$

(a) – Horizontal scale: time index   (b) – Horizontal scale: range in meters
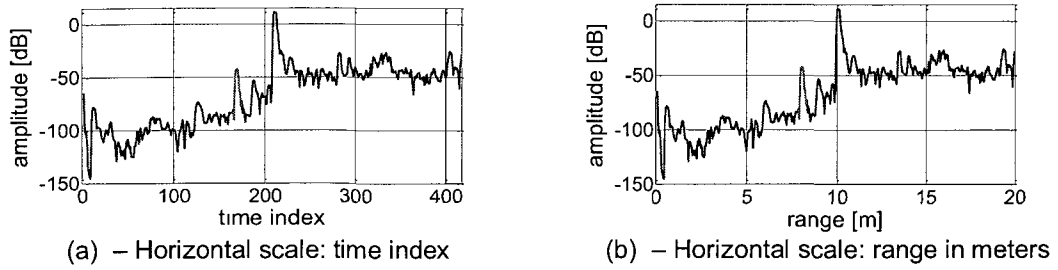
Figure 4.21 – Sp values from EK60 record

(a) – Alongship angles   (b) – Athwartship angles
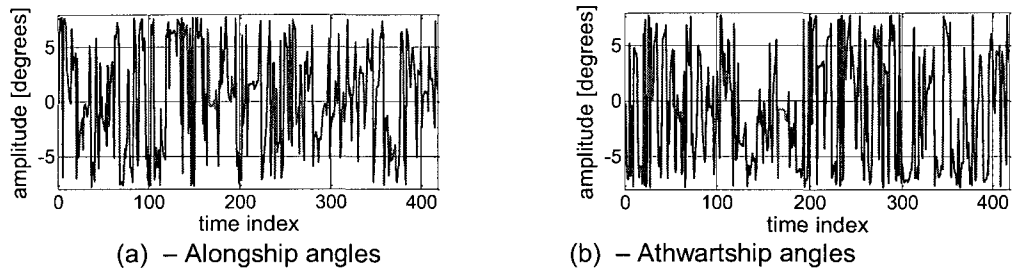
Figure 4.21 – Angles from EK60 record

Next, the MBES raw file is read, providing for each ping the amplitude of

the returned signal for the whole range of the record for all of the 256 beams

($Amp7125\_o$), the sound velocity ($SoundVel7125$), and the sample rate

($SampleRate7125$). Similarly as is done for the EK60 record, the position of the

target sphere in this record is determined by finding the time index of the largest

amplitude in the target region ($indMaxAmp7125$) defined by $minRange$ and

$maxRange$ values. The time indices corresponding to the target region in the

MBES record are given by

$$ibr7125 = (minRange * 2)/(SoundVel7125 / SampleRate7125) \qquad (4.7.4)$$

and

$$isr7125 = (maxRange * 2)/(SoundVel7125 / SampleRate7125). \qquad (4.7.5)$$

The amplitude corresponding to the sphere return for each of the 256

beams ($Amp7125$) is calculated by taking an average value of the amplitude

record $Amp7125\_o$ around the $indMaxAmp7125$ time index. This time index

interval was defined from 5 time indices below to 5 time indices above

$indMaxAmp7125$. Figure 4.22 shows the MBES returned signal: the blue line

corresponds to the entire range while the red line corresponds to the target

sphere region defined by the indexes $ibr7125$ and $isr7125$. Figure 4.23 shows

the details of the $Amp7125$ calculation.
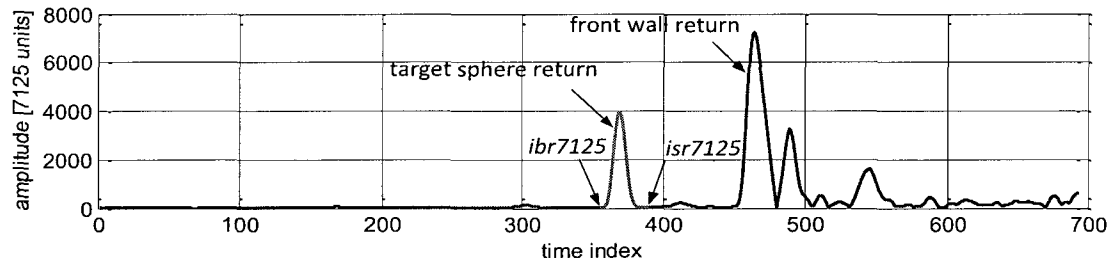
(a) – horizontal axis: time index
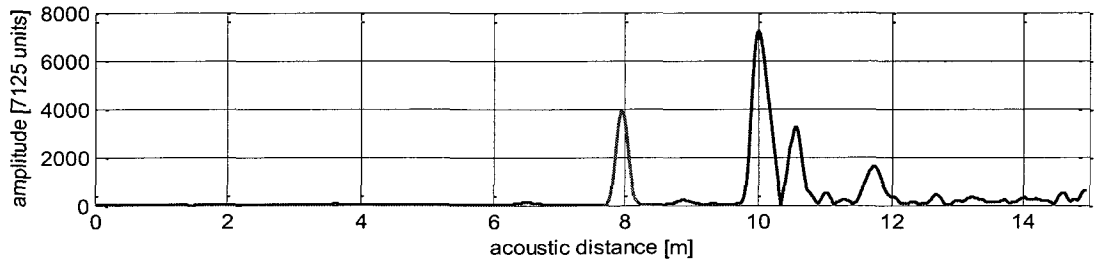
(b) – Horizontal axis: acoustic distance

Figure 4.22 – $Amp7125$ calculation
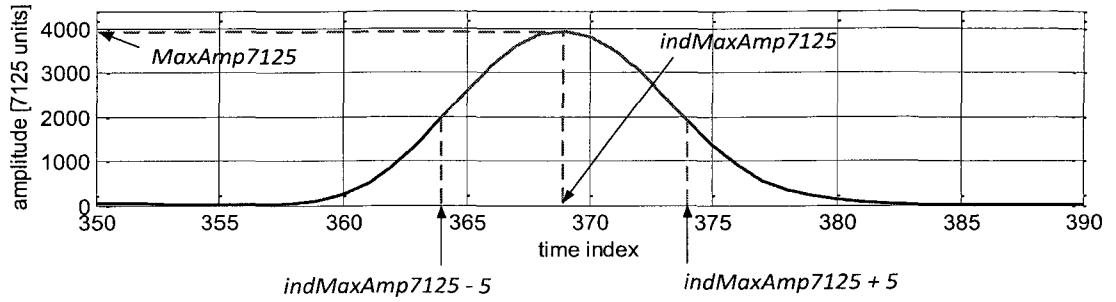
Figure 4.23 – *Amp7125* calculation detail

The time interval corresponding to the travel of the transmitted signal from the MBES transducer to the target sphere and then back to the MBES transducer (t_1) is obtained by first finding the time index of the beam with the maximum amplitude value corresponding to the target sphere return, *maxBeamAmpIdx*. Then, the time interval t_1 is given by

$$t_1 = indMaxAmp7125(maxBeamAmpIdx) / SampleRate7125. \tag{4.7.6}$$

The values of alongship and athwartship angles (β_{EK60} and α_{EK60}, respectively) and the time intervals t_1 and t_2 are averaged between the 50 pings and are used to calculate the system time delay ($t_{system\ delay}$). The distance between the target sphere and the MBES transducer (d_{7125}) is given by

$$d_{7125} = SoundVel7125 * \left(t_1 / 2\right). \tag{4.7.7}$$

The distance between the target sphere and the split-beam transducer (d_{EK60}) is given by using (4.4.16):

$$d_{EK60} = \sqrt{d_{7125}^2 + y_t^2}, \tag{4.7.8}$$

where y_t is the distance between the split-beam transducer to the MBES transducers. The expected time interval for the travel of the transmitted signal

from the MBES transducer to the target sphere and then to the split-beam

transducer ($t_{2\_expected}$) is calculated using (4.4.17):

$$t_{2\_expected} = \left(d_{7125} + d_{EK60}\right)\big/ SoundVel7125 \tag{4.7.9}$$

and the time delay between the triggers from both sonar systems is calculated by

applying (4.4.18):

$$t_{system\ delay} = t_2 - t_{2\_expected}. \tag{4.7.10}$$

The athwartship angle offset between the MRAs (α_o) is determined using

4.4.8, where α_{EK60} is the split-beam system athwartship angle found for the target

sphere position. Figure 4.24 depicts the block diagram of the algorithm employed

in part 1 of the data processing.

v, yt, minRange, maxRange

Read SBES raw file for target at EK60 MRA

athwartship and alongship angles in EK60 coordinates,
SoundVelEK60, numPingsEK60, TimeEK60, SpEK60

EK60 range indexes of target position:
ibrEK60 =
(minRange * 2) / (SampleIntervalEK60 * SoundVelEK60)
isrEK60 =
(maxRange * 2) / (SampleIntervalEK60 * SoundVelEK60)

Find index of maximum value in SpEK60 for
index range [ibrEK60 isrEK60]:
indMaxSpEK60

Get alonship and athwartship angle values corresponding
to index indMaxSpEK60

Get time interval t2 (7125 – target – EK60):
t2 = SampleIntervalEK60 * indMaxSpEK60

all pings

Read MBES raw file for target at MBES MRA

Amplitude of return signal
Amp7125_o

7125 range indexes of target position:
ibr7125 =
(minRange * 2) / (SoundVel7125 / SampleRate7125)
ibr7125 =
(maxRange * 2) / (SoundVel7125 / SampleRate7125)

Find index of maximum amplitude value for
index range [ibr7125 isr7125]:
indMaxAmp7125

Amplitude of 7125 is the average around index
indMaxAmp7125

Find beam with max amplitude (beamMaxAmp)

Get time interval t1 (7125 – target – 7125):
t1 =
indMaxPower7125(beamMaxAmp) / SampleRate7125

Take the average of pings for:
alongship_angle_EK60, athwartship_angle_EK60, t1, t2

all pings

Distance between target and 7125:   d7125 = SoundVelEK60 * (t1 / 2)
Distance between target and EK60:   dEK60 = sqrt(yt^2 +d7125^2)
Expected time t2 (7125 – target – EK60):   t2_expectd = (d7125 + dEK60) / SoundVelEK60
Time delay between the sonar systems: t_system delay = t2 – t2_expected
Athwartship angle offset between 7125 MRA and EK60 MRA:
   alpha_o = 90 - cos (yt / dEK60) + athwartship_angle_EK60

t_system delay, alpha_o

Figure 4.24 – Block diagram of data processing: part 1

96

4.7.2 – Part 2: Target Sphere at Arbitrary Position

The target sphere was used to sweep an area corresponding to approximately an angular range from –6° to +6° in both alongship and athwartship directions relative to the MRA of the split-beam sounder, while the two sonar systems recorded data. The raw datasets from both sonar systems were processed by part 2 of the MATLAB code *fcbp_7125_EK60.m*, which uses the results from part 1 to compute the beam pattern of the MBES. Details of the operations performed in part 2 of this algorithm are explained next.

The EK60 raw file from the split-beam system is read and processed in the same way as explained in part 1 to get for each ping: the alongship and athwartship angular position of the target sphere in the split-beam coordinates (*AlongAngEK60* and *AthwartAngEK60* respectively), the time interval t_2, and the time stamp of the ping *TimeEK60*. However, one more step is added: pings with *Sp* values corresponding to the target sphere position which are smaller than a threshold of -60 dB are discarded. This is done to minimize the presence of outliers in the final beam pattern plot.

Following the same procedure as in part 1, the raw file from the MBES record is read and processed to provide for each ping: the amplitude of the signal corresponding to the target sphere return (*Amp7125*), the time interval t_1, and the time stamp of the ping *Time7125*.

The next step in this algorithm is to check for missing pings in the records of both systems and discard the corresponding recorded pings using the time stamp data (*TimeEK60* and *Time7125*), as explained in Section 4.5.2. The

resulting valid pings from the missing pings checking algorithm are used to calculate the distance between the target sphere and the MBES transducers ($d7125$) employing (4.7.6) and (4.7.7), the travel time from the MBES transducer to the target and then to the split-beam system ($t_{2\_corrected}$), and the distance between the target sphere and the split-beam transducer ($dEK60$). The values of $t_{2\_corrected}$ and $dEK60$ are given by applying (4.4.19):

$$t_{2\_corrected} = t_2 - t_{system\ delay} \qquad (4.7.11)$$

and (4.4.21):

$$dEK60 = SoundVelEK60 * \left(t_{2\_corrected} - \left(t_1 / 2 \right) \right). \qquad (4.7.12)$$

The alongship and athwartship angles corresponding to the target sphere position given by the split-beam system are then transformed into the MBES coordinates. Values of alongship angles from the split-beam coordinate system ($AlongAngEK60$) are assigned to the alongship angles in the MBES coordinate system ($AlongAng7125$) without transformation. The alongship angle offset between the two systems is compensated at a later stage of the data processing. Athwartship angles are converted using (4.4.8), (4.4.9), (4.4.10), (4.4.11), and (4.4.12), as follows:

$$d7125xy = d7125 * cos\left(AlongAng7125 \right), \qquad (4.7.13)$$

$$dEK60xy = dEK60 * cos\left(AlongAng7125 \right), \qquad (4.7.14)$$

$$dy\_sph = dEK60xy * sin^{-1}\left(alpha\_o - AthwartAngEK60 \right), \qquad (4.7.15)$$

$$y\_sph = dy\_sph + yt, \qquad (4.7.16)$$

$$AthwartAng7125 = sin^{-1}\left(\frac{y\_sph}{d7125xy} \right). \qquad (4.7.17)$$

98

The amplitude of the signal corresponding to the target sphere return in the MBES system ($Amp7125$) is converted to decibel relative to its maximum value ($Amp7125dB$),

$$Amp7125dB = 20 * log_{10}\left(\frac{Amp7125}{MaxAmp7125}\right). \qquad (4.7.18)$$

The beam pattern of the MBES is then computed using $Amp7125dB$ as the beam pattern magnitude along the angles $AlongAng7125$ and $AthwartAng7125$. The alongship angle offset between the two systems is determined by inspection of the beam pattern plot and compensated to compute the final beam pattern plot of the MBES. Figure 4.25 depicts the block diagram of the MATLAB code fcbp_7125_EK60.m corresponding to part 2 of the data processing.

v, minRange, maxRange, EK60SpThreshold, t_system delay, alpha_o

---

Read SBES raw file for target at general position

Read MBES raw file for target at general position

---

athwartship and alongship angles in EK60 coordinates,
SoundVelEK60, numPingsEK60, TimeEK60, SpEK60

Amplitude of return signal
Amp7125_o, Time7125

EK60 range indexes of target position
ibrEK60 =
  (minRange * 2) / (SampleIntervalEK60 * SoundVelEK60)
isrEK60 =
  (maxRange * 2) / (SampleIntervalEK60 * SoundVelEK60)

7125 range indexes of target position:
ibr7125 =
  (minRange * 2) / (SoundVel7125 / SampleRate7125)
ibr7125 =
  (maxRange * 2) / (SoundVel7125 / SampleRate7125)

Find index of maximum value in SpEK60 for
index range [ibrEK60 isrEK60]·   indMaxSpEK60

Find index of maximum amplitude value for
index range [ibr7125 isr7125]:
indMaxAmp7125

Get alonship and athwartship angle values corresponding
to index indMaxSpEK60

Amplitude of 7125 is the average around index
indMaxAmp7125

Get time interval t2 (7125 – target – EK60).
t2 = SampleIntervalEK60 * indMaxSpEK60

Find beam with max amplitude (beamMaxAmp)

Discard pings if
SpEK60 < EK60SpThreshold

Get time interval t1 (7125 – target – 7125):
t1 =
  indMaxPower7125(beamMaxAmp) / SampleRate7125

---

all pings

all pings

Check for missing pings: missPingsIDX.m

Distance between target and 7125:   d7125 = SoundVelEK60 * (t1 / 2)
travel time 7125-target-EK60.   t2_corrected = t2 -t_system delay
Distance between target and EK60:   dEK60 = SoundVelEK60 * (t2_corrected – (t1 /2))

Conversion of Coordinates
AlongAng7125 = AlongAngEK60
d7125xy = d7125 * cos(AlongAng7125)
dEK60xy = dEK60 * cos(AlongAng7125)
dy_sph = dEK60xy * sin(-AthwartAngEK60 + alpha_o)
y_sph = dy_sph + yt
AthwartAng7125 = asin(y_sph / d7125xy)

Amp7125db = 20 * log10(Amp7125 / MaxAmp7125)
Compute 7125 beam pattern using: Amp7125dB, AlongAng7125, AthwartAng7125
determine and compensate for alongship offset from beam pattern plot

---

7125 Beam Pattern.
Amp7125dB, AlongAng7125 – Along_offset, AthwartAng7125

Figure 4.25 – Block diagram of data processing: part 2

4.8 – Beam Pattern Measurements Results

The first results from the beam pattern measurements revealed some inconsistencies which are observed in the beam pattern plots. Figure 4.26 shows the computed beam pattern for beam 129.

(a) – Data without interpolation

(b) – Interpolated data

Figure 4.26 – RESON 7125 beam pattern: beam 129

The plot of Figure 4.26.a shows the alongship angular region from 0° to +1° with denser data population than for other regions, which could be evidence of acoustic interference caused by the monofilament line which holds the target sphere. These inconsistencies were investigated by looking in the data provided from the records of the SIMRAD EK60 split-beam system. Figure 4.27 presents the values of athwartship and alongship angles and the Sp values provided by the split-beam system corresponding to the target sphere return.
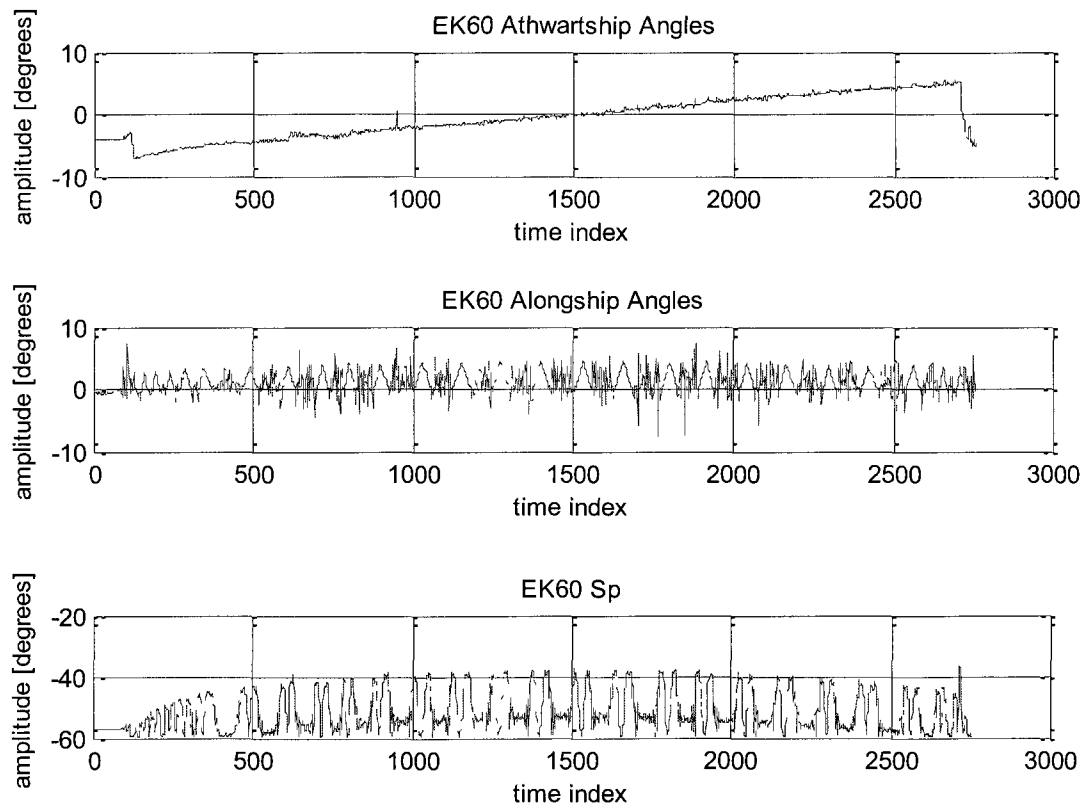
Figure 4.27 – Angular position and Sp data corresponding to the target sphere from split-beam system

By observing the three plots from Figure 4.27, it is possible to notice that the values of alongship angles are noisier for certain time index regions, as well as the Sp values. The knowledge of how the target sphere was moved along the

area of interest during the tests can help to identify time indices of regions of

invalid data to compute the radiation beam pattern of the MBES. The sphere was

moved vertically down, and then moved horizontally to the side before being

moved vertically up, and then moved horizontally to the side before being moved

again vertically down in the acoustic tank, as depicted by Figure 4.28.
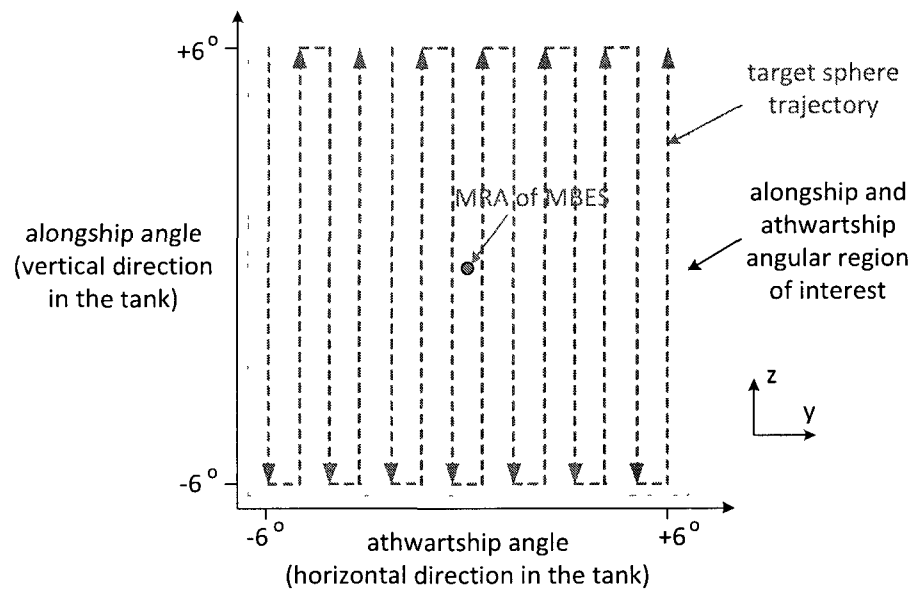
Figure 4.28 – Target sphere trajectory during beam pattern measurements

The alongship angle plot of Figure 4.27 reveals noisy measurements for

regions where alongship angle values corresponding to the target sphere

position are below 0°. This may be evidence of acoustic interference from the

monofilament line, since in these regions the amplitude of the transmitted signal

from the MBES becomes weaker at the sphere position and higher signal

amplitudes are scattered back from the monofilament line, as depicted by Figure

4.29. Consequently, another step in the data processing was performed: data

corresponding to the noisy regions of the alongship angle plot were removed

manually by inspection. Figure 4.30 shows the regions were the noisy data were

discarded highlighted in red.
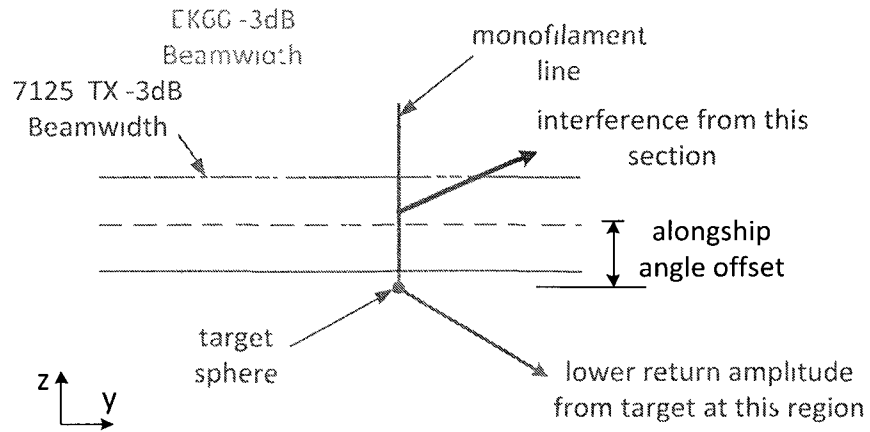
Figure 4.29 – Discarding bad data from split-beam record
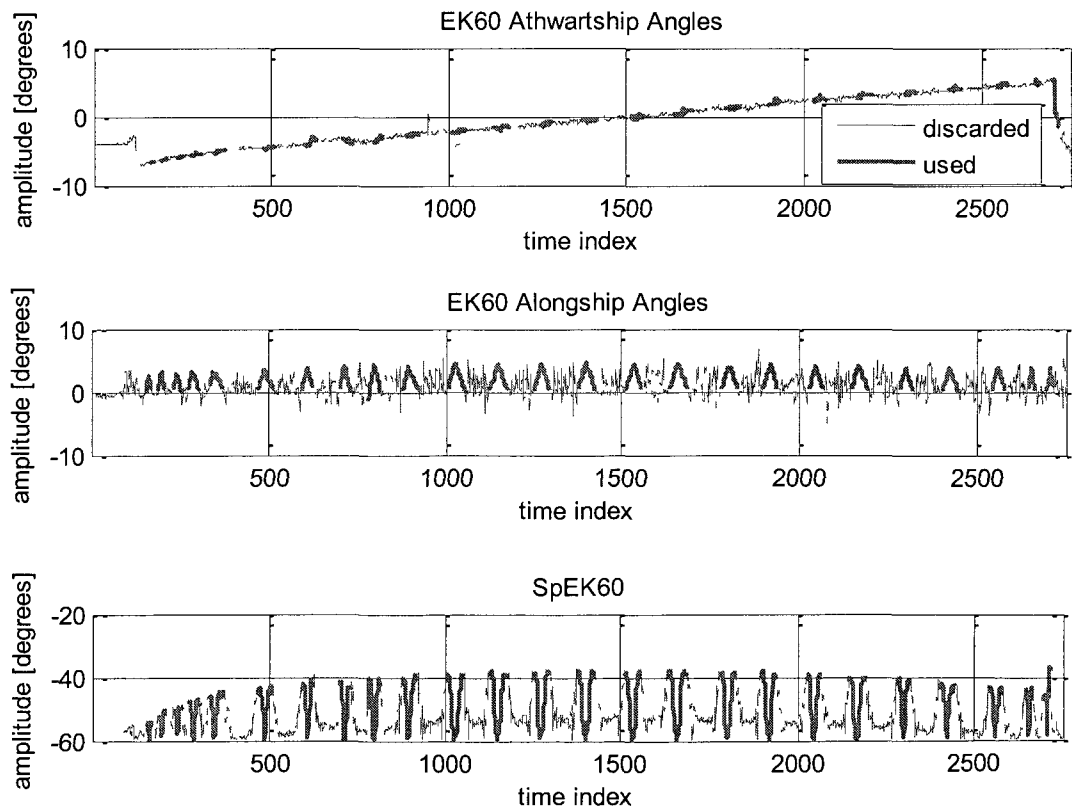
Figure 4.30 – Discarding bad data from split-beam records

After this data cleaning stage, the radiation beam pattern of the MBES was computed again. Figure 4.31 shows the beam pattern plot corresponding to beam 129 of the RESON 7125 multibeam system. This figure presents a much cleaner beam pattern, which still needs to be adjusted for the alongship angle offset between the coordinates of the two sonar systems.
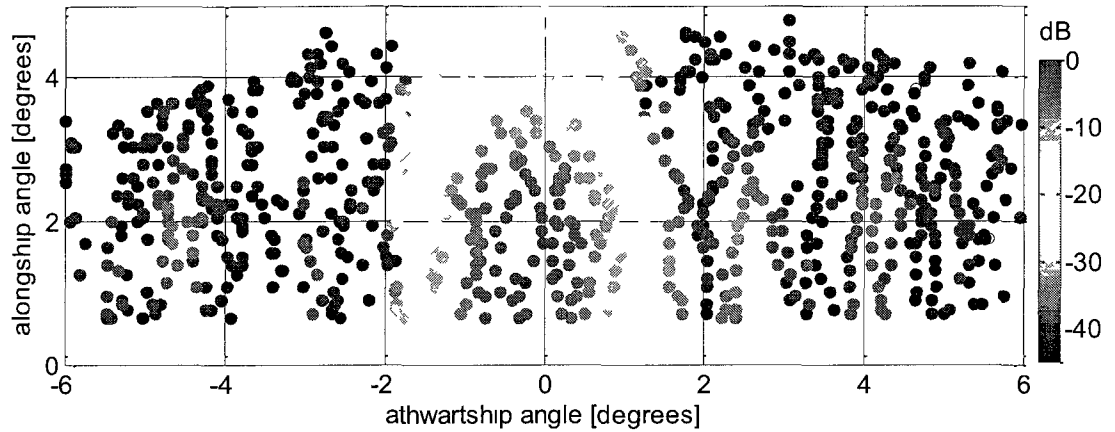
(a) – Data without interpolation
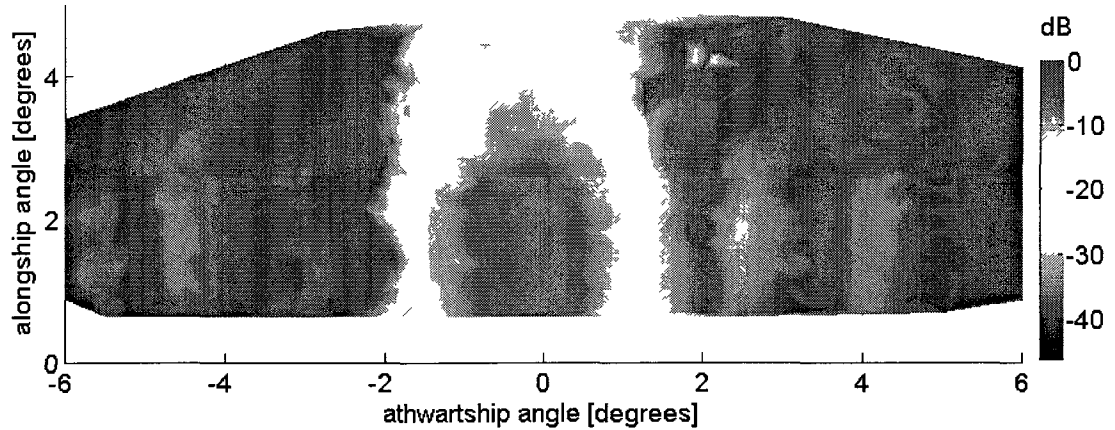
(b) – Interpolated data

Figure 4 31 – RESON 7125 beam pattern after data cleaning – beam 129

The alongship offset is approximately 1.6°, which was determined by inspection of the radiation beam pattern from figure 4.33. This angular offset was

used to compute the final radiation beam pattern of the RESON 7125 MBES.

Figure 4.32 presents the final combined transmit/receive beam pattern plot for

beam 129, compensated for the alongship angle offset and showing contour lines

at −3, −10, −20, and −30 dB. Figure 4.33 shows the three-dimensional plot of the

beam pattern for beam 129.

(a) − Data without interpolation

(b) − Interpolated data
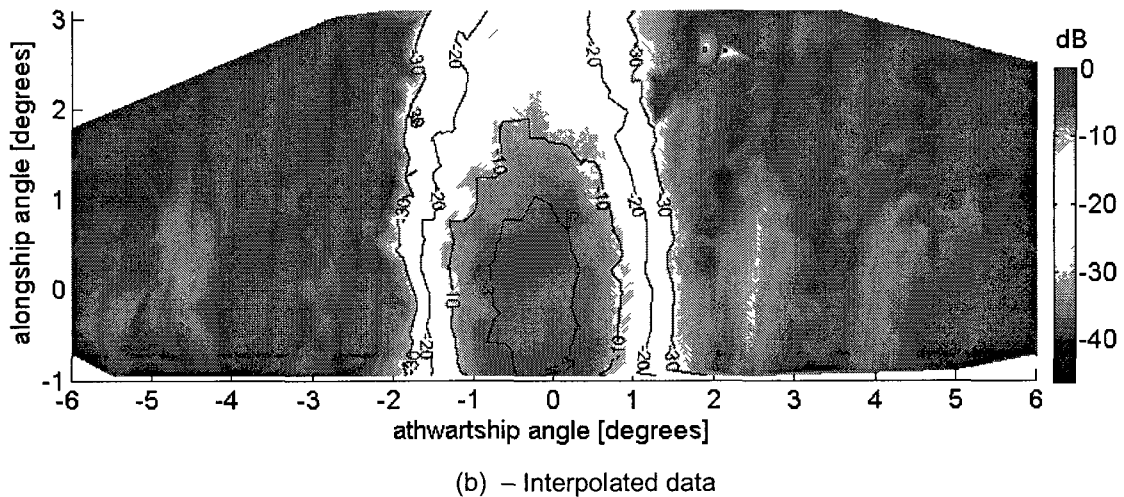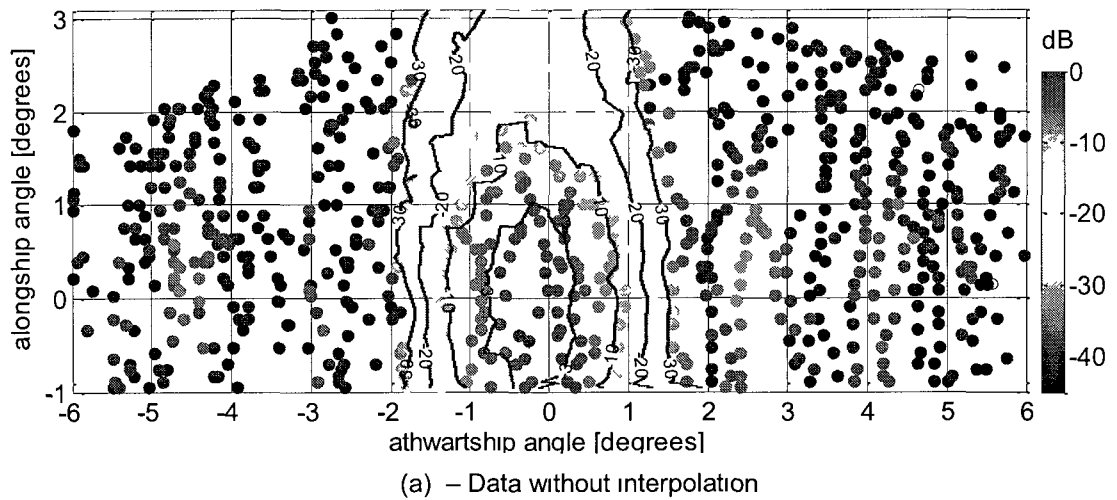
Figure 4.32 − RESON 7125 beam pattern after data cleaning and alongship angle offset
compensation − beam 129
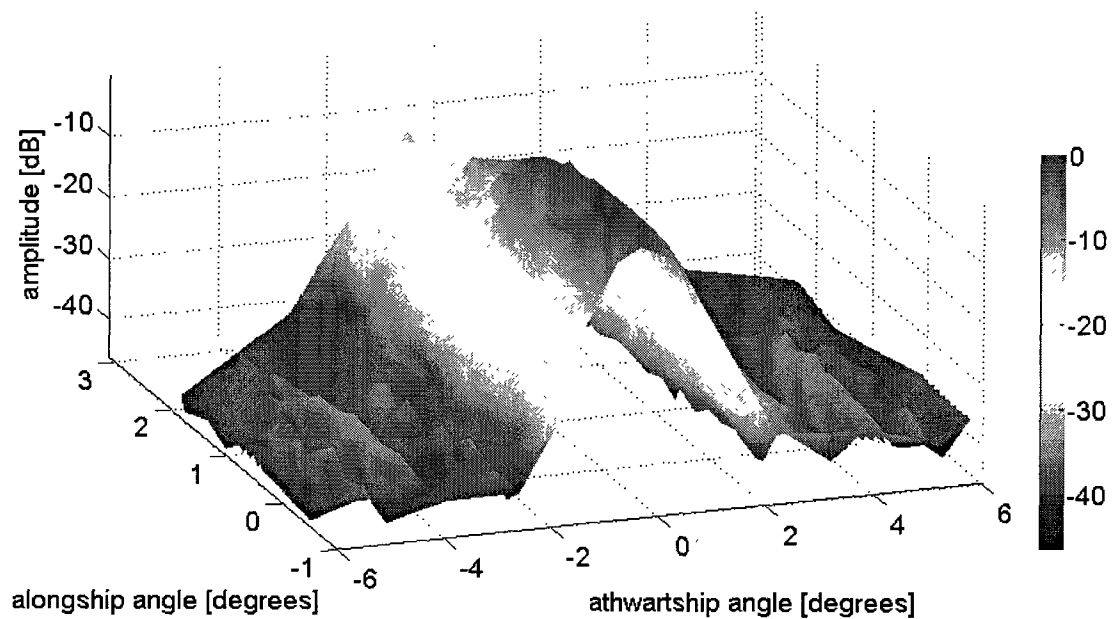
Figure 4.33 – Three dimensional plot of the RESON 7125 radiation beam pattern – beam 129

The –3 dB beamwidth of the computed beam pattern for the RESON 7125 MBES (beam 129) is approximately $1.1°$ in the athwartship direction and approximately $2.0°$ in the alongship direction, which agrees with the manufacturer specification ($1°$ for athwartship direction and $2°$ for alongship direction). Figure 4.34 depicts the plots used to determine these values. The dynamic range, as shown in Figure 4.36.a, is approximately 40 dB relative to the maximum; which limits the ability to resolve side-lobes.
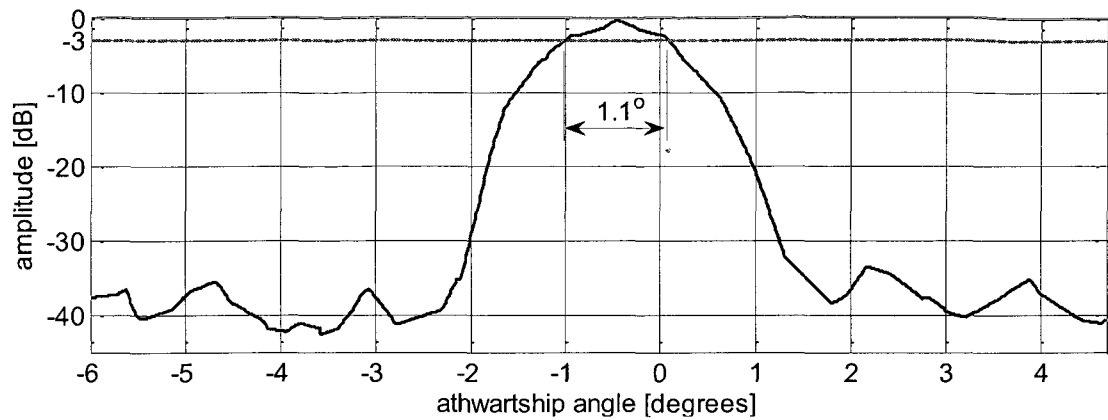
(a) – Athwartship direction
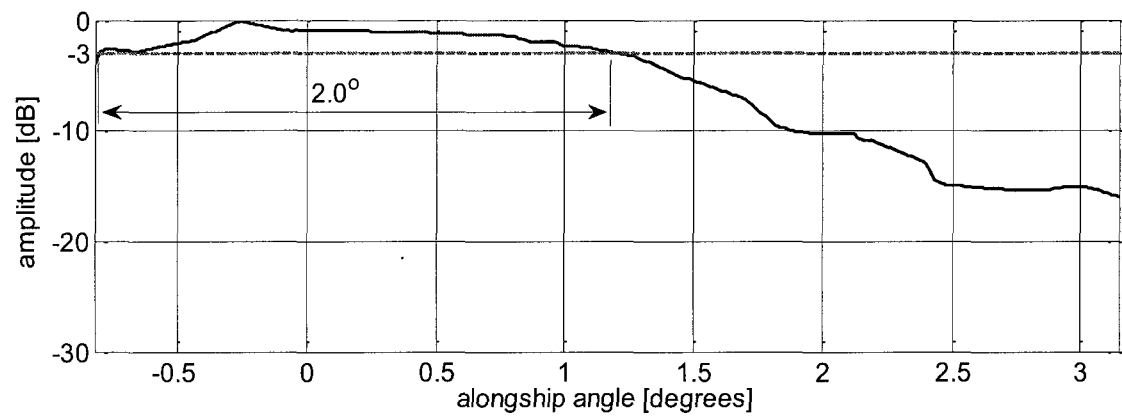
(b) – Alongship direction

Figure 4.34 – -3 dB beamwidth of RESON 7125 for beam 129

Figure 4.35 shows the computed radiation beam pattern plots of the

RESON 7125 MBES for beams 117 to 128 and Figure 4.36 shows the plots for

beams 129 to 140.
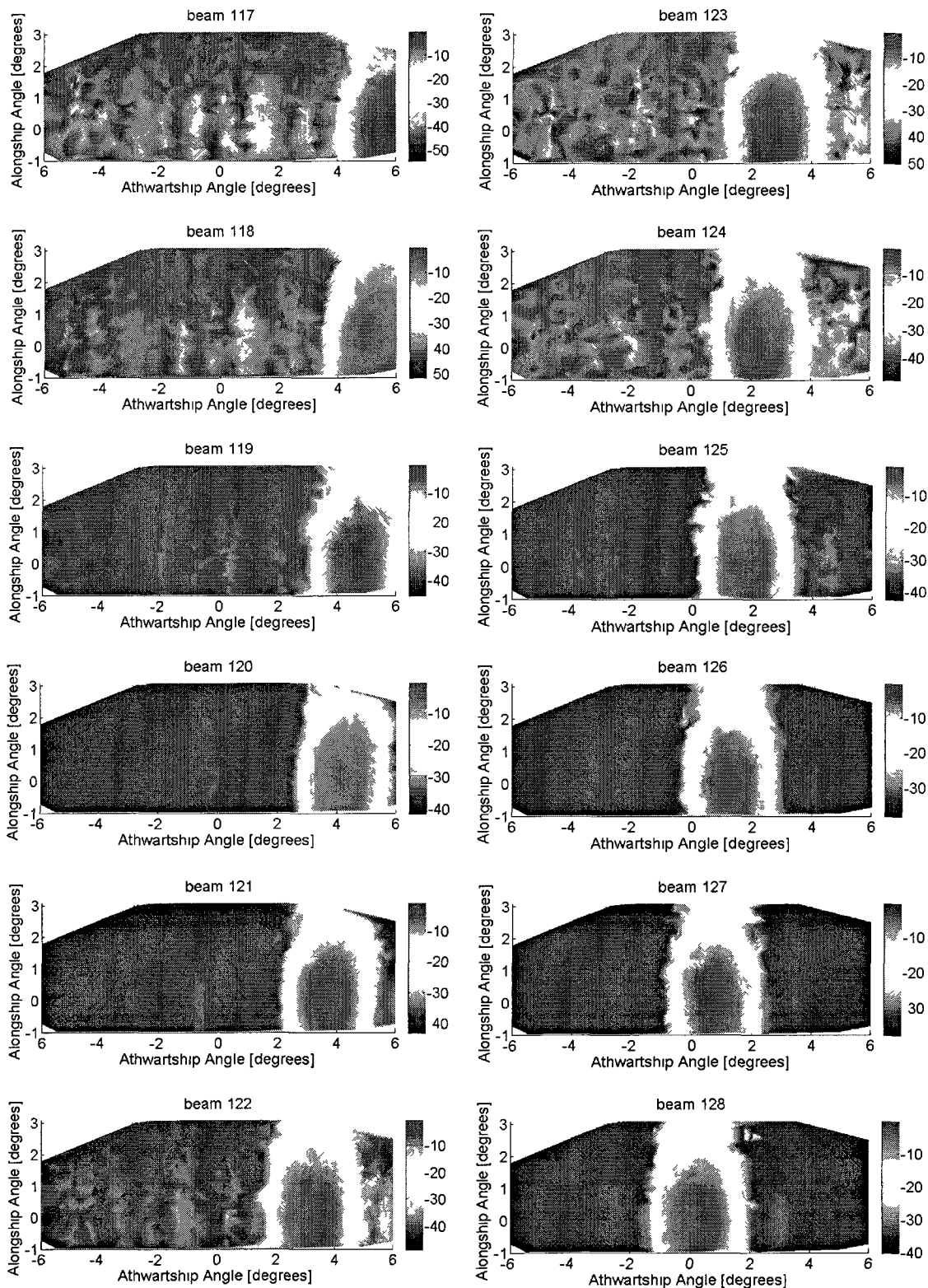
Figure 4 35 – RESON 7125 radiation beam pattern for beam 117 to 128
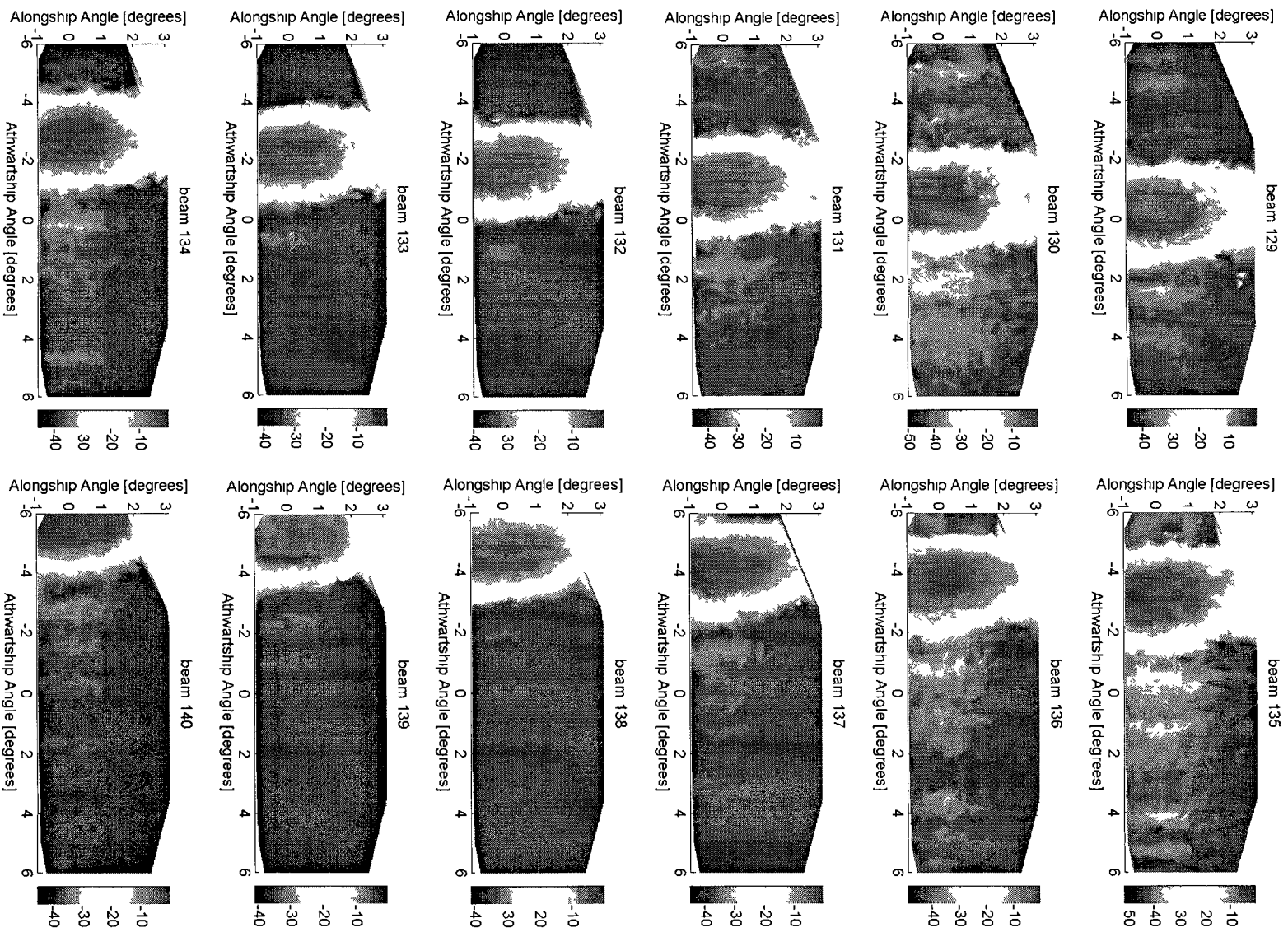
Figure 4 36 – RESON 7125 radiation beam pattern for beam 129 to 140

Figure 4.37 depicts the theoretical composite (transmit/receive) beam

pattern of a Mills cross system. The combined transmit/receive beam pattern

from this figure is very similar to the one measured employing the described field

calibration methodology. Side-lobes corresponding to the receive array can be

observed in the measured beam pattern albeit with some difficulty due to the 40

dB dynamic range. Side-lobes corresponding to the transmit array are not

observed in the measured beam pattern due to the alongship angular range

limits.

(a) – Transmit   (b) – Receive   (c) – Combined
transmit/receive
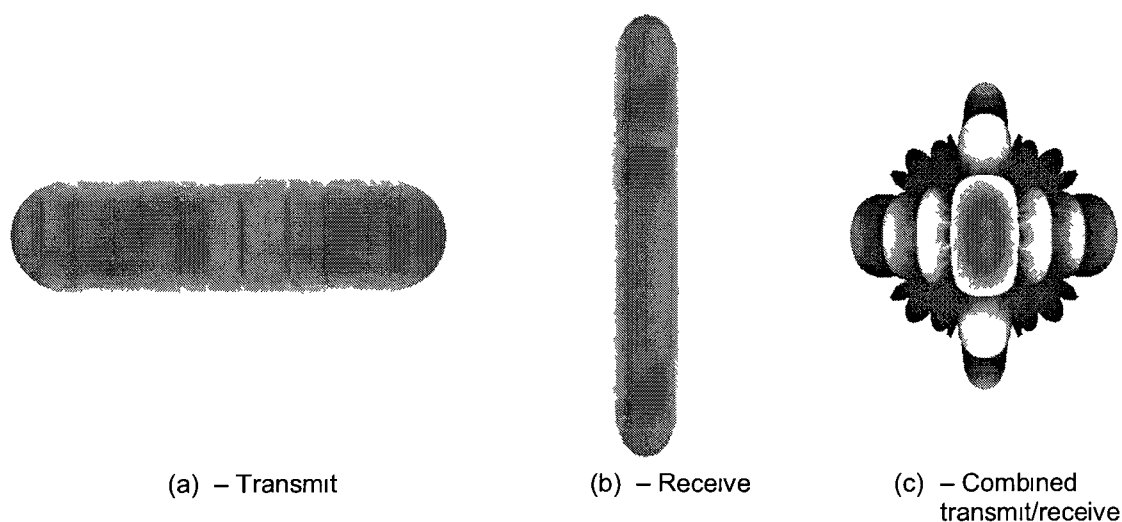
Figure 4.37 – Model of radiation beam pattern for a Mills Cross MBES

4.9 – Remarks

The field calibration methodology tests in the acoustic tank provided

satisfactory results. The MBES was set to transmit with maximum power, with a

fixed gain properly adjusted to maximize the amplitude of the signal return from

the target sphere while keeping the operation region in a linear range, minimizing nonlinearities and saturation effects. These power and gain settings were determined from the power/gain curves of the MBES as described in Appendix A.

The limited range in the athwartship direction in the beam pattern plots is due to the -3 dB beamwidth of $7.0°$ of the SIMRAD EK60 split-beam system. The same angular range limits would be expected in the alongship direction. However, the alongship range is more limited due the combination of this -3 dB beamwidth, the alongship angle offset of $1.6°$ between the systems, and the acoustic interference which is believed to be from the monofilament line, as suggested by the tests of the split-beam accuracy described in Chapter 3.

The measured -3 dB beamwidth in the alongship direction is $2.0°$ and in the athwartship direction it is $1.1°$ for beam 129. These beamwidth values are in line with the manufacturer specifications, which are $2°$ and $1°$, respectively. Side-lobes from the beam pattern estimated from data are difficult to be resolved due to the dynamic range of the measurements being at approximately the same level as the expected side-lobe amplitudes relative to the maximum.

The results from this methodology may be improved for field calibration of ship-mounted systems by using of a thinner monofilament line to suspend the target sphere in the water column and by reducing the offsets between the MRAs of both systems. Different geometry of the shipboard measurement scheme may also improve the results.

CHAPTER 5

CONCLUSION

The use of multibeam echo sounders (MBES) is becoming more frequent in applications like seafloor mapping and characterization, fisheries, and habitat mapping. Beam pattern calibration is of fundamental importance to understanding the performance of MBES and to increase the utility of MBES backscatter measurements. The need for a field calibration methodology for ship-mounted Mills cross multibeam sonar systems was illustrated in Chapter 2. It is clear that despite the high accuracy/high resolution measurements provided by the calibration conducted in a controlled environment, the effort does not account for acoustic interference caused by objects near the transducer mount during field operations and needs a large amount of time to completion. Furthermore, it is not always feasible to bring multibeam echo sounders to a test tank facility for these measurements.

The calibration methodology for multibeam echo sounders (MBES) proposed here employs a split-beam sonar and a standard target. The approach was tested in the fresh water tank of the University of New Hampshire, demonstrating that it is a potential candidate for field calibration of multibeam sonars. This methodology addresses possible mount-related acoustic

interference in ship-mounted systems, allowing 3D (three-dimensional) beam pattern estimates in much less time when compared to methodologies conducted in controlled environments, like the one presented in Chapter 2.

Split-beam echo sounders are commonly calibrated in the field using the standard target method. Employing a transducer with four quadrants, this type of sonar system can detect the standard target position in two dimensions (alongship and athwartship directions). However, when this method is applied to a Mills Cross MBES, the target position can be determined only in the athwartship direction, since the receiver transducer is a line array.

In the methodology described in this document, a standard target and a split-beam echo sounder are used together; the task of the split-beam system is to identify the position of the target during the calibration procedure. This target position information is combined with the magnitude of the signal return corresponding to the standard target to compute the combined transmit/receive beam pattern of the multibeam system.

This methodology was tested on a RESON Seabat 7125 MBES, employing a SIMRAD EK60 split-beam echo sounder with a 200 kHz split-beam transducer ES200-7C and a tungsten-carbide target sphere of 38.1 mm diameter (WC38.1). The tank used to perform the tests has dimensions of 18 m long, 12 m wide and 6 m deep, allowing measurements of combined transmit and receive directional characteristics of the multibeam system at an acoustic distance up to 8 m, while avoiding multi-path interference from the tank walls. The MBES was configured for 256 beams equi-angle mode at an operating frequency of 200

kHz; the split-beam was set to work passively (receive mode) at the same frequency. The calibration procedure allowed the computation of the combined transmit/receive beam pattern for athwartship angular range of –6° and +6° and alongship angular range between –1° and +3° at the range of 8 m. The target sphere, with target strength of –39 dB at 200 kHz, was suspended in the water column by a 30 lbs. test monofilament fishing line (0.3 mm diameter) and moved manually along the athwartship and alongship angles.

The split-beam echo sounder used for this work has a –3 dB beamwidth of 7.0° in athwartship and alongship directions. This characteristic caused the limitation on the angular range of the computed radiation beam pattern of the MBES under test. In addition, possible acoustic interference caused by the monofilament line (as indicated by the tests of the accuracy of the target angle estimates discussed in Chapter 5) combined with the alongship angle offset of 1.6° between the maximum response axes (MRA) of both systems contributed to limiting the alongship angular range of the beam pattern.

The –3 dB beamwidth of the computed beam pattern for the most inner beams is approximately 1.1° in the athwartship direction and approximately 2.0° in the alongship direction. These values agree with the manufacturer specification, which is 1.0° in the athwartship direction and 2.0° in the alongship direction. The dynamic range of the beam pattern measurements was approximately of 40 dB relative to the maximum response, limiting the ability to resolve side-lobes.

Tests to evaluate the accuracy of the split-beam echo sounder were conducted employing the same configuration used for the beam pattern measurements. The first set of tests was performed to identify an optimal value for the pulse length of the transmitted signal based on the angular errors. Three different pulse length values (64 μs, 130 μs, and 260 μs) were used and it was concluded that the longer pulse length provided more consistent and accurate results for measured angular positions by the split-beam system. Longer pulse length values for the transmitted signal cause longer echo return from the target sphere, improving the detection of the target by the split-beam system. A second set of tests was conducted using the pulse length value of 260 μs (same value employed in the calibration procedure) to compute measured athwartship and alongship angular errors from the split-beam system. These tests employed two different configurations: MBES passive/split-beam system active and MBES active/split-beam passive.

The results from the angular accuracy tests show that athwartship angle errors were smaller when the MBES is active than when the split-beam is active. This is likely due to the higher transmitted power provided by the MBES, with larger covered range in athwartship direction than when the split-beam system is active. Alongship angle errors are slightly higher than the athwartship angle errors for the two cases. These angle errors become larger than 1° for alongship angles lower than −1.9° when the MBES is active (after correcting for the alongship angle offset of 1.6° between the MRAs of the two systems); these angle errors are higher than the corresponding alongship angle errors for the

case when the split-beam system is active. This suggests that the monofilament line used to hold the target sphere may have been an interfering factor in the measurements, as was further investigated in subsequent tests. For angular values inside the –3 dB beamwidth range of the split-beam system (+/–3.55° in both alongship and athwartship directions), the athwartship angle errors for both cases (split-beam active and MBES active) vary from +/–0.2°, with smaller angle errors for angular positions closer to the MRA of the split-beam system. Inside this –3 dB beamwidth range, alongship angle errors when the split-beam is active vary from 0° to 0.2° for alongship angles from –0.3° to +3.5° and from 0° to 0.6° for alongship angles from –0.3° to –3.5°. For the case when the MBES is active, the alongship angle errors vary from 0° to 0.3° for alongship angles from –0.3° to +3.5° and from 0° to more than 1° for alongship angles from –0.3° to –3.5°.

Tests employing both 30 lb. and 6 lb. test monofilament lines suggest that when the thinner monofilament line used to suspend the target sphere in the water column there was less acoustic interference, allowing more accurate and stable alongship angle measurements from the split-beam sonar system. The observed interference may have been due to the particular configuration of the setup employed in the acoustic tank, where the MRAs of both sonar systems were pointed parallel to the water level and approximately perpendicular to the monofilament line. Better results may be observed during a field calibration of ship-mounted systems, were the position of the monofilament line would not be in a plane perpendicular to the MRA of any of the transducers.

Despite the restriction imposed by the tank dimensions (18 m long, 12 m wide, and 6 m deep), which could only allow measurements close to the near field of the MBES, the results from the tests provided confidence to extend this methodology to field applications for ship-mounted systems. The results shown here may be improved for field calibration by reducing angular offsets between MRAs of both systems and also by using a thinner monofilament line to avoid acoustic interferences. Even with the limitation in the covered angular region and reduced angular accuracy when compared to an indoor calibration procedure, a field calibration procedure offers the advantages of being applicable to ship-mounted systems operating in the field, with significant reduced operation time.

Future research should include testing the described methodology in field operations. After validating the methodology of employing the split-beam in a fixed position to determine the beam pattern of the MBES under test for a limited angular region, a mechanism should be designed and built to rotate the split-beam transducer in one direction. This rotation would make the MRA of the split-beam transducer point in different positions along the athwartship axis of the MBES, and a more complete beam pattern could be determined in steps using the principles described in this methodology. Some of the issues that should be addressed to apply this calibration procedure in the field are the construction of a split-beam transducer mount with the necessary rigidity to avoid vibrations that could cause interference with the measurements, the determination of a place with acceptable ambient noise to perform the procedure, and possibly an approach to position the target sphere at the MRA of the MBES with sufficient

stabilization as required by the first step in the described field calibration procedure.

.

LIST OF REFERENCES

[1] K.G. Foote, D. Chu, T.R. Hammar, K.C. Baldwin, L.A. Mayer, L.C. Hufnagle, Jr., and J.M. Jech, "Protocols for Calibrating Multibeam Sonar," J. Acoust. Soc. Am., vol. 114, pp. 2013-2027 (2005)

[2] J.C. Lanzoni and T.C. Weber, "High-resolution Calibration of a Multibeam Echo Sounder", Proc. MTS/IEEE Oceans 2010 Conf., Sep. 20-23, Seattle, WA

[3] W.S. Burdic, "Underwater Acoustic System Analysis," 2nd ed., Prentice Hall, New Jersey, 1991

[4] S.F. Greenaway and T.C. Weber, "Test Methodology for Evaluation of Linearity of Multibeam Echosounder Backscatter Performance", Proc. MTS/IEEE Oceans 2010 Conf., Sep. 20-23, Seattle, WA

[5] D. Chu, K.C. Baldwin, K.G. Foote, Y. Li, L.A. Mayer, and G.D. Melvin, "Multibeam Sonar Calibration: Removal of Static Surface Reverberation by Coherent Echo Subtraction," Proc. Oceans 2001, Nov. 6-8, Honolulu, HI, vol. 4, pp. 2498-2502.

[6] Meinberg, *Network Time Protocol (NTP)*, [Online], Available: http://www.meinberg.de/english/info/ntp.htm

[7] T.K. Stanton and D. Chu, "Calibration of Broadband Active Acoustic Systems Using a Single Spherical Target," J. Acoust. Soc. Am. 124, 128-136 (2008)

[8] D. Chu, K.G. Foote, L.C. Hufnagle, Jr., T.R. Hammar, S.P. Liberatore, K.C. Baldwin, L.A. Mayer, and A. McLeod, "Calibrating a 90-kHz Multibeam Sonar," Proc. MTS/IEEE Oceans 2003 Conf., Sep. 22-26, San Diego, CA, pp. 1633–1636

[9] R.J. Urick, "Principles of Underwater Sound," 3rd ed., McGraw–Hill, New York, 1983

[10] L.E. Kinsler, A.R. Frey, A.B. Coppens, and J.V. Sanders, "Fundamentals of Acoustics," 4th ed., Wiley, New York, 2000

[11] X. Lurton, "An Introduction to Underwater Acoustics," 1st ed., Springer, New York, 2002

[12] K.G. Foote, "Optimizing Copper Spheres for Precision Calibration of Hydroacoustic Equipment," J. Acoust. Soc. Am. 71, 742–747 (1982)

[13] K.G. Foote, "Maintaining Precision Calibrations with Optimal Copper Spheres," J. Acoust. Soc. Am. 73, 1054–1063 (1983)

[14] D. Chu, K.G. Foote, and L.C. Jr. Hufnagle, "Measurement of Multibeam Sonar Directivity Patterns," Proc. MTS/IEEE Oceans 2002 Conf., Oct. 29-31, vol. 3, pp. 1411–1414

[15] G.C. Gaunaurd, "Sonar Cross Section of Bodies Partially Insonified by Finite Sound Beams," IEEE J. Ocean. Eng. OE-10, 213–230 (1985)

[16] K.G. Foote and D.N. MacLennan, "Comparison of Copper and Tungsten Carbide Calibration Spheres," J. Acoust. Soc. Am. 75, 612–616 (1984)

[17] T.R. Hammar, K.G. Foote, and S.P. Liberatore, "Advances in Developing a High-frequency Sonar Calibration Facility," Proc. MTS/IEEE Oceans 2003 Conf., Sep. 22-26, vol. 3, pp. 1622–1624

[18] R. Hickling, "Analysis of Echoes from a Solid Elastic Sphere in water," J. Acoust. Soc. Am. 34, 1582–1592 (1962)

[19] K.W. Doherty, T.R. Hammar, and K.G. Foote, "Transducer Mounting and Rotating System for Calibrating Sonars in a Sea Well," Proc. MTS/IEEE Oceans 2002 Conf., Oct. 29-31, vol. 3, pp. 1407–1410

[20] K.C. Baldwin, L.A. Mayer, A. McLeod, and J. Millar, "Acoustic Transducer Calibration System," Proc. MTS/IEEE Oceans 2003 Conf., Sep. 22-26, vol. 4, pp. 2093–2099

[21] D. Chu, K.C. Baldwin, K.G. Foote, Y. Li, L.A. Mayer, and G. D. Melvin, "Multibeam Sonar Calibration: Target Localization in Azimuth," Proc. MTS/IEEE Oceans 2001 Conf., Nov. 5-8, vol. 4, pp. 2506–2510

[22] D. Chu, K.G. Foote, T.R. Hammar, L.C. Hufnagle, Jr., and J.M. Jech, "Calibrating a 90-kHz Multibeam Sonar: Illustrating protocols," Proc. MTS/IEEE Oceans 2004 Conf., Sep. 22-26, vol. 3, pp. 438–442

[23] J.M. Jech, K.G. Foote, D. Chu, and S.P. Liberatore. "Comparing Two Scientific Echo Sounders," Proc. MTS/IEEE Oceans 2003, Sep. 22- 26, San Diego, CA, vol. 3, pp. 1630

[24] E. Ona, V. Mazauric, and L. N. Andersen, "Calibration Methods for Two Scientific Multibeam Systems," ICES Journal of Marine Science, 66: 1326-1334 (2009)

[25] L.R. Dragonette, S.K. Numrich, and L.J. Frank, "Calibration Technique for Acoustic Scattering Measurements," J. Acoust. Soc. Am. 69, 1186-1189 (1981)

[26] S. Vagle, K.G. Foote, M.V. Trevorrow, and D.M. Farmer, "A Technique for Calibration of Monostatic Echosounder Systems," IEEE Journal of Oceanic Engineering, 1996, 21, 298-305 (1996)

[27] K.G. Foote, D.T. Francis, and P.R. Atkins, "Calibration Sphere for Low-frequency Parametric Sonars," J. Acoust. Soc. Am. 121, 1482–1490 (2007)

[28] K.G. Foote, A. Aglen, and O. Nakken, "Measurement of Fish Target Strength with a Split-beam Echo sounder," J. Acoust. Soc. Am. 80, 612–621 (1986)

[29] K.G. Foote, "Coincidence Echo Statistics," J. Acoust. Soc. Am. 99, 266–271 (1996)

[30] J.J. Faran, Jr., "Sound Scattering by Solid Cylinders and Spheres," J. Acoust. Soc. Am. 23, 405–418 (1951)

[31] F.E. Tichy, H. Solli, and H. Klaveness, "Non-linear Effects in a 200-kHz Sound Beam and the Consequences for Target-strength Measurement," ICES Journal of Marine Science, 60, 571-574 (2003)

[32] Y. Miyanohana, K. Ishii, and M. Furusawa, "Spheres to Calibrate Echo Sounders at Any Frequency," Nippon Suisan Gakkaishi, 59(6), 933-942 (1993)

[33] K.G. Foote, "Acoustic Robustness of Two Standard Spheres for Calibrating a Broadband Multibeam Sonar," Proc. Oceans 2007 – Europe Conf., Jun. 18-21

[34] K.G. Foote, "Optimizing Two Targets for Calibrating a Broadband Multibeam Sonar," Proc. Oceans 2006 Conf., Boston, MA, Sep. 18-21

[35] K.G. Foote, "Target-tracking in a Parametric Sonar Beam, with Applications to Calibration," Proc. MTS/IEEE Oceans 2010 Conf., Seattle, WA, Sep. 20-23

[36] D. Chu and L.C. Hufnagle, Jr., "Time Varying Gain (TVG) Measurements of a Multibeam Echo Sounder for Applications to Quantitative Acoustics," Proc. Oceans 2006 Conf., Boston, MA, Sep. 18-21

[37] E. Bernard, C.J. Jakubiak, J.L.Miksis-Olds, J. Penvenne, and D.V. Holliday, "Calibration of a Steered Phased-Array Sonar for Use in Fish Detection," Proc. Oceans 2006 Conf., Boston, MA, Sep. 18-21

[38] T. Meurling, M. Baldwin, D. Lockhart, and C. Malzone, "The Ultra-High Resolution Future of Hydrography," [Online], Available: http://www.fugro-pelagos.com/papers/High-Res_Future.pdf

APPENDICES

APPENDIX A

MULTIBEAM ECHO SOUNDER SATURATION CURVES

A.1 – Introduction

A beam pattern calibration procedure must be conducted in the linear region of operation of the MBES under test. If the region of operation is nonlinear, the measured radiation beam pattern can become deformed from its actual values, where smaller amplitudes would appear more amplified than higher ones, as discussed in Chapter 2 and in more detail by Greenaway and Weber [4].

During transmission, an active sonar system generates electrical energy which are converted into acoustic energy by an electro-acoustic transducer (projector). Before sending the signal to the projector, the signal is amplified to an amplitude level according to the transmit power setting. When a sonar system receives a returned acoustic signal, this signal is converted into an electrical one also by an electro-acoustic transducer (hydrophone). The receive electrical signal is then amplified to higher amplitude electrical signal according to the system gain setting for further processing.

The amplification process needs to be linear with the same effective gain at different signal amplitudes. In practice, however, this process can only be linear over a certain operation range. As the amplitude of the electrical input signal to an amplifier increases, the amplifier may start to operate in a nonlinear region, and eventually it will saturate. Figure A.1 shows two response curves from a typical amplifier. The blue curve on this figure has a smaller gain than the purple curve. It can be observed from this figure that the maximum input voltage to operate the amplifier in the linear region diminishes as the applied gain increases.
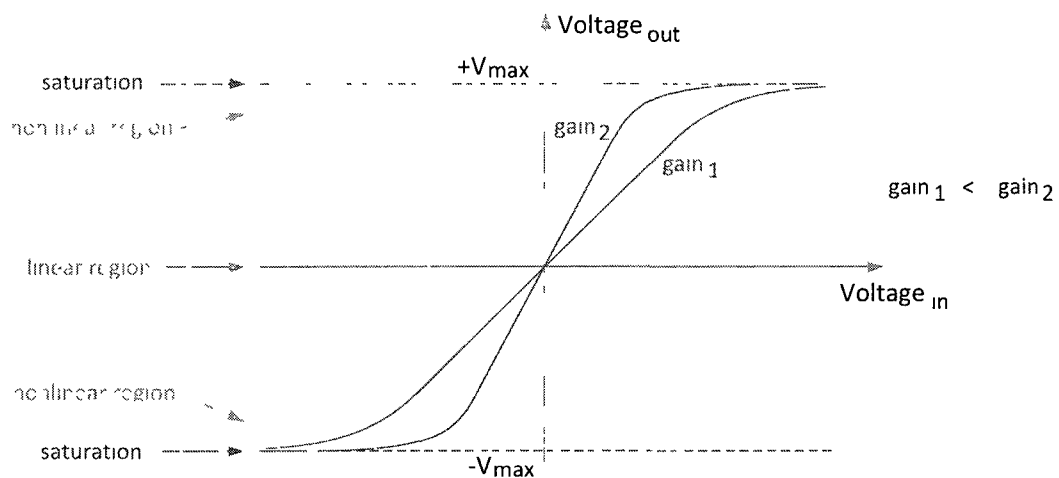
Figure A.1 – Response curves of a typical amplifier

Measurements to determine the gain curves of the MBES RESON 7125 used in this project at the frequency of 200 kHz were performed to identify its linear region of operation with different gain and power settings while using the same target sphere that would be employed in the field calibration methodology.

A.2 – Gain Curves Measurements Setup/Procedure

The MBES RESON 7125 was mounted in the acoustic tank of the University of New Hampshire according to Figure A.2. The target sphere was suspended by a monofilament fishing line (30 lbs. test, 0.3 mm diameter) and positioned at the MRA of the MBES at a distance of 8 m, avoiding interference from the tank walls on the acoustic measurements.

Beamformed data was collected for the MBES for power settings varying from 170 dB to 220 dB in 1 dB increments for each gain setting varying from 0 dB to 80 dB in 5 dB increments. The target sphere was centered at beam 129, which is one of the most inner beams of the MBES. The measurements were performed with the sonar system pinging at a rate of 2 pings per second and pulse length of 260 µs. It was collected data for 20 pings per power/gain setting pair, and the magnitude of the received signal corresponding to the target sphere position was averaged over the pings.
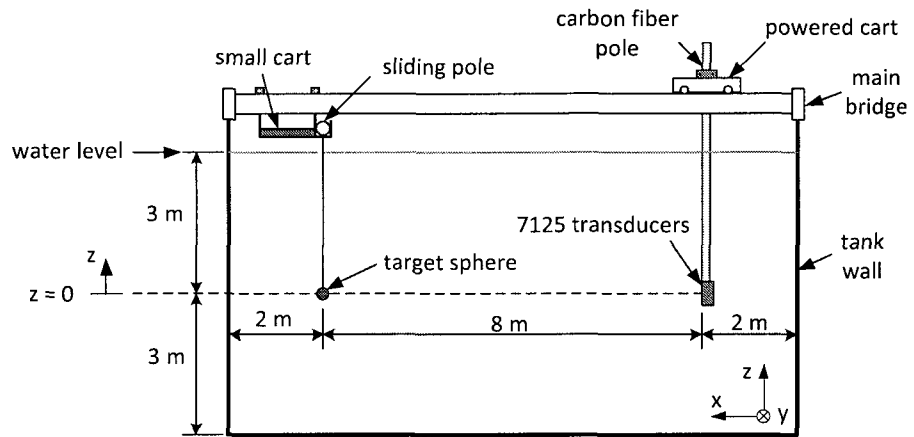
(a) – Side view
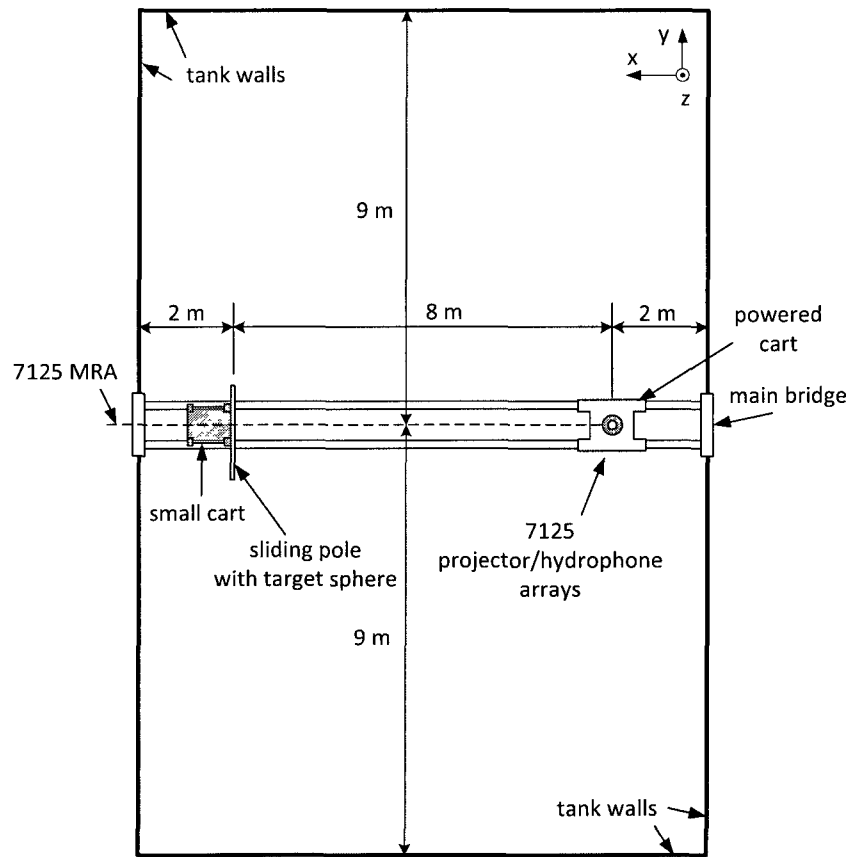
(b) – Top view

Figure A.2 – Setup for measurements of MBES gain curves in curves in the acoustic tank

A.3 – Gain Curves Measurement Results

Figure A.3 shows the gain curves of the RESON 7125 MBES. As expected, there is a region of linearity for each gain setting, as well as the nonlinear behavior as the power setting gets larger, leading to saturation. Also, the linear region of operation decreases as the gain increases. Another nonlinear effect can be noticed for received signal amplitudes below 20 dB. This is caused by the dynamic range of the system, where very small amplitudes are not amplified properly.

It is desirable that the MBES operates in a linear range and with a large power setting. The large power setting is to help increase the signal to noise ratio of the measured return signals from the target sphere, as discussed in Chapter 1. A linear fit was applied to these gain curves to choose the best power and gain settings to always operate the MBES in a linear region during the field calibration procedure. To operate with maximum power, a gain setting of 40 dB was chosen. The maximum deviation from the linear fit on this curve is approximately 0.8 dB at a power setting of 220 dB. Figure A.4 depicts the gain curves along with the linear fit for the gain setting of 40 dB (black line).
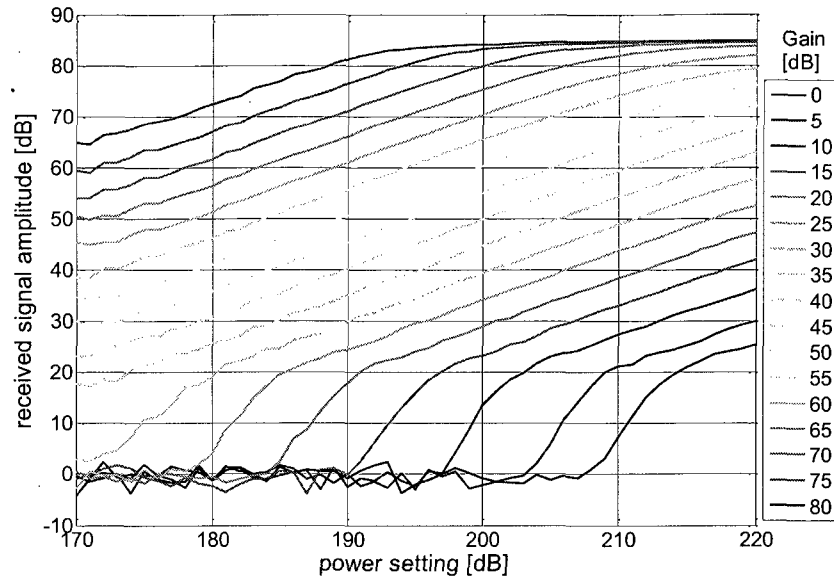
Figure A.3 – RESON 7125 gain curves – beam 129
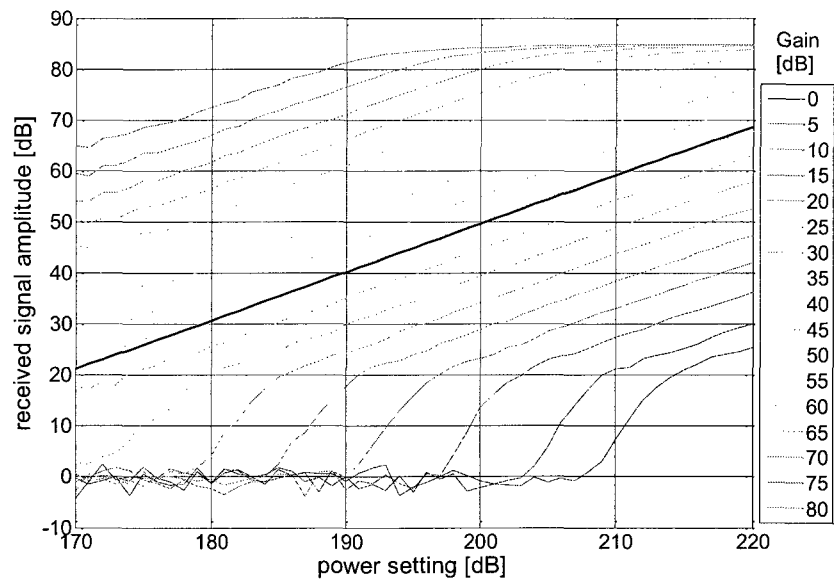
Figure A.4 – Linear fit for gain setting of 40 dB on RESON 7125 gain curves – beam 129

A.4 – Power Offset (Calibration Offset)

The power offset of the MBES was also investigated using the

measurements from the gain curves. The acoustic source level (SL) can be

expressed in terms of the received level (RL), the transmission losses (TL), the target strength (TS), and the gain applied to the sonar system (G) by

$$SL = RL + 2\,TL - TS - G.$$
$$\hspace{10cm}\text{(A.4.1)}$$

The power offset of the sonar system, P_{offset}, is given by the difference between its power setting (PS) and the source level (SL):

$$P_{offset} = PS - SL.$$
$$\hspace{10cm}\text{(A.4.2)}$$

Substituting A.4.1 in A.4.2 gives

$$P_{offset} = PS - RL - 2\,TL + TS + G.$$
$$\hspace{10cm}\text{(A.4.3)}$$

RL and TL are given by

$$RL = 20\,log_{10}(Receive\ Amplitude)$$
$$\hspace{10cm}\text{(A.4.4)}$$

and

$$TL = 20\,log_{10}(target\ distance) + \alpha\,(target\ distance).$$
$$\hspace{8cm}\text{(A.4.5)}$$

where α is the absorption coefficient and the target distance is 8 m. The term containing α is very small and is considered negligible in A.4.5. The target strength of the sphere is −39 dB. Figure 4.5 shows the power offset for the RESON 7125 MBES calculated using these equations. It was expected a constant power offset for the linear range of the gain curves. However, it can be observed a small slope for the linear section of these curves. Figure A.5 shows power offset values ranging from approximately 110 dB for a power setting of 170 dB to approximately 118 dB for a power setting of 220 dB.
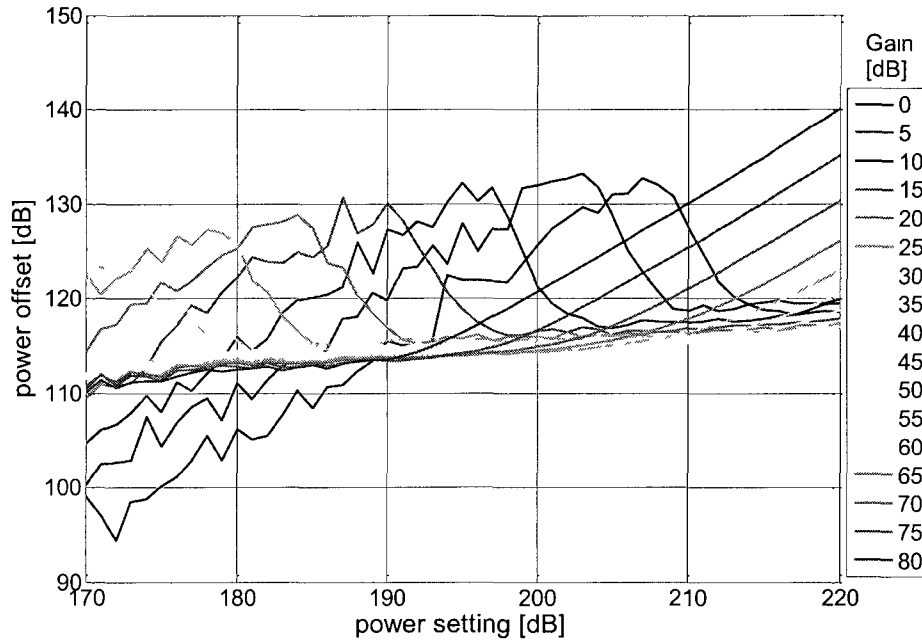
Figure A.5 – Power offset for RESON 7125 – beam 129

A.5 – Remarks

Measurements for beam pattern calibration need to be performed in a linear range of operation to ensure that the same gain values are effectively applied to different amplitude levels of received acoustic signals. Nonlinearities are typically present in the response of electrical amplifiers. Therefore, for the investigation of gain curves of the sonar system it was necessary to define the settings which would allow the system to operate linearly over a larger dynamic range, in order to minimize the nonlinear effects on the system response.

It is desirable to set the MBES to operate at a high power setting to increase the signal to noise ratio of the received signals during the calibration procedure using the target sphere. Hence, a power setting of 220 dB was chosen

along with a gain setting of 40 dB for the operation of the RESON 7125 during the beam pattern calibration tests which used the 38.1 mm diameter target sphere at a distance of 8 m from the MBES transducers. With these settings, the system could operate over a larger linear range, reducing nonlinear effects on the return signals from the target.

The resulting gain curves provided evidence of nonlinearities in the region of very small signal amplitudes. This effect is caused by the limited dynamic range of the system, which makes it more difficult to reliably measure very small amplitude.

The power offset plot of the tested MBES was calculated from the gain curves measurements. It was expected that the power offset of the system would be a constant value. However, this plot shows that the power offset increases from 110 dB at a power setting of 170 dB to 118 dB at a power setting of 220 dB.

APPENDIX B

MATLAB CODES

B.1 – fcbp_7125_EK60.m

```
% SECTION 1:
% * Reads EK60 and 7125 raw files for target at 7125 MRA (n pings)
% * Calculates EK60 angles offsets, the time delay between the two systems,
%   and the angle between the 7125 MRA and the EK60 MRA:
%
%   athw_o --> EK60 athwartship angle offset
%   along_o --> EK60 alongship angle offset
%   dto     --> time delay between the 7125 and EK60 systems
%   alpha_o --> angle between the 7125 MRA and the EK60 MRA
%
% SECTION 2:
% * Reads EK60 and 7125 raw files for target in different positions
%   (covering radiation beam pattern area)
% * Calculates EK60 angles (from EK60 coordinate system) and convert these
%   angles to 7125 angles (to 7125 coordinate system)
% * Check for missing pings in both EK60 and 7125 systems and correct for
%   proper pair of pings (discarding the corresponding missing ping)
% * Calculate amplitude of 7125 ping (average over a narrow section around
%   the max amplitude)
% * Normalize amplitude and calculate amplitude value in dB
% * Compute and plot the 3-D beam pattern of 7125 for each beam
%
% INPUTS:
% * EK60 and 7125 raw files for target at MRA (specify directory in code):
%   EK60File1.raw, 7125File1.s7k
% * EK60 and 7125 raw files for target at radiation beam pattern measurement
%   range (specify directory in code):
%   EK60File2.raw, 7125File2(1).s7k, 7125File2(2).s7k, ....
% * sound speed:
%   v
% * Distance from EK60 transducer to 7125 transducers along y-axis (7125
%   coordinates):
%   yt
% * range of target from 7125:
%   minRange, maxRange
%
% MATLAB Functions Used:
% * missPingsIdx.m
```

```
% * jday2matlab.m
% * read7125_7000Record.m
% * read7125_7008Record.m
% * readEKRaw EK/ES60 ME/MS70 MATLAB toolkit


clear all; close all;
v = 1490;                   % measured sound speed declared here
yt = 0.955;                 % distance from 7125 to EK60 on y-axis
                            % (7125 coord system)
minRange = 7.9;             % minimum range of target
maxRange = 8.3;             % maximum range of target
SpEK60Threshold = -60;      % Filters out data with TS lower than this threshold
n7125files = 4;             % number of 7125 files to read:
                            % 7125File2(1).sk7, 7125File2(2).sk7, ...


%% ************** SECTION 1: Target at MRA of 7125 ******************


%% **** EK60 ****


%% read EK60 raw file for target at MRA position:


% read EK60 raw data:
[headerEK60, dataEK60] = readEKRaw('EK60File1.raw');


% get EK60 calibration parameters:
calParmsEK60 = readEKRaw_GetCalParms(headerEK60, dataEK60);


% transform electrical angles into physical angles:
dataEK60 = readEKRaw_ConvertAngles(dataEK60, calParmsEK60);


% convert power to Sp
dataEK60 = readEKRAW_Power2Sp(dataEK60,calParmsEK60);


%% EK60 physical angles, PowerEK60_o, SoundVelEK60.SampleIntervalEK60.
%% numPingsEK60 TimeEK60:
% discard first 4 pings:
AthwartAngEK60_phys_o = cast(dataEK60.pings.athwartship(:,5:end), 'double');
AlongAngEK60_phys_o = cast(dataEK60.pings.alongship(:,5:end), 'double');
SpEK60_o = dataEK60.pings.Sp(:,5:end);
SoundVelEK60 = cast(dataEK60.pings.soundvelocity(1), 'double');
SampleIntervalEK60 = dataEK60.pings.sampleinterval(1);
SampleRangeEK60 = cast(dataEK60.pings.samplerange, 'double');
RangeTimeEK60 = 0:SampleIntervalEK60:(SampleRangeEK60(2)-1)* SampleIntervalEK60;
RangeDistanceEK60 = RangeTimeEK60 * SoundVelEK60 / 2;
numPingsEK60 = dataEK60.pings.number(end) - 4;
TimeEK60 = (datestr(dataEK60.pings.time(5:end),'yyyy-mm-dd HH:MM:SS.FFF'));


%% Calculate EK60 range indexes (acoustic distance) for the target position
ibrEK60 = int16((minRange * 2) / (SampleIntervalEK60 * SoundVelEK60));
isrEK60 = int16((maxRange * 2) / (SampleIntervalEK60 * SoundVelEK60));


%  *******************************************************************
% --> PowerEK60_o, AlongAngEK60_phys_o, AthwartAngleEK60_phys_o.
%     numPingsEK60, TimeEK60
%  *******************************************************************
```

```
%% Find indexes of maximum Power values, EK60 Angles, and time t2:
MaxSpEK60_vector = zeros(numPingsEK60,1);
indMaxSpEK60_vector = zeros(numPingsEK60,1);
indMaxSpEK60 = zeros(numPingsEK60,1);
AlonAngEK60_o = zeros(numPingsEK60,1);
AthwAngEK60_o = zeros(numPingsEK60,1);

for i = 1:numPingsEK60
    [MaxSpEK60_vector(i), indMaxSpEK60_vector(i)] = max(SpEK60_o(ibrEK60:isrEK60,i));
    indMaxSpEK60(i) = indMaxSpEK60_vector(i) + ibrEK60;
    % EK60 Angles:
    AthwAngEK60_o(i) = AthwartAngEK60_phys_o(indMaxSpEK60(i),i);
    AlonAngEK60_o(i) = AlongAngEK60_phys_o(indMaxSpEK60(i), i);
end

% time interval t2 (7125-target-EK60):
t2_vector_o = double(SampleIntervalEK60 .* indMaxSpEK60);

% ******************************************************************
% --> numPingsEK60, TimeEK60, AthwAngEK60_o, AlonAngEK60_o. t2_vector_o
% ******************************************************************

%% **** 7125 ****

%if file 7125File2.s7k is in the current directory:
fid = fopen('7125File1.s7k','r','ieee-le');

% % or specify file location.
% [filename, pathname] = uigetfile('*.s7k', 'Open Reson 7125 Data File for Target at 7125 MRA'),
% fid = fopen([pathname filename],'r'.'ieee-le');

Time7125 = zeros(5,numPingsEK60);      % time7k_2 = ([day; year: hour; min; sec], num_pings)
MaxPower7125 = zeros(numPingsEK60,256);
indMaxPower_o = zeros(numPingsEK60,256);
indMaxPower7125 = zeros(numPingsEK60,256);
t1_vector_o = zeros(numPingsEK60,1);
maxBeamAmp = zeros(numPingsEK60,1);
maxBeamAmpIdx = zeros(numPingsEK60,1);
Amp7125_o = zeros(numPingsEK60,256);
gainSetting = zeros(numPingsEK60,1);

stopp = 0;
firstRecord = 1;
pingidx = 0;
pingidx7125 = 0;

while ~stopp
    % read 7125 dataframe
    protocolVers = fread(fid,1,'uint16');
    offset = fread(fid,1,'uint16');
    syncPatt = fread(fid,1,'uint32');
    sizey = fread(fid,1,'uint32');
    optdataOffset = fread(fid,1,'uint32');
    optdataId = fread(fid,1,'uint32');
    year_ = fread(fid,1,'uint16');
```

```
day_ = fread(fid,1,'uint16');
sec_ = fread(fid,1,'single');
hour_ = fread(fid,1,'uint8');
min_ = fread(fid,1,'uint8');
time7k = [day_; year_; hour_; min_; sec_];
recordVers = fread(fid,1,'uint16');
recordType = fread(fid,1,'uint32');        % this identifies the type
                                           % of data in this record
deviceId = fread(fid,1,'uint32');
fread(fid,1,'uint16');                     % reserved
systemEnum = fread(fid,1,'uint16');
recordCount = fread(fid,1,'uint32');
flags = fread(fid,16,'ubit1');
fread(fid,1,'uint16');                     % reserved
fread(fid,1,'uint32');                     % reserved
totFragRecords = fread(fid,1,'uint32');
fragNum = fread(fid,1,'uint32');

% data section
if recordType == 7000
    [PowerSel,RangeSel,GainSel,TxpulseWidth,Absorption,SoundVel,...
        Spread,PingNum,SampRate] = read7125_7000Record(fid);

    if firstRecord
        PingNumOffset = PingNum - 1;
        firstRecord = 0;
    end
    gainSetting(PingNum - PingNumOffset) = GainSel;

elseif recordType == 7008

    pingidx = pingidx + 1;

    %% Calculate 7125 range indexes (acoustic distance) for the target
    if pingidx == 1
        ibr7125 = int16((minRange * 2) / (SoundVel / SampRate));
        isr7125 = int16((maxRange * 2) / (SoundVel / SampRate));
    end

    %% Find indexes of maximum Power values and time t1

    if pingidx > 4          % discard 1st 4 pings

        pingidx7125 = pingidx7125 + 1;
        display(pingidx7125)

        [amntRead,amp,phs,PingNum] = read7125_7008Record(fid);

        fread(fid,sizey-68-amntRead,'uint8');

        Time7125(:,pingidx7125) = time7k;        % time7k = [day, year, hour, min, sec]
        [MaxPower7125(pingidx7125,:), indMaxPower_o(pingidx7125,:)] = ...
            max(amp(ibr7125:isr7125,:));
        indMaxPower7125(pingidx7125,:) = ...
            int16(indMaxPower_o(pingidx7125,:)) + ibr7125;
```

```matlab
        % Amplitude of 7125 is the average around indMaxPower7125:
        for k = 1:256
           Amp7125_o(pingidx7125, k) = ...

           mean(amp(indMaxPower7125(pingidx7125,k)-5:indMaxPower7125(
              pingidx7125,k)+5, k));
        end

        % find beam with max amplitude in each ping
        [maxBeamAmp(pingidx7125), maxBeamAmpIdx(pingidx7125)] = ...
           max(Amp7125_o(pingidx7125,:));

        % time interval t1 (7125-target-7125) for each ping,  t1 (#pings,1):
        t1_vector_o(pingidx7125) = ...
           indMaxPower7125(pingidx7125,maxBeamAmpIdx(pingidx7125)) ./ SampRate;
     else
        [amntRead_junk,amp_junk,phs_junk,PingNum_junk] = read7125_7008Record(fid);
     end

  else
     if ~feof(fid)
        fseek(fid,sizey-68,'cof');
     end
  end

  if ~feof(fid)
     checksum = fread(fid,1,'uint32');
  end

  if feof(fid)
     disp('stop!')
     stopp = 1;
  end

end
numPings7125 = pingidx7125;

fclose(fid);

Time7125 = Time7125(:,1:numPings7125);% time7k_2 = ([day; year; hour; min; sec], num_pings)
t1_vector_o = t1_vector_o(1:numPings7125,1);
Amp7125_o = Amp7125_o(1:numPings7125,:);


% ***************************************************************
% --> numPingsEK60, TimeEK60, AthwAngEK60_o, AlonAngEK60_o, t2_vector_o
% --> numPings7125, Time7125, Amp7125_o, t1_vector_o
% ***************************************************************


%% Check for missing Pings

if numPingsEK60 ~= numPings7125
   % call function of time check to obtain idx_discard vectors:
   [idx_discard7125, idx_discardEK60, numPingsValid, ErrorPingCheck] = ...
      missPingsIdx(Time7125, TimeEK60);
```

137

```
if ErrorPingCheck == 1
    error('myApp1:pingChk1', 'Error checking pair of pings for target at MRA!')
end
t1_vector = zeros(numPingsValid, 1);
t2_vector = zeros(numPingsValid, 1);
Amp7125_ = zeros(numPingsValid, 256);
AthwAngEK60 = zeros(numPingsValid);
AlonAngEK60 = zeros(numPingsValid);

k = 0;
n = 0;

for m = 1:numPings7125
    if idx_discard7125(m) == 0
        k = k + 1;

        t1_vector(k) = t1_vector_o(m);
        Amp7125_(k) = Amp7125_o(m);     % 7125 power for /125 MRA
    end
end

for m = 1:numPingsEK60
    if idx_discardEK60(m) == 0
        n = n + 1;
        t2_vector(n) = t2_vector_o(m);
        AthwAngEK60(n) = AthwAngEK60_o(m);
        AlonAngEK60(n) = AlonAngEK60_o(m);
    end
end
else
    t1_vector = t1_vector_o;
    t2_vector = t2_vector_o;
    Amp7125_ = Amp7125_o;
    AthwAngEK60 = AthwAngEK60_o;
    AlonAngEK60 = AlonAngEK60_o;
end

Amp7125_0 = mean(Amp7125_);        % 7125 power amplitude for MRA

%% EK60 Angles, time t1, and time t2 for target at 7125 MRA:
AthwAngEK60_0 = mean(AthwAngEK60);
AlonAngEK60_0 = mean(AlonAngEK60);
t1 = mean(t1_vector);
t2 = mean(t2_vector);

% ***********************************************************
% --> t1, t2, AthwAngEK60_0, AlonAngEK60_0, SoundVelEK60, yt
% ***********************************************************

%% delay between systems dto for target in 7125 MRA:
d7125 = SoundVelEK60 * (t1 / 2);        % distance between target and 7125
dEK60 = sqrt(yt^2 + d7125^2);           % distance between target and EK60
t2_expected = (d7125 + dEK60) / SoundVelEK60;   % expected time travel 7125-target-EK60
dt_o = t2 - t2_expected;                % time delay between systems, (old: t2_expected - t2;)
                                        % t1: 7125 travel time 7125-target-7125
                                        % t2: EK60 travel time 7125-target-EK60
```

138

```
% ********************************************************
% --> t1, t2, AthwAngEK60_0, AlonAngEK60_0, Amp7125_0, dt_o
% ********************************************************

%% alpha_o --> angle between EK60 MRA and 7125 MRA (xy plane):

% d7125xy = d7125;      % distance target-7125 projected on xy plane
dEK60xy = dEK60;        % distance target-EK60 projected on xy plane

do = sqrt(dEK60xy^2 - yt^2);
alpha3 = rad2deg(acos(yt / dEK60xy));
alpha2 = alpha3 - AthwAngEK60_0;
alpha_o = 90 - alpha2;

% ********************************************************
% --> AthwAngEK60_0, AlonAngEK60_0, delay dto, alpha_o, Amp7125_0
% ********************************************************

clearvars -except yt AthwAngEK60_0 AlonAngEK60_0 alpha_o dt_o Amp7125_0 ...
    minRange maxRange SpEK60Threshold n7125files
```

```
%% ************* SECTION 2: Target at General Position **************

%% **** EK60 ****

%% read EK60 raw file for target at general position:
[headerEK60, dataEK60] = readEKRaw('EK60File2.raw');      % read raw data

% get EK60 calibration parameters:
calParmsEK60 = readEKRaw_GetCalParms(headerEK60, dataEK60);

% transform electrical angles into physical angles:
dataEK60 = readEKRaw_ConvertAngles(dataEK60, calParmsEK60);

% convert power to Sp
dataEK60 = readEKRaw_Power2Sp(dataEK60,calParmsEK60);

%% EK60 physical angles, PowerEK60_o, SoundVelEK60,SampleIntervalEK60,numPingsEK60
%% TimeEK60:
% discard first 4 pings:
AthwartAngEK60_phys_o = cast(dataEK60.pings.athwartship(:,5:end), 'double');
AlongAngEK60_phys_o = cast(dataEK60.pings.alongship(:,5:end), 'double');

%PowerEK60_o = dataEK60.pings.power(:,5:end);
SpEK60_o = dataEK60.pings.Sp(:,5:end);

SoundVelEK60 = cast(dataEK60.pings.soundvelocity(1), 'double');
SampleIntervalEK60 = dataEK60.pings.sampleinterval(1);
numPingsEK60_ = dataEK60.pings.number(end) - 4;    % discard first 4 pings
TimeEK60_ = (datestr(dataEK60.pings.time(5:end),'yyyy-mm-dd HH:MM:SS.FFF'));

%% Calculate EK60 range indexes (acoustic distance) for the target position
```

```matlab
ibrEK60 = int16((minRange * 2) / (SampleIntervalEK60 * SoundVelEK60));
isrEK60 = int16((maxRange * 2) / (SampleIntervalEK60 * SoundVelEK60));

% *****************************************************************
% --> PowerEK60_o, AlongAngEK60_phys_o, AthwartAngleEK60_phys_o,
%     numPingsEK60, TimeEK60
% *****************************************************************

%% Find indexes of maximum Power values, EK60 Angles, and time t2:
MaxSpEK60_vector = zeros(numPingsEK60_,1);
indMaxSpEK60_vector = zeros(numPingsEK60_,1);
indMaxSpEK60 = zeros(numPingsEK60_,1);

AlonAngEK60_o = zeros(numPingsEK60_,1);
AthwAngEK60_o = zeros(numPingsEK60_,1);

for i = 1:numPingsEK60_
    [MaxSpEK60_vector(i), indMaxSpEK60_vector(i)] = max(SpEK60_o(ibrEK60:isrEK60,i));
    indMaxSpEK60(i) = indMaxSpEK60_vector(i) + ibrEK60;
    % EK60 Angles:
    AthwAngEK60_o(i) = AthwartAngEK60_phys_o(indMaxSpEK60(i),i);
    AlonAngEK60_o(i) = AlongAngEK60_phys_o(indMaxSpEK60(i), i);
end

% time interval t2 (7125-target-EK60):
t2_vector_o = double(SampleIntervalEK60 .* indMaxSpEK60);

%% set MaxSpEK60 threshold value to discard invalid EK60 received pings:
idxEK60 = find(MaxSpEK60_vector > SpEK60Threshold);

MaxSpEK60_vector_o = MaxSpEK60_vector(idxEK60);
AthwAngEK60_o = AthwAngEK60_o(idxEK60);
AlonAngEK60_o = AlonAngEK60_o(idxEK60);
t2_vector_o = t2_vector_o(idxEK60);
numPingsEK60 = length(AthwAngEK60_o);
TimeEK60 = TimeEK60_(idxEK60,:);

% *****************************************************************
% --> numPingsEK60, TimeEK60, AthwAngEK60_o, AlonAngEK60_o, t2_vector_o
% *****************************************************************

%% **** 7125 *****

Time7125 = zeros(5,numPingsEK60_);    % time7k_2 = ([day; year; hour; min; sec], num_pings)

MaxPower7125 = zeros(numPingsEK60_,256);
indMaxPower_o = zeros(numPingsEK60_,256);
indMaxPower7125 = zeros(numPingsEK60_,256);
t1_vector_o = zeros(numPingsEK60_,1);
maxBeamAmp = zeros(numPingsEK60_,1);
maxBeamAmpIdx = zeros(numPingsEK60_,1);
Amp7125_o = zeros(numPingsEK60_,256);
gainSetting = zeros(numPingsEK60_,1);

pingidx = 0;
pingidx7125 = 0;
```

```
 firstRecord = 1;
dataidx = 0;
m = 0;

p = 0;
amp7125_x = zeros(10, 694, 256);

for nf = 1:n7125files

    aa = '7125File2';
    ab = '(';
    bb = int2str(nf);
    bc = ')';
    cc = '.s7k';
    File = [aa ab bb bc cc];
    fid = fopen(File,'r','ieee-le');

    stopp = 0;

    while ~stopp

        % read the dataframe
        protocolVers = fread(fid,1,'uint16');
        offset = fread(fid,1,'uint16');
        syncPatt = fread(fid,1,'uint32');
        sizey = fread(fid,1,'uint32');
        optdataOffset = fread(fid,1,'uint32');
        optdataId = fread(fid,1,'uint32');
        year_ = fread(fid,1,'uint16');
        day_ = fread(fid,1,'uint16');
        sec_ = fread(fid,1,'single');
        hour_ = fread(fid,1,'uint8');
        min_ = fread(fid,1,'uint8');
        time7k = [day_; year_; hour_; min_; sec_];
        recordVers = fread(fid,1,'uint16');
        recordType = fread(fid,1,'uint32');        % this identifies the type of data in this record
        deviceId = fread(fid,1,'uint32');
        fread(fid,1,'uint16');  % reserved
        systemEnum = fread(fid,1,'uint16');
        recordCount = fread(fid,1,'uint32');
        flags = fread(fid,16,'ubit1');
        fread(fid,1,'uint16');  % reserved
        fread(fid,1,'uint32');  % reserved
        totFragRecords = fread(fid,1,'uint32');
        fragNum = fread(fid,1,'uint32');

        % data section
        if recordType == 7000

[PowerSel,RangeSel,GainSel,TxpulseWidth,Absorption,SoundVel,Spread,PingNum,SampRate] =
...
            read7125_7000Record(fid);

        if firstRecord
            PingNumOffset = PingNum - 1;
            firstRecord = 0;
```

```matlab
        end
        gainSetting(PingNum - PingNumOffset) = GainSel;
    elseif recordType == 7008

        pingidx = pingidx + 1;

        %% Calculate 7125 range indexes (acoustic distance) for the target
        if pingidx == 1
            ibr7125 = int16((minRange * 2) / (SoundVel / SampRate));
            isr7125 = int16((maxRange * 2) / (SoundVel / SampRate));
        end

        %% Find indexes of maximum Power values and time t1.

        if pingidx > 4                % discard 1st 4 pings

            pingidx7125 = pingidx7125 + 1;
            display(pingidx7125)

            [amntRead,amp,phs,PingNum] = read7125_7008Record(fid);

            fread(fid,sizey-68-amntRead,'uint8');

            Time7125(:,pingidx7125) = time7k;    % time7k = [day, year, hour, min, sec]

            [MaxPower7125(pingidx7125,:), indMaxPower_o(pingidx7125,:)] = ...
                max(amp(ibr7125:isr7125,:));
            indMaxPower7125(pingidx7125,:) = int16(indMaxPower_o(pingidx7125,:)) + ibr7125;

            % Amplitude of 7125 is the average around indMaxPower7125
            for k = 1:256
                Amp7125_o(pingidx7125, k) = ...
                    mean(amp(indMaxPower7125(pingidx7125,k)-3:indMaxPower7125(...
                        pingidx7125,k)+3, k));
            end

            if rem(pingidx7125,30) == 0
                p = p + 1;
                amp7125_x(p,:,:) = amp(:,:);
            end

            % find beam with max amplitude in each ping
            [maxBeamAmp(pingidx7125), maxBeamAmpIdx(pingidx7125)] = ...
                max(Amp7125_o(pingidx7125,:));

            % time interval t1 (7125-target-7125) for each ping, t1 (#pings.1).
            t1_vector_o(pingidx7125) = ...
                indMaxPower7125(pingidx7125,maxBeamAmpIdx(pingidx7125)) ./ SampRate;
        else
            [amntRead_junk,amp_junk,phs_junk,PingNum_junk] = read7125_7008Record(fid);
        end

else
    if ~feof(fid)
        %fread(fid,sizey-68,'uint8');
        fseek(fid,sizey-68,'cof');
```

```
            end
        end
        if ~feof(fid)
            checksum = fread(fid,1,'uint32');
        end

        if feof(fid)
            disp('stop!')
            stopp = 1;
        end
    end
end
numPings7125 = pingidx7125;
fclose(fid);

% adjust variables size to proper number of pings
amp7125_x = amp7125_x(1:p,:,:);
Time7125 = Time7125(:,1:numPings7125);% time7k_2 = ([day, year, hour, min, sec], num_pings)
MaxPower7125 = MaxPower7125(1:numPings7125,:);
indMaxPower_o = indMaxPower_o(1:numPings7125,:);
indMaxPower7125 = indMaxPower7125(1:numPings7125,:);
t1_vector_o = t1_vector_o(1:numPings7125,1);
maxBeamAmp = maxBeamAmp(1:numPings7125,1);
maxBeamAmpIdx = maxBeamAmpIdx(1:numPings7125,1);
Amp7125_o = Amp7125_o(1:numPings7125,:);
gainSetting = gainSetting(1:numPings7125,1);


% ***********************************************************
% --> numPingsEK60, TimeEK60, AthwAngEK60_o, AlonAngEK60_o, t2_vector_o
% --> numPings7125  Time7125, Amp7125_o, t1_vector_o
% ***********************************************************

%% Check for missing Pings

if numPingsEK60 ~= numPings7125

    % call function of time check to obtain idx_discard vectors.
    [idx_discard7125, idx_discardEK60, numPingsValid, ErrorPingCheck] = ...
        missPingsIdx(Time7125, TimeEK60);

    if ErrorPingCheck
        error('myApp2 pingChk2', 'Error checking pair of pings for target at general position!')
    end

    t1_vector = zeros(numPingsValid, 1);
    t2_vector = zeros(numPingsValid, 1);
    Amp7125 = zeros(numPingsValid, 256);
    AthwAngEK60 = zeros(numPingsValid,1);
    AlonAngEK60 = zeros(numPingsValid,1);
    MaxSpEK60_vector_f = zeros(numPingsValid,1);

    k = 0;
    n = 0;

    for m = 1:numPings7125
        if idx_discard7125(m) == 0
```

```
        k = k + 1;
        t1_vector(k) = t1_vector_o(m);
        Amp7125(k,:) = Amp7125_o(m,:);      % 7125 power for 7125 MRA
      end
    end

    for m = 1:numPingsEK60
      if idx_discardEK60(m) == 0
        n = n + 1;
        t2_vector(n) = t2_vector_o(m);
        AthwAngEK60(n,:) = AthwAngEK60_o(m,:);
        AlonAngEK60(n,:) = AlonAngEK60_o(m,:);
        MaxSpEK60_vector_f(n,:) = MaxSpEK60_vector_o(m,:);
      end
    end
  else
    t1_vector = t1_vector_o;
    t2_vector = t2_vector_o;
    Amp7125 = Amp7125_o;
    AthwAngEK60 = AthwAngEK60_o;
    AlonAngEK60 = AlonAngEK60_o;
    MaxSpEK60_vector_f = MaxSpEK60_vector_o;

  end

% **********************************************
%  have: AthwEK60, AlonEK60, Amp7125, t1, t2, alpha_o
% **********************************************

%% acoustic distances
% distance d7125 for any target position:
d7125 = SoundVel .* (t1_vector ./ 2);      % distance between target and 7125

% distance dEK60 for any target position:
t2_ = t2_vector - dt_o;              % t2_. travel time 7125-target-EK60 accounting for delay dto
t3 = t2_ - (t1_vector ./ 2);         % t3: travel time target-EK60
dEK60 = SoundVel .* t3;              % distance between target and EK60

%% convert angles from EK60 coordinates to 7125 coordinates

AlongAng7125 = AlonAngEK60; % - AlonAngEK60_0:
d7125xy = d7125 .* cos(deg2rad(AlongAng7125)); % dist target-7125 projected on xy plane|7125
dEK60xy = dEK60 .* cos(deg2rad(AlongAng7125));% dist target-EK60 projected on xy
                                              % plane|7125

% with alpha_o --> calculate 7125 Athwartship Angles:
dy_sph = dEK60xy .* sin(deg2rad(- AthwAngEK60 + alpha_o));

y_sph = - dy_sph +  yt;

AthwAng7125 = rad2deg(asin(y_sph ./ d7125xy));

%% Convert Amp7125 into dB:
% Normalize Amp7125 using its maximum value

% [MaxAmp7125_1(1,256) idxMaxAmp7125_1(1,256)]:
```

```matlab
[MaxAmp7125_1, idxMaxAmp7125_1] = max(Amp7125);

% [MaxAmp7125_2(1), idxMaxAmp7125_2(1)]:
[MaxAmp7125_2, idxMaxAmp7125_2] = max(MaxAmp7125_1);

% Location of maximum amplitude:
pingMaxAmp7125 = idxMaxAmp7125_1(idxMaxAmp7125_2);
beamMaxAmp7125 = idxMaxAmp7125_2;

Amp7125_dB = 20 .* log10(Amp7125 ./ MaxAmp7125_2);

%% Beam Pattern Plots
% Interpolated BP 3D plot:
for beamNumber = 129:129   % choose beams
    close all
    beamLabel = ['beam ' num2str(beamNumber)];
    xlin = linspace(min(AthwAng7125),max(AthwAng7125),1000);
    ylin = linspace(min(AlongAng7125),max(AlongAng7125),1000);

    [X,Y] = meshgrid(xlin,ylin);

    f = TriScatteredInterp(AthwAng7125,AlongAng7125,Amp7125_dB(:,beamNumber));
    Z = f(X,Y);

    figure(1)
    mesh(X,Y,Z) %interpolated
    axis tight; hold on
    xlabel('Athwartship Angle [degrees]','FontSize',12)
    ylabel('Alongship Angle [degrees]','FontSize',12)
    zlabel('Amplitude [dB]','FontSize',12)
    title(beamLabel,'FontSize',12)
    set(gca,'FontSize',18)
% view([0 90])
    colorbar
    hold on

    fh = figure(1);
    set(fh,'color', 'white');

    Xa = 5; Ya = 700;
    set(gcf,'PaperUnits','centimeters')
    xSize = 16; ySize = 6;
    xLeft = (21-xSize)/2; yTop = (30-ySize)/2;
    set(gcf,'PaperPosition',[xLeft yTop xSize ySize])
    set(gcf,'Position',[Xa Ya xSize*50 ySize*50])

    set(gca,'FontSize',12)
    pause
end

%% 2D plot of Beam Pattern - No Interpolation

figure(4)
plot(AthwAng7125,AlongAng7125,'ko');
hold on
```

```
AmpThres = -45:0;
c = colormap(jet(length(AmpThres)));
 for i = 1:length(AmpThres)
   idxXdB = find(abs(Amp7125(:,129) - AmpThres(i)) <= 0.5);
   plot(AthwAng7125(idxXdB),AlongAng7125(idxXdB),'.','MarkerSize', 20,'color',c(i,:));
   hold on
end

xlabel('Athwartship Angle [degrees]','FontSize',12)
ylabel('Alongship Angle [degrees]','FontSize',12)
xlim([-6 6])
ylim([-1 3.1])
grid on

colorbar

contourLevels = [-30 -20 -10 -3];
[c h] = contour(X,Y,Z,contourLevels, 'b-');
clabel(c,h);

fh = figure(4);
set(fh,'color', 'white');

Xa = 850; Ya = 700;
set(gcf,'PaperUnits','centimeters')
xSize = 16; ySize = 6;
xLeft = (21-xSize)/2; yTop = (30-ySize)/2;
set(gcf,'PaperPosition',[xLeft yTop xSize ySize])
set(gcf,'Position',[Xa Ya xSize*50 ySize*50])
```

B.2 – missPingsIdx.m

```
function [idx_discard7125, idx_discardEK60, NumPingsValid, Error] = ...
        missPingsIdx(Time7125, TimeEK60)
% [idx_discard7125, idx_discardEK60, NumPingsValid, Error] =
%    missPingsIdx(Time7125, TimeEK60)
%
% Time7125 and TimeEK60
% * Converts to the same format
% * Converts number of hours, minutes, and seconds to seconds
% * Tests for missing pings and returns two vectors indicating the indexes
%   of missing pings, one for the 7125 system and one for the EK60 system
%   0 --> ping is not missing
%   1 --> ping is missing


%% **** Section 1 - Convert Time7125 and Time EK60 to the same format ****

%% EK60

TimeEK60hour = str2num(TimeEK60(:,12:13));   %#ok<ST2NM>
TimeEK60min = str2num(TimeEK60(:,15:16));    %#ok<ST2NM>
TimeEK60sec = str2num(TimeEK60(:,18:end));   %#ok<ST2NM>

%% 7125

DayMonthYear_7125 = zeros(length(Time7125),1);  % DayMonthYear_7125(# pings,1)
DDMMMYYYY_7125 = zeros(length(Time7125),10);
Time7125_cell = cell(length(Time7125),1);

for i = 1:length(Time7125)
    % conversion of Julian Day and Year to Day MonthYear
    DayMonthYear_7125(i) = jday2matlab(Time7125(1,i),Time7125(2,1));   % conv into num
    DDMMMYYYY_7125(i,:) = datestr(DayMonthYear_7125(i), 'yyyy-mm-dd'); % conv into string
    % put everything together (time string).
    Time7125_cell(i) = {char([DDMMMYYYY_7125(i,:) ' ' sprintf('% 2d', Time7125(3,i)) ' ' ...
        sprintf('% 2d', Time7125(4,i)) ' ' num2str(Time7125(5,i))])};
end

Time7125_char = char(Time7125_cell);  % convert to the same format as TimeEK60

Time7125hour = str2num(Time7125_char(:,12:13));    %#ok<ST2NM>
Time7125min = str2num(Time7125_char(:,15:16));     %#ok<ST2NM>
Time7125sec = str2num(Time7125_char(:,18:end));    %#ok<ST2NM>

%% Convert HMS to seconds
delayWriteEK60 = 0 ;%0 9987, % this is the delay between 7125 write and EK60 write
(timestamp)
Time7125SEC = Time7125sec + 60 * Time7125min + 3600 * Time7125hour + delayWriteEK60;
TimeEK60SEC = TimeEK60sec + 60 * TimeEK60min + 3600 * TimeEK60hour;

%% **** Section 2 - Test for Missing Pings using (Time7125,TimeEK60)  ****
```

```
maxPings = max([length(Time7125SEC) length(TimeEK60SEC)]); % get max # pings
idx_discard7125_ = ones(length(Time7125SEC),1);
idx_discardEK60_ = ones(length(TimeEK60SEC),1);
k = 0;      % number of missing 7125 pings
n = 0;      % number of missing EK60 pings
m = 1;

while m <= (maxPings + max([k n]))

    if ((m-n) <= length(TimeEK60SEC)) && ((m-k) <= length(Time7125SEC))

        if (TimeEK60SEC(m-n) - Time7125SEC(m-k)) > 0.1

            idx_discard7125_(m) = 1;    % discard 7125 ping
            n = n + 1;

        elseif (TimeEK60SEC(m-n) - Time7125SEC(m-k)) < - 0.1

            idx_discardEK60_(m) = 1;    % discard EK60 ping
            k = k + 1;

        else
            idx_discard7125_(m-k) = 0;
            idx_discardEK60_(m-n) = 0;

        end

    end

    m = m+1;

end

idx_discard7125 = idx_discard7125_(1:length(Time7125SEC));
idx_discardEK60 = idx_discardEK60_(1:length(TimeEK60SEC));

numPings7125valid = length(Time7125) - sum(idx_discard7125);
numPingsEK60valid = length(TimeEK60) - sum(idx_discardEK60);

if numPings7125valid ~= numPingsEK60valid
    Error = 1;
else
    Error = 0;
end

NumPingsValid = numPings7125valid;
```

B.3 – readEK60raw_ErrorTest_25x25_Files.m

```
%% EK60 Error Investigation
% Reads all 25 x 25 raw files (7125 active and EK60 active),
% each file corresponds to one position in the angular grid
% Use mean values of the 50 pings per position

clear all; close all;

nn = 25;                % number of points per line
minRange = 7.9;         % minimum range of target
maxRange = 8.3;         % maximum range of target

%% initialize arrays
AthwMean1 = zeros(nn,nn);
AlonMean1 = zeros(nn,nn);
AthwMean2 = zeros(nn,nn);
AlonMean2 = zeros(nn,nn);
AthwStd1 = zeros(nn,nn);
AlonStd1 = zeros(nn,nn);
AthwStd2 = zeros(nn,nn);
AlonStd2 = zeros(nn,nn);

%%
for m = 1:1:25
    m
    i = 0;

    for n = 1:2:49
        %% clear variables (updatable) to be used inside FOR loop:
        clearvars -except AlonMean1 AthwMean1 AlonMean2 AthwMean2 nn n m i ...
            AlonStd1 AthwStd1 AlonStd2 AthwStd2 index_start_range ...
            index_end_range AthwartTRUE AlongTRUE minRange maxRange

        %% read individual raw files:
        i = i + 1;
        s1 = 'RAW DATA\Final\Sequence\';
        s2 = int2str(m);
        s3 = '\';
        s4_1 = int2str(n);
        s4_2 = int2str(n+1);
        s5 = '.raw';
        File1 = [s1 s2 s3 s4_1 s5];
        File2 = [s1 s2 s3 s4_2 s5];

        [header1, data1] = readEKRaw(File1);    % read raw data EK60 active
        [header2, data2] = readEKRaw(File2);    % read raw data 7125 active

        % get EK60 calibration parameters.
        calParms_1 = readEKRaw_GetCalParms(header1, data1);
        calParms_2 = readEKRaw_GetCalParms(header2, data2);

        % transform electrical angles into physical angles.
```

```
data1 = readEKRaw_ConvertAngles(data1, calParms_1);
data2 = readEKRaw_ConvertAngles(data2, calParms_2);

% discard first 4 pings:
AthwartAng_phys_1 = cast(data1.pings.athwartship(:,5:end), 'double');
AlongAng_phys_1 = cast(data1.pings.alongship(:,5:end), 'double');
AthwartAng_phys_2 = cast(data2.pings.athwartship(:,5:end), 'double');
AlongAng_phys_2 = cast(data2.pings.alongship(:,5:end), 'double');

power_1 = data1.pings.power(:,5:end);
power_2 = data2.pings.power(:,5:end);

SoundVel = cast(data1.pings.soundvelocity(1), 'double');
SampleInterval = data1.pings.sampleinterval(1);
SampleRange = cast(data1.pings.samplerange, 'double');
RangeTime = 0:SampleInterval:(SampleRange(2)-1)* SampleInterval;
RangeDistance = RangeTime * SoundVel / 2;
numPings_1 = data1.pings.number(end) - 4;
numPings_2 = data2.pings.number(end) - 4;

%% Calculate EK60 range indexes (acoustic distance) for the target position
ibrEK60 = int16((minRange * 2) / (SampleInterval * SoundVel));
isrEK60 = int16((maxRange * 2) / (SampleInterval * SoundVel));

%% Find indexes of maximum Power values, EK60 Angles:
MaxPower_vector_1 = zeros(numPings_1,1);
MaxPower_vector_2 = zeros(numPings_2,1);
indMaxPower_vector_1 = zeros(numPings_1,1);
indMaxPower_vector_2 = zeros(numPings_2,1);
indMaxPower_1 = zeros(numPings_1,1);
indMaxPower_2 = zeros(numPings_2,1);

AlonAng_1 = zeros(numPings_1,1);
AthwAng_1 = zeros(numPings_1,1);
AlonAng_2 = zeros(numPings_2,1);
AthwAng_2 = zeros(numPings_2,1);

for k = 1:numPings_1
    [MaxPower_vector_1(k), indMaxPower_vector_1(k)] = max(power_1(ibrEK60:isrEK60,k));
    indMaxPower_1(k) = indMaxPower_vector_1(k) + ibrEK60;
    % EK60 Angles 1:
    AthwAng_1(k) = AthwartAng_phys_1(indMaxPower_1(k),k);
    AlonAng_1(k) = AlongAng_phys_1(indMaxPower_1(k), k);
end

for k = 1:numPings_2
    [MaxPower_vector_2(k), indMaxPower_vector_2(k)] = max(power_2(ibrEK60:isrEK60,k));
    indMaxPower_2(k) = indMaxPower_vector_2(k) + ibrEK60;
    % EK60 Angles 2:
    AthwAng_2(k) = AthwartAng_phys_2(indMaxPower_2(k),k);
    AlonAng_2(k) = AlongAng_phys_2(indMaxPower_2(k), k);
end

% Calculate the mean angles across pings:
% (Athwarship angles were reversed for this configuration)
AthwMean1(m,i) = mean(AthwAng_1);
```

```matlab
        AlonMean1(m,i) = mean(AlonAng_1);
        AthwMean2(m,i) = mean(AthwAng_2);
        AlonMean2(m,i) = mean(AlonAng_2);
        % Standard deviation across pings:
        AthwStd1(m,i) = std(AthwAng_1);
        AlonStd1(m,i) = std(AlonAng_1);
        AthwStd2(m,i) = std(AthwAng_2);
        AlonStd2(m,i) = std(AlonAng_2);

    end
end

%% Angular Offsets Between MRAs:
AthwOffset1 = AthwMean1(13,13);      % (13,13) are the indexes
AlonOffset1 = AlonMean1(13,13);      % corresponding to position
AthwOffset2 = AthwMean2(13,13);      % of (y,z) = (0,0)
AlonOffset2 = AlonMean2(13,13);

%% true Athwartship angles
yt = 0.955;
y7125 = [-0.84 -0.77 -0.70 -0.63 -0.56 -0.49 -0.42 -0.365 -0.28 -0.21 -0.14 ...
    -0.07 0 0.07 0.14 0.21 0.28 0.35 0.42 0.49 0.56 0.63 0.70 0.77 0.84];
r = 8.05;
b = rad2deg(atan(yt/r));
% EK60 active:
a1 = b + AthwOffset1;
ya1 = r * tan(deg2rad(a1));
yo1 = yt - ya1;
dxyo1 = sqrt(r^2 + ya1^2);
yEK60_1 = y7125 - yo1;
dxy_sph_1 = sqrt(r^2 + (ya1 - yEK60_1).^2);
sin_c1 = r ./ dxy_sph_1;
AthwTRUE_1 = rad2deg(asin((yEK60_1 .* sin_c1) ./ dxyo1));
% 7125 active:
a2 = b + AthwOffset2;
ya2 = r * tan(deg2rad(a2));
yo2 = yt - ya2;
dxyo2 = sqrt(r^2 + ya2^2);
yEK60_2 = y7125 - yo2;
dxy_sph_2 = sqrt(r^2 + (ya2 - yEK60_2).^2);
sin_c2 = r ./ dxy_sph_2;
AthwTRUE_2 = rad2deg(asin((yEK60_2 .* sin_c2) ./ dxyo2));

%% true Alongship angle
z7125 = [-0.84 -0.77 -0.70 -0.63 -0.56 -0.49 -0.42 -0.35 -0.28 -0.21 -0.14 ...
    -0.07 0 0.07 0.14 0.21 0.28 0.35 0.42 0.49 0.56 0.63 0.70 0.77 0.84];
% EK60 active:
zo1 = r * tan(deg2rad(AlonOffset1));
zEK60_1 = z7125 + zo1;
dxzo1 = sqrt(r^2 + zo1.^2);
dxz_sph_1 = sqrt(r^2 + (zEK60_1 - zo1).^2);
sin_e1 = r ./ dxz_sph_1;
AlonTRUE_1 = rad2deg(asin((zEK60_1 .* sin_e1) ./ dxzo1));
% 7125 active:
zo2 = r * tan(deg2rad(AlonOffset2));
zEK60_2 = z7125 + zo2;
```

```
dxzo2 = sqrt(r^2 + zo2.^2);
dxz_sph_2 = sqrt(r^2 + (zEK60_2 - zo2).^2);
sin_e2 = r ./ dxz_sph_2;
AlonTRUE_2 = rad2deg(asin((zEK60_2 .* sin_e2) ./ dxzo2));

%% Calculate Error:
Athw1 = AthwMean1;
Athw2 = AthwMean2;
Along1 = AlonMean1;
Along2 = AlonMean2;

AlongError1 = zeros(nn,nn);
AlongError2 = zeros(nn,nn);
AthwError1 = zeros(nn,nn);
AthwError2 = zeros(nn,nn);

for j = 1:nn
    AthwError1(j,:) =  Athw1(j,:) - AthwTRUE_1;
    AthwError2(j,:) =  Athw2(j,:) - AthwTRUE_2;
    AlongError1(:,j) = Along1(:,j) - AlonTRUE_1';
    AlongError2(:,j) = Along2(:,j) - AlonTRUE_2';
end

magAthwError1 =  abs(AthwError1);
magAthwError2 =  abs(AthwError2);
magAlongError1 = abs(AlongError1);
magAlongError2 = abs(AlongError2);

%% Plot of Errors:
figure(1)
AmpErrorAthw = -0.5:0.1:0.5;
c = colormap(jet(length(AmpErrorAthw)));
for m =1:25
    for n = 1:25
        for p = 1 : length(AmpErrorAthw)
            if(abs(AthwError1(m,n) - AmpErrorAthw(p)) <= 0.05)
                plot(AthwTRUE_1(n), AlonTRUE_1(m),'.','MarkerSize', 20,'color',c(p,:));
                hold on
            end
        end
    end
end
grid on
colorbar
xlim([-7 7]);
ylim([-7 7]);
title('EK60 Athwartship Angle Error')
xlabel('Athwartship Angles [degrees]','FontSize',14)
ylabel('Alongship Angles [degrees]','FontSize',14)

fh = figure(1);
set(fh,'color', 'white');
set(gca,'FontSize',14)

X = 5; Y = 395;
set(gcf,'PaperUnits','centimeters')
```

```
xSize = 10.5; ySize = 8;
xLeft = (21-xSize)/2; yTop = (30-ySize)/2;
set(gcf,'PaperPosition',[xLeft yTop xSize ySize])
set(gcf,'Position',[X Y xSize*50 ySize*50])

figure(2)
AmpErrorAlon = -0.5:0.1:0.5;
c = colormap(jet(length(AmpErrorAlon)));
for m =1:25
    for n = 1:25
        for p = 1 : length(AmpErrorAlon)
            if (abs(AlongError1(m,n) - AmpErrorAlon(p)) <= 0.05)
                plot(AthwTRUE_1(n), AlonTRUE_1(m),'.','MarkerSize', 20,'color',c(p,:));
                hold on
            end
        end
    end
end
grid on
colorbar
xlim([-7 7]);
ylim([-7 7]);
title('EK60 Alongship Angle Error')
xlabel('Athwartship Angles [degrees]','FontSize',14)
ylabel('Alongship Angles [degrees]','FontSize',14)

fh = figure(2);
set(fh,'color', 'white');
set(gca,'FontSize',14)

X = 475; Y = 395;
set(gcf,'PaperUnits','centimeters')
set(gcf,'PaperPosition',[xLeft yTop xSize ySize])
set(gcf,'Position',[X Y xSize*50 ySize*50])

figure(3)
c = colormap(jet(length(AmpErrorAthw)));
for m =1:25
    for n = 1:25
        for p = 1 : length(AmpErrorAthw)
            if (abs(AthwError2(m,n) - AmpErrorAthw(p)) <= 0.05)
                plot(AthwTRUE_2(n), AlonTRUE_2(m),'.','MarkerSize', 20,'color',c(p,:));
                hold on
            end
        end
    end
end
grid on
colorbar
xlim([-7 7]);
ylim([-7 7]);
title('7125 Athwartship Angle Error')
xlabel('Athwartship Angles [degrees]','FontSize',14)
ylabel('Alongship Angles [degrees]','FontSize',14)

fh = figure(3);
```

```matlab
set(fh,'color', 'white');
set(gca,'FontSize',14)

X = 945; Y = 395;
set(gcf,'PaperUnits','centimeters')
set(gcf,'PaperPosition',[xLeft yTop xSize ySize])
set(gcf,'Position',[X Y xSize*50 ySize*50])

figure(4)
c = colormap(jet(length(AmpErrorAlon)));
for m =1:25
    for n = 1:25
        for p = 1 : length(AmpErrorAlon)
            if (abs(AlongError2(m,n) - AmpErrorAlon(p)) <= 0.05)
                plot(AthwTRUE_2(n), AlonTRUE_2(m),' ','MarkerSize', 20,'color',c(p,:));
                hold on
            end
        end
    end
end
grid on
colorbar
xlim([-7 7]);
ylim([-7 7]);
title('7125 Alongship Angle Error')
xlabel('Athwartship Angles [degrees]','FontSize',14)
ylabel('Alongship Angles [degrees]','FontSize',14)

fh = figure(4);
set(fh,'color', 'white');
set(gca,'FontSize',14)

X = 1415; Y = 395;
set(gcf,'PaperUnits','centimeters')
set(gcf,'PaperPosition',[xLeft yTop xSize ySize])
set(gcf,'Position',[X Y xSize*50 ySize*50])

%% Standard Deviation Plots
figure(5)
AmpStdDevAthw = 0:0.1:0.5;
c = colormap(jet(length(AmpStdDevAthw)));
for m =1:25
    for n = 1:25
        for p = 1 : length(AmpStdDevAthw)
            if (abs(AthwStd1(m,n) - AmpStdDevAthw(p)) <= 0.05)
                plot(AthwTRUE_1(n), AlonTRUE_1(m),' ','MarkerSize', 20,'color',c(p,:));
                hold on
            end
        end
    end
end
grid on
colorbar
xlim([-7 7]);
ylim([-7 7]);
title('EK60 Athwartship Angle Standard Deviation')
```

```
xlabel('Athwartship Angles [degrees]','FontSize',14)
ylabel('Alongship Angles [degrees]','FontSize',14)

fh = figure(5);
set(fh,'color', 'white');
set(gca,'FontSize',14)

X = 5; Y = 395;
set(gcf,'PaperUnits','centimeters')
xSize = 10.5; ySize = 8;
xLeft = (21-xSize)/2; yTop = (30-ySize)/2;
set(gcf,'PaperPosition',[xLeft yTop xSize ySize])
set(gcf,'Position',[X Y xSize*50 ySize*50])

figure(6)
AmpStdDevAlon = 0:0.1:0.5;
c = colormap(jet(length(AmpStdDevAlon)));
for m =1:25
    for n = 1:25
        for p = 1 : length(AmpStdDevAlon)
            if (abs(AlonStd1(m,n) - AmpStdDevAlon(p)) <= 0.05)
                plot(AthwTRUE_1(n), AlonTRUE_1(m),'.','MarkerSize', 20,'color',c(p,:));
                hold on
            end
        end
    end
end
grid on
colorbar
xlim([-7 7]);
ylim([-7 7]);
title('EK60 Alongship Angle Standard Deviation')
xlabel('Athwartship Angles [degrees]','FontSize',14)
ylabel('Alongship Angles [degrees]','FontSize',14)

fh = figure(6);
set(fh,'color', 'white');
set(gca,'FontSize',14)

X = 475; Y = 395;
set(gcf,'PaperUnits','centimeters')
set(gcf,'PaperPosition',[xLeft yTop xSize ySize])
set(gcf,'Position',[X Y xSize*50 ySize*50])

figure(7)
c = colormap(jet(length(AmpStdDevAlon)));
for m =1:25
    for n = 1:25
        for p = 1 : length(AmpStdDevAlon)
            if (abs(AthwStd2(m,n) - AmpStdDevAlon(p)) <= 0.05)
                plot(AthwTRUE_2(n), AlonTRUE_2(m),'.','MarkerSize', 20,'color',c(p,:));
                hold on
            end
        end
    end
end
```

```
grid on
colorbar
xlim([-7 7]);
ylim([-7 7]);
title('7125 Athwartship Angle Standard Deviation')
xlabel('Athwartship Angles [degrees]','FontSize',14)
ylabel('Alongship Angles [degrees]','FontSize',14)

fh = figure(7);
set(fh,'color', 'white');
set(gca,'FontSize',14)

X = 945; Y = 395;
set(gcf,'PaperUnits','centimeters')
set(gcf,'PaperPosition',[xLeft yTop xSize ySize])
set(gcf,'Position',[X Y xSize*50 ySize*50])

figure(8)
c = colormap(jet(length(AmpStdDevAlon)));
for m =1:25
    for n = 1:25
        for p = 1 : length(AmpStdDevAlon)
            if (abs(AlonStd2(m,n) - AmpStdDevAlon(p)) <= 0.05)
                plot(AthwTRUE_2(n), AlonTRUE_2(m),'.','MarkerSize', 20,'color',c(p,:));
                hold on
            end
        end
    end
end
grid on
colorbar
xlim([-7 7]);
ylim([-7 7]);
title('7125 Alongship Angle Standard Deviation')
xlabel('Athwartship Angles [degrees]','FontSize',14)
ylabel('Alongship Angles [degrees]','FontSize',14)

fh = figure(8);
set(fh,'color', 'white');
set(gca,'FontSize',14)

X = 1415; Y = 395;
set(gcf,'PaperUnits','centimeters')
set(gcf,'PaperPosition',[xLeft yTop xSize ySize])
set(gcf,'Position',[X Y xSize*50 ySize*50])
```